A Framework for Further Transparency of Supplier Energy Waste Streams in Multi-layer Production Enterprises

By

Kevin Masataka Ninomiya

A thesis submitted in partial satisfaction of the

requirements for the degree of

Master of Science

in

Mechanical Engineering

in the

Graduate Division

of the

University of California, Berkeley

Committee in charge:

Professor David Dornfeld, Chair
Professor Tarek Zohdi
Professor Sara Beckman

Fall 2014

A Framework for Further Transparency of Supplier Energy Waste Streams in Multi-layer Production Enterprises

by

Kevin Masataka Ninomiya

Abstract

A Framework for Further Transparency of Supplier Energy Waste Streams in Multi-layer Production Enterprises

by

Kevin Masataka Ninomiya

Master of Science in Mechanical Engineering

University of California, Berkeley

Professor David Dornfeld, Chair

Regulatory agencies and compliance measures have obligated manufacturers to reduce its corporate-wide environmental impact in the recent years with economic penalties and social stigma otherwise. Manufacturers undertake constant, inherent risk of affecting their environmental footprint and increased costs while they depend on suppliers. Frameworks for energy audits are undefined between production enterprises and are dependent on self-reported, unit-inconsistent data by individual suppliers. Traditional energy audit methods are detailed, but possible developments can also be implemented in its analysis with real-time data that is of higher granularity, which may aid in the optimization of the overall process plan. This thesis aims to further develop an energy auditing methodology which enables energy streams to be more transparent for detecting waste points at a higher specificity within a production enterprise and suggesting precise improvements that can add greater value, especially in high volumes of production. This framework may be used in applications such as supplier selection and/or evaluation by manufacturers and footprint improvements by non-compliant suppliers.

To Takahisa and Yasuyo Ninomiya

Who provided me with the love and motivation to aspire.

Acknowledgements

I would like to thank Professor David Dornfeld for his guidance and support throughout my undergraduate and graduate career, here at University of California, Berkeley. I would also like to thank my dear friends, mentors, colleagues, and collaborators, who I have met through the research activities in the Laboratory for Manufacturing and Sustainability for both my personal and professional growth. Lastly, I would like to thank the numerous professional support staff including personnel from the Mechanical Engineering machine shop, Departmental Information Technology office, and the Academic Affairs office for their kind assistance.

Additional Project Partner Acknowledgements

- B. Linke, M. Hutchins, M. Helu, N. Diaz, S. Robinson, A. D'Alessio, R. Bhinge, M. Fuge, K. McKinstry, Y. Huang, S. McMains, S. Pavanaskar, S. Pande, C. Chen, Z. Hu, J. Noble, D. Berthold, T. Keller, L. Clemon, A. Srinivasan, R. Verma, V. Schulze, H. Meier
- Laboratory for Manufacturing and Sustainability, DMG/Mori Seiki, Autodesk, KIT wbk

Table of Contents

List of Figures

List of Tables

Chapter 1 Introduction and Motivation

In recognition of the significance of environmental impacts to both the economy and society, many global regions started to implement new regulations and compliance measures for corporations to keep up-to-date with the market trend. Triple Bottom Line (TBL) is a concept that supports the notion that an enterprise is ultimately built on three foundational pillars: economic, environmental, and social factors as shown in Figure 1 [1].

Figure 1: Triple bottom line [1]

A variant concept called, Integrated Bottom Line (IBL) consolidates the TBL factors on the same accounting sheet for measuring business activities [2]. Historically, some enterprises, have considered economic factors to be the only pillar, if not the most important. However, due to emerging regulations, compliance measures, and new type of costs associated with these, corporations have become more concerned with the IBL during their business activities. Supplier selection and evaluation has become increasingly important. Most credible corporations have now adopted auditing measures that monitor supplier behavior and decisions with respect to each of the factors in the TBL. For the purpose of this study, the environmental pillar, specifically energy, will be emphasized over the IBL. This will be done with references to relationship between economic and social aspects; hence, for applications in selecting or evaluating one's green supplier.

Section 1 Environmental policy and compliance and their effects on production enterprises
Section 1.a. Regulation

Environmental policies began to emerge in the latter half of the 1900s, especially with the birth of the United States Environmental Protection Agency (USEPA), which oversees corporations on US soil [3]. Some past notable regulations include the Clean Water Act (CWA), Clean Air Act (CAA), and the Resource Conservation and Recovery Act. Although the US opted out of the international agreement, Kyoto Protocol, other industrialized nations who ratified the agreement were legally bound to act in accordance with the Protocol.

Section 1.a.i. Domestic regulatory climate

The Clean Water Act was last amended in 1972. The CWA primarily affected industries that directly discharge wastewater to navigable surface water with regulations surrounding wastewater quality as part of the pollution control program [4]. The Clean Air Act, which was last amended in 1990, aims to protect public health and welfare and to regulate emissions of hazardous air pollutants [5]. The CAA included emission sources that are both stationary and mobile such as factories and transportation modes, respectively. One can imagine that industries and production enterprises, especially, were affected greatly as changes to their strategies became necessary. Similar to the CWA and CAA, the RCRA was concerned with solid and hazardous waste [6]. Industries were motivated to detect point sources within the enterprise that may violate these regulations. Enterprises that violate such regulations were penalized with a fine through Power Conservation Programs such as the excessive energy use sanction in countries like South Africa [7].

Section 1.a.ii. International regulatory climate

As cited above for South Africa, the international community became more active during this period as well. The most notable legally-binding agreement was called the Kyoto Protocol. Many industrialized nations were involved in its ratification with the United States being one of the exceptions. The Kyoto Protocol aimed to promote industrialized economies to regulate greenhouse gas emissions under a certain level per amendment period. The latest amendment was made in 2012 whereby the target for participating nations was to reduce its greenhouse gas emissions by 18 percent below that of 1990 levels between the 8-year period of 2013-2020 [8]. Although the US rejected the ratification of the Kyoto Protocol and it still lacks an effective nationwide program, some states and localities began to impose a "carbon tax" that penalizes businesses for CO_2 emissions. Examples include the Bay Area Air Quality Management District in the form of a permit. Another program obligates businesses to reduce their greenhouse gas emissions through regulations such as the Global Warming Solutions Act of 2006 (AB 32) in the state of California [9, 10].

Section 1.a.iii. Future regulatory climate

There are future ecological policies foreseen as well. The European Environmental Bureau, for example, have laid out visions that hint at future environmental regulations such as further decreases in natural resource use [11]. The international shipping industry already has 2020 visions set for upcoming regulations according to Nyhus, E. [12]. The implications of such future policies on to production enterprises are unknown, though one can safely speculate an increased complexity when making business decisions that also satisfy the IBL of an enterprise.

Section 1.a.iv. Importance of product life cycle footprint

All of the above regulations have had or may have significant influence over corporate decision-making processes especially for a production enterprise who that manufactures heavy consumer products. These enterprises are heavily dependent on utility such as electricity during the product's manufacturing phase. An example is the automotive industry. A product life cycle contains five basic stages from cradle-to-grave as shown in Figure 2 [13].

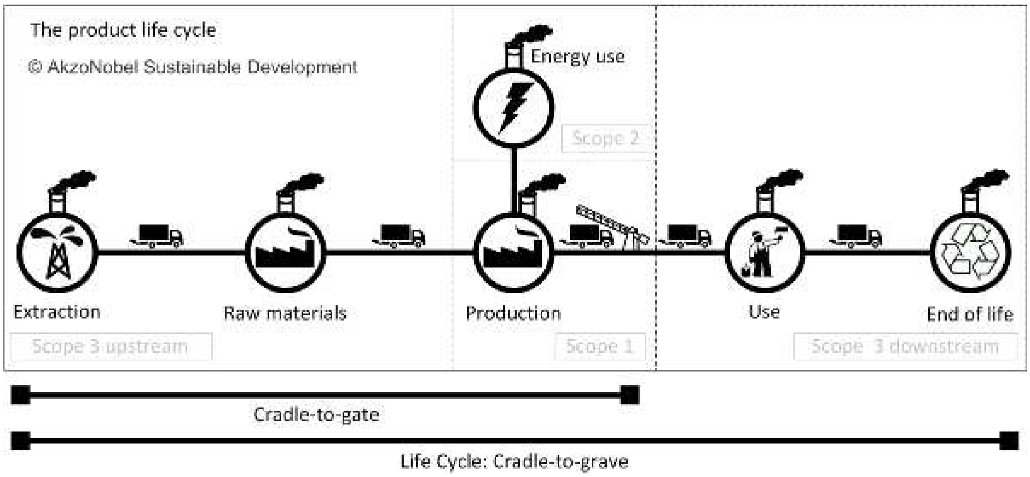

Figure 2: Product life cycle [13]

In the past, industries were merely obligated to reduce their footprint at point sources; hence, their impact during the manufacturing phase of a product life cycle. Studies quickly showed that other phases of a product life cycle also contributed for a significant portion of the life cycle footprint. Consequently, for example, manufacturers were encouraged to become mindful about their product's use phase contribution to the footprint as well. In this framework, however, the topic is narrowed to the manufacturing phase of the life cycle. The framework's purpose is for the selection of new green suppliers or evaluation of existing ones while being able to suggest improvements at a higher level of granularity with a quicker response time. The reason being, each large production enterprises have the most influence over their own grounds including supplier behaviors over consumer behaviors of their products. Therefore, the argument focus for the thesis is that by having energy waste stream transparency and relevant data at a higher (more micro) granular level, it is better because it allows change enablers at the enterprise to make a larger impact by giving them more control of facility or supplier's energy impact, especially if the data is real-time so that their changes can become effective immediately in some cases. This is based on an assumption that the higher data granularity is proportional to “data at a lower level” within a production facility or supplier hierarchy. The hierarchy shown in Figure 3, that was assumed in this thesis is an adaptation of the “manufacturing Google Earth View” shown in Figure 4 [Dornfeld REF of GEV].

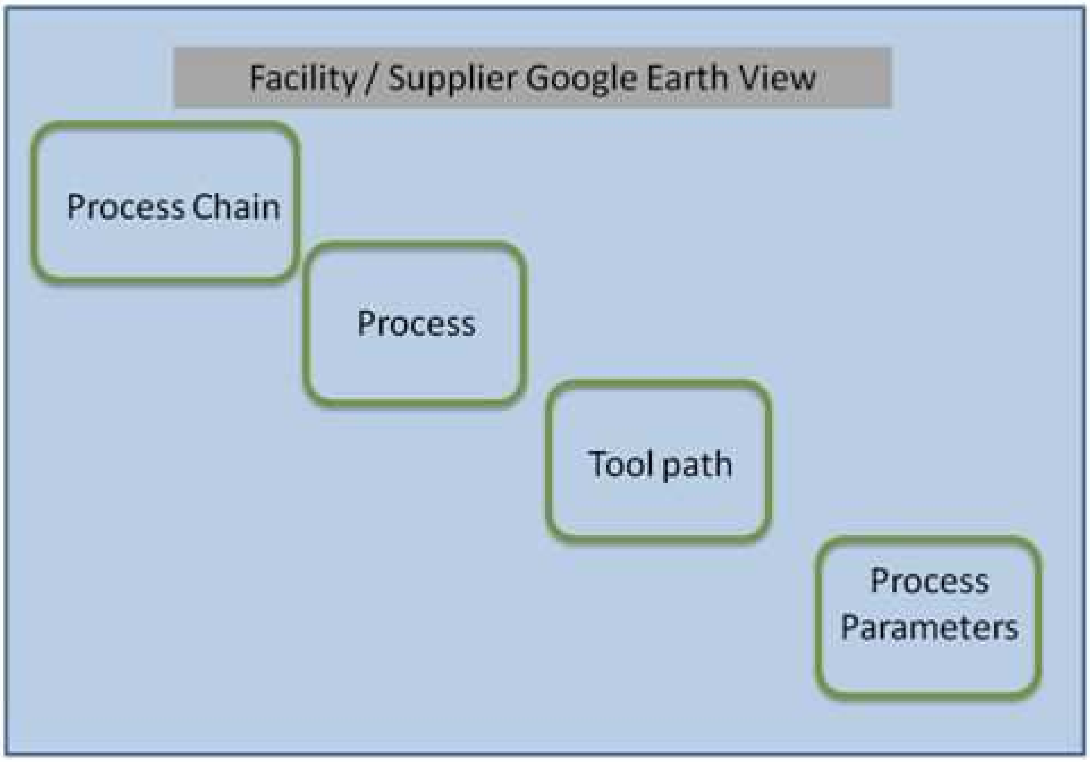

Figure 3: Facility/supplier Google earth view

Figure 4: Manufacturing Google earth view

Section 1.b. Compliance measure

Compliance measures have been agreed at both national and international scale. These include green initiatives such as Leadership in Energy and Environmental Design (LEED) certification, sustainable production standards such as ISO 14001, and responsible supplier selection efforts made by corporations such as Hewlett and Packard (HP) and recent issues with enterprises such as Apple [14, 15].

Section 1.b.i. Green initiative

LEED is a green certification program administered by the U.S. Green Building Council with different levels of certification and rating systems. The levels of certification are Certified, Silver, Gold, and Platinum [16]. Due to the heavy demand in utility, resources, and maintenance involved in operating a factory, production enterprises have tougher times obtaining a certification. It may be inferred that industries, however, are inclined to obtain such certifications in order to maintain a competitive edge for both technological and branding reasons. Companies such as Volkswagen have obtained LEED Platinum certification for their assembly plant in Chattanooga, TN [17].

Section 1.b.ii. Environmental standards

Sustainable production standards such as the ISO 14000 family, specifically ISO 14001:2004 and ISO 14004:2004, address environmental management of facilities. Companies or organizations aiming to improve their environmental performance are encouraged to conform to the ISO 14000 family standards such as reduction of energy consumption as part of ISO 14001:2004 [18]. Notable companies such as IBM maintains to be at the forefront of sustainable practices through the employment of ISO 50001 as well [19].

Section 1.b.iii. Inherent risks from suppliers

Enterprises with a large network of global suppliers are constantly exposed to risks through supplier behavior that is non-compliant. For example, Apple was recently scrutinized for their Chinese suppliers with regards to labor conditions [15]. Apple was specifically cited for their Chinese suppliers dumping excessive amounts of chemicals into nearby rivers [20]. HP performed a comprehensive audit to survey their suppliers in 2013. They found that 12% of non-conformance issues were attributed to environmental compliance standards [14].

Section 1.b.iv. Importance of conformance

The inherently higher risk of compliance measures over environmental regulations is arguable due to the unpredictable nature of an outcome. For this reason, companies, especially production enterprises, are motivated to be within compliance. Although non-conformance to compliance measures does not necessarily result in direct monetary penalties, though this is dependent on local jurisdictions, it presents vulnerability for corporations to lose their competitive edge via opportunity losses such as customer attrition. For this reason, having a framework that allow for further transparency of error sources is critical.

An ignorance of such policies and compliance measures trigger penalties for industries to pay large fines or in worst case scenario, halt production and sales which would be detrimental to company performance. For this type of study, it is ideal to conduct a comprehensive study using IBL data. However, due to the difficulty in defining a universal metric for certain TBL factors such as social metrics, it is limited to the environmental factors, and specifically the energy assessment aspect due to data availability. An energy assessment, namely - energy audit – enables corporate decision-makers to understand the current energy usage situation of their enterprise and plan their strategies accordingly to minimize cost and impacts.

Section 2 Industrial energy audit
Section 2.a. Current process

Industrial energy audits are a comprehensive assessment of a facility's energy management practice. An energy audit can be categorized into two main types: a preliminary audit and a detailed audit [21]. According to the Industrial Energy Audit Guideline by Lawrence Berkeley National Laboratory (LBNL), energy audits are generally based on assessments of utility bills, historical usage, inventory and energy balance using energy measurements, production patterns and their relationship to energy usage, benchmarking and comparative energy performance analysis [21]. Most audits tend to follow a similar process flow as shown in Figure 5 [21].

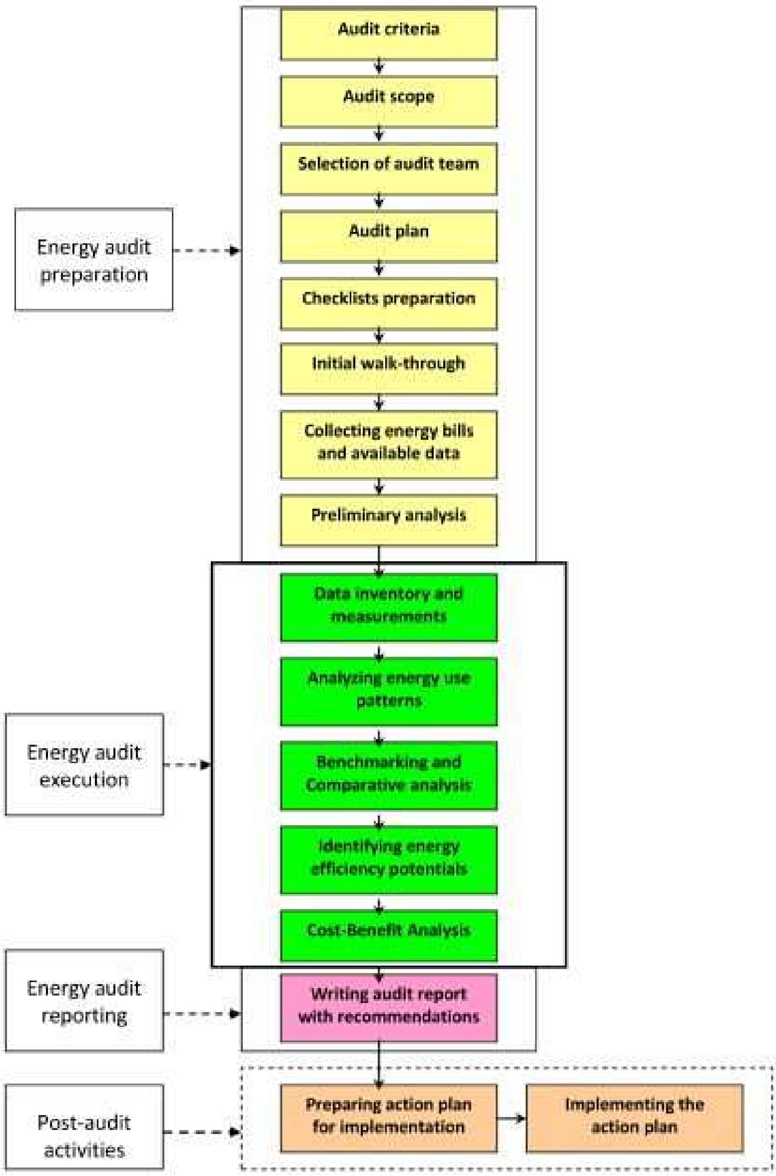

Figure 5: Industrial energy audit process flow [21]

Figure 5 shows a general auditing process that includes improvement suggestions, cost-benefit analysis, report generation, and improvement implementation plans. Industries rely heavily on audits in order to make cost-effective improvements while being compliant.

Section 2.b. Avenues of improvement

Although the current methods are detailed with a certain level of granularity, it is important to note that these audits are a discrete process and that the suggestions are descriptive-based improvements on a lower level of data granularity.

Section 2.b.i. Discrete process

Energy audits are conducted based on requests made to in-house or outsourced auditors. These requests, however, are made on a periodic, not continuous, basis. Although the collected data maybe representative of a set of historical samples, this mean that changes will take time before they are implemented. According to Figure 5 from Chapter 1, Section 2.a., the implementation process for change only comes after the report generation stage. It may be of concern to fast-paced industries to react against negative audit marks as quickly as possible and have their facility or supplier contribute more to their value chain. This requires audits to be made continuously while enabling key players to implement change with a short turnaround time. For this reason, it is important for production facilities to obtain real-time data.

Section 2.b.ii. Granular descriptive-based improvements

According to [21], collected data include those that generate Load/Demand profiles and/or Scatter diagram for presenting the dynamics of the energy-production relationship. Although these profiles and plots are detailed in nature, they only enable suggestions for improvements at the same level of granularity as the data. If the collected data plots are low in sensitivity, their suggestions will also be low quality. This may negate the purpose of conducting an energy audit if meaningful changes are overlooked due to frameworks of low sensitivity. For key players, who make decisions for a facility based on audit reports, it is safe to assume that they would like suggestions based on data that have high level of granularity (sensitivity).

Section 3 Example of target users
Section 3.a. Example of multi-layer production enterprise structure

Many different types of production enterprises exist. They will differ by industry type and size. This framework focuses on large production enterprises that could consist of multiple layers. An example of an organizational structure for a production enterprise is shown in Figure 6.

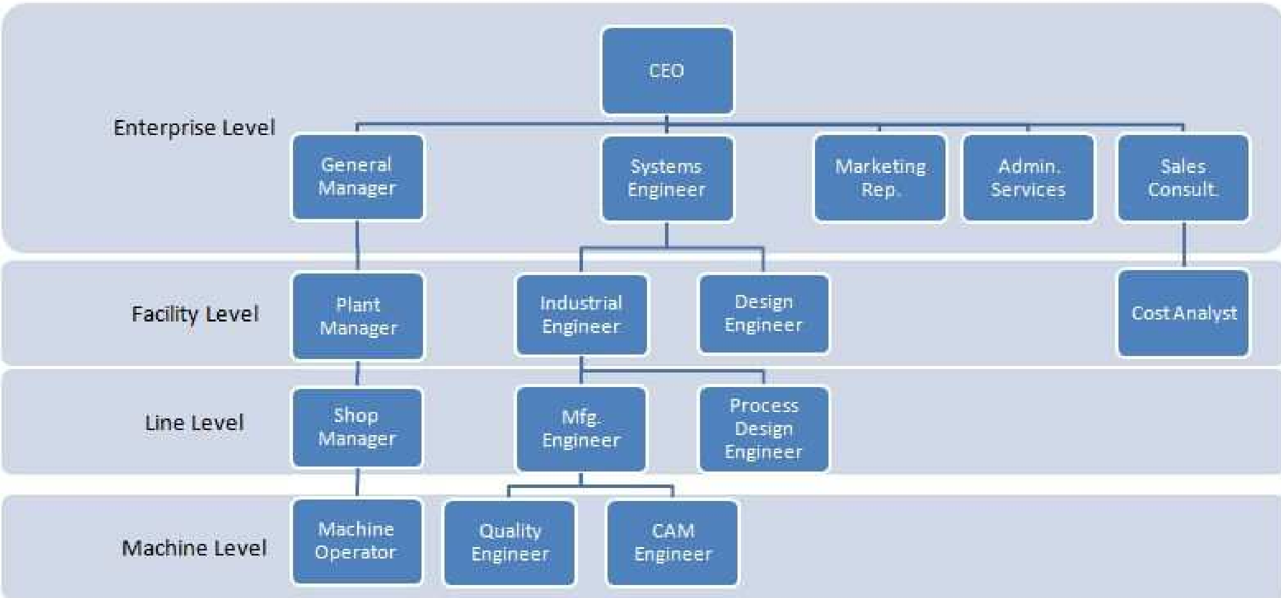

Figure 6: Example enterprise hierarchy [22]

One can imagine that opportunities for energy loss and inefficient production concerning environmental management exist at each layer of Figure 4. It is important that the energy auditing process considers energy loss opportunities at each level down to the parameter level, which ultimately governs the production process on a per unit basis. This will allow the user to understand a cause-and-effect relationship for a bottom-up improvement approach. For example, is the energy consumption, which is proportional to energy utility bills, high because of a milling process that moves at twice the cutting speed than it needs to be? Not only the higher energy consumption, but due to the high production rate (from the faster cutting speed), is it producing excessive inventory costs? By enabling the key players to view energy losses at a higher granularity, it results in making error sources more transparent; hence, improving the bottom line more effectively.

Section 3.b. Example players within each layer

A key player can exist at each of the enterprise levels in Figure 6. For example, at the Facility Level, an Industrial Engineer might be concerned with the energy consumption of the entire facility as opposed to the Process Design Engineer in the Line Level who may only be concerned with energy consumptions of the assembly line. Basic energy audits tend to be concerned with surface level direct energy data with low granularity. Although a Line Level individual could be satisfied with such a level of granularity, this can only affect two more layers above as opposed to a level of granularity that exists at the Machine Level. Data at the Machine Level of granularity will have a greater effect, especially for high volume enterprises, a high level of granularity enables facilities and suppliers to further pinpoint the root cause of their energy loss.

Section 4 Framework's purpose

The framework's purpose is to cut the energy loss throughout a production enterprise through a higher granularity of descriptive, real-time analysis. This would ultimately enable decision-makers to implement effective changes that improve the corporate bottom-line. It will also aid a production enterprise to maintain a corporate-wide compliance to industry standards and the green market mindset through an effective selection and evaluation of green suppliers. It will also enable non-compliant suppliers to identify the source of energy loss and make a greater change in a shorter amount of response time.

Section 5 Framework by analysis level

Section 5.a. Parameter

The parameter level is the highest level of data granularity that one can obtain and it corresponds to the lowest layer of the enterprise structure from Figure 6 in Chapter 1, Section 3.a. It allows for the greatest impact to be made through an energy audit since a change in a production parameter may alter the production outcome significantly. This level is considered to be under the process plan-influencing family. The author's contribution is an algorithm for prediction of energy consumption and optimal parameter selection at a high confidence level based on the energy audit.

Section 5.b. Tool path

The tool path level can provide parameter-like impacts since it has a greater influence on a process plan than the subsequent levels. This level would also correspond to the lowest layer of the enterprise structure. The author's contribution in this level is a methodology to generate energy-efficient roughing process tool path based on the energy audit.

Section 5.c. Process

The process level data starts to become similar to the traditional granularity as seen in [21]. Both this level and the subsequent process chain level influence the operations scheduling, but the process level still maintains influence on the process plan. The data and improvement suggestions in this level are concerned with comparisons between different machines of the same process. For example, if a CNC Mori Seiki milling machine was used over a CNC HAAS milling machine for a drilling process, what would have been the difference in energy consumption. For each of the machines, what would be the embodied energy versus the process energy? The author's contribution for this level was more on the data post-processing, organization, and visualization aspect rather than an improvement suggestion since the improvement suggestion at this level will be very similar to existing methods already. By providing key change enablers with effective post-processing, organization, and visualization technique, it would enable them to execute changes more quickly and effectively.

Section 5.d. Assembly line/process chain

The process chain level data is meant for operations scheduling and energy reduction through utilization of an optimal process chain [23]. It lacks granular data compared to the previous three levels; thus, it might be less impactful for implementing improvements but it can provide a general overview of the energy usage at a facility quickly. The author's contribution here was the data organization and visualization of energy consumption at facilities or suppliers.

Section 6 Assumptions and disclaimers

Due to data and time constraints, some goals are considered as future steps. This study provides the preliminary steps for making energy loss points more transparent for a more effective improvement strategy. For this reason, certain concepts were neglected. For example, error values should exist for every analysis and each level, but it was assumed that errors were constant for each level of analysis. Only environmental effects from the TBL were considered due to data availability. Lastly, all products manufactured as part of experiment and future manufactured products in question were assumed to be produced with a certain, satisfactory level of product quality.

Chapter 2 Related Works

Section 1 Supplier selection/evaluation

Proper supplier selection has become increasingly important, yet represents a set of complicated tasks for supply chain specialists. Many research efforts exist that explore strategies for selection/evaluation. Some studies focus on the supplier selection/evaluation process while others focus on refining selection/evaluation criteria (parameters). Due to high investments of financial resources in making supply chain decisions, it is vital that specialists utilize the optimal process and parameter based framework. Beil describes the typical supplier selection process starting from the identification stage to the evaluation stage. It describes how each step is interrelated and why each step is important [24]. Akili describes a scorecard that contains green supplier selection criterion [25]. Walmart became famous for implementing a green supplier selection scorecard in 2006 for its suppliers' packaging performance [25]. Vance et. al. introduced a computer-aided methodology that uses a P-graph framework to determine a supply chain based on cost, cost of electricity production, ecological footprint, and emergy. They defined emergy as a measure of energy used in production, directly or indirectly [26]. Xie examined the impacts of energy saving policies created by policy-makers. Xie analyzed the decisions by observing the tradeoffs between energy saving and profits made by two types of supply chain structures: vertical integration and decentralized setting [27]. Although the application is for policy decisions over business decisions, this type of study enables decision-makers to conduct tradeoff analysis when generating strategies for their particular supply chain design. Waldemarsson et. al. takes an interesting approach where they consider energy surplus as a revenue-generating product [28]. This suggests that energy savings have both a cost-saving and revenue-generating effect on production.

Section 2 Proposed framework levels
Section 2.a. Parameter

A force model was developed by Kishawy et. al. using collected energy signals from the broaching experiment [29]. The surfaces were then used to examine the subsurface micro hardness and microstructure. The objective was to develop an energy-based force model and estimate depth of cold-working from broaching tools. The force model contained energy and dynamic factors such as friction at the tool-chip interface, friction at the tool-work piece interface, power spent on plastic deformation zones, formation of a new surface and influence of minor cutting edges. All of these contained separate but related equations. The model was verified between the simulated and measured data. Cold-working of material increased the cutting force. Analysis was done by the Vickers micro hardness test. Severe elongation and plastic deformation was seen during the subsurface microstructure test. These conclusions were used as a basis for modifying the shear flow stress in the energy based force prediction model, most likely as their future work since no new model was actually presented other than their original one [29]. Yoon et. al. proposed a model that enabled machine operators to determine the optimal set of machining parameters for both minimum energy and minimum cost. They studied milling and drilling processes to identify the optimal parameters when considering energy consumption and cost savings [30]. Liu et. al. proposed a method to predict the energy consumption of a machine tool. They broke the cycle into three period: start-up, idle, and cutting in order to determine characteristic models for the first two periods using a fitted curve of energy consumption data. They then used the cutting power based on machining parameters in order to predict the energy consumption [31].

Section 2.b. Tool path [32]

In the Fall 2013 term, a class project was conducted to explore energy-efficient tool path generation algorithms. The tool path level is an adaptation of the project for the purpose of making energy-saving suggestions at a higher granularity than a mere machine utilization improvement at the process-level and above, which are related to operations scheduling [23]. This level has frequent references to the collaborative course report as [32]. For this reason, please consider the tool path level (sub-)sections (and subsequent ones) as a block reference to [32].

Section 2.b.i. Tool path introduction

Kong et. al. [33] showed that tool path generation schemes affected the amount of energy and the processing time required to machine the same part. Rangarajan et. al. [34] showed that tool path segment length influenced machining cycle time, thus affecting the energy consumed. Therefore, it was indicated that the tool path strategy was related to the energy demanded to produce a product. It was preferred that CNC milling machines have longer tool paths in the advantageous axis where less energy was consumed [33]. Common characteristics of energy efficient tool paths included, but were not limited to, making fewer and gradual changes in tool path cutting direction, avoiding sharp corners, and having longer paths with near constant cutting load.

Section 2.b.ii. Chord error introduction

It was equally important to consider precision manufacturing errors associated with machining as well as its energy consumption. It is important to note here though that this process was merely assumed to be categorized under the roughing process at this stage based on previous roughness observations made by Youngwok [35]. For this reason, this particular project assumed that it was more accurate and applicable for a roughing process only. Chord error was the focus for the project. Chord error is the maximum error that occurs when a chord line is to be drawn under the supposed arc. Theoretically, the maximum error/deviation was considered to occur at the middle of the arc and the drawn chord line. Figure 7 shows an illustration of this phenomenon. The point where the deviation is calculated is shown as W(X,Y).

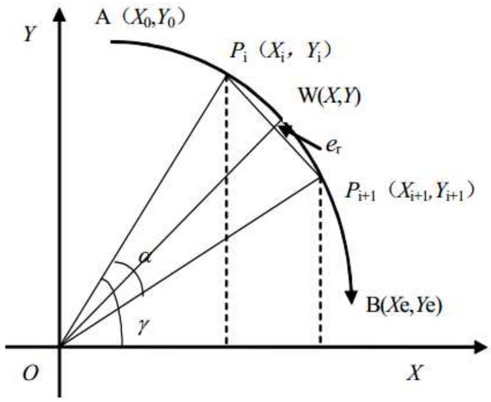

Figure 7: The schematic diagram of error in CNC interpolation [36]

Other planar errors such as parallelism, planarity, surface roughness, and form errors were also considered for the project, but chord error was ultimately selected to be the focus within this project. It was less investigated than other errors in relation to energy consumption. Chord error could be predicted analytically based on input process parameters. It is the difference between the ideal arc section and the approximation using segments [36] as aforementioned. Figure 8 shows an illustration of the ideal arc-segment difference as chord error.

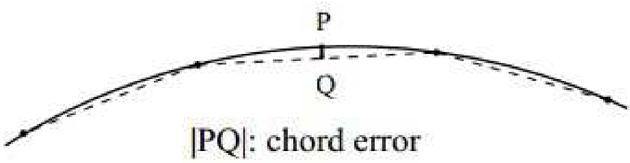

Figure 8: Chord error [37]

Yeh and Hsy [38] proposed an algorithm that reduced the chord error within a specified tolerance range during the interpolation process. They pointed out that chord error was closely related to the curve speed and the radius of curvature. They introduced an adaptive-feed rate interpolation algorithm in which the feed rate was automatically adjusted for chord error reduction. Yong and Narayanaswam [39] proposed a speed-error controlled interpolator based on offline predetermination of feed rate sensitive corners. The interpolator controlled the speed and acceleration/deceleration of machining during the interpolation process as an additional aspect compared to Yeh and Hsy.

Section 2.b.iii. Tool path generation and connectivity

There have been several automatic tool path generation algorithms presented in literature. The majority of these were related to machining free form surfaces especially in three dimensions. The focus of this project's collaborative literature review was on studying automatic tool path generation algorithms for 3-axis milling machines.

Standard Computer Aided Manufacturing (CAM) software commonly generates zigzag or circular paths. However, these may be suboptimal depending on the specific application. Lin and Koren [40] came up with an optimized tool path for free form surfaces which relies on variable offsets from the previous tool path to minimize redundant machining. Linares and Sprauel [41] came up with Spade and Triangular tool paths in order to achieve uniform tool wear. Trochoidal tool paths [42] were also commonly used because they generated constant feed and increased material removal rate by moving the tool along a path of constant radius. In order to further optimize redundant tool movements, a topological approach was developed by Choi and Cheung [43] who used a hierarchical data structure to address this problem. Choi and Cheung [43] also used a dynamic priority-based approach.

The digital micrography algorithm generated a sufficiently smooth vector field over the domain subject to boundary constraints. It then generated a set of streamlines in the interior of the domain. The algorithm then proceeded to fit text along the streamlines. One of the major objectives of generating an efficient tool path for the project's application essentially boiled down to finding a way to connect streamlines minimally with little time where no cutting would occur. From observation, this was equivalent to a shortest Hamiltonian Path problem, which is a graph traversal technique such that all the vertices were visited exactly once.

Both the Hamiltonian Path problem and this project based their modified algorithm on the traditional Traveling Salesman Problem (TSP) approach. The TSP found the shortest possible route for the tool to hit all nodes within the vector field. The TSP guaranteed that the tool would visit all nodes and return to the starting point. The TSP limited the tool from returning to the starting point, so a dummy variable was introduced as "zero" distance from all points as the initial point.

Section 2.b.iv. Tool path, machining, and energy efficiency

An energy or facilities auditor may be able to obtain relevant data and results through basic life cycle assessments, but this may still be considered preliminary for detailed audits. Suggested by Diaz et. al. [44], a large part of the energy consumption will be produced during the use phase in machining. Diaz et. al. [44] also observed that energy consumption for the particular NVD 1500 DCG machine could be characterized on a specific energy curve based on the Material Removal Rate, *MRR*. *MRR* is a product of feed rate, F_T, depth of cut, *doc*, and width of cut, *woc*. Scholars have worked on studying machine tools for different stages of the cutting process to analyze the energy consumption more specifically [33].

The three broad stages were constant, run-time and cutting energy portions. The tool path can only change the cutting energy when the machine is running. The acceleration and deceleration could cause more energy consumption. Shorter cycle times can generate less constant tare energy. Shorter tool path segment length and orientation can lead to longer machining cycle time. The ideal cutting direction can reduce the energy consumption as well. Considering the dominance of the tare power demand in electricity consumption, the electrical energy decreases when the process rate increases. The cutting time can be related to the energy consumption as well, which can also use a non-constant offset to reduce machining time such as letting the tool path begin and end at the surface boundary.[40] The accuracy of the predicted energy was based on the average error and the standard deviation.[33]

Process time and energy demand for five various tool paths are shown in Figure 9(a-e) [33].

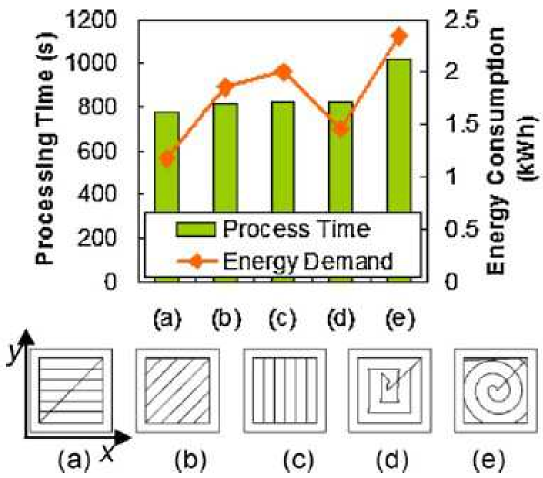

Figure 9(a–e): Processing time and energy consumption of various tool paths [33]

From the example, one can see that the Figure 9(a) is mainly in the x-direction and Figure 9(c) is mainly in the y-direction. The travelling distance involved in case Figure 9(e) generates the highest energy consumption while Figure 9(b) is between cases Figure 9(a) and Figure 9(c). Based on this example, cases Figure 9(a) and Figure 9(d) were chosen as the model tool paths since the influence of the moving direction on energy demands were smallest. [33]

As an important note and disclaimer, the objective of this project was to verify that the tool path generated via the connection of streamline vector fields, which were created from UBC's micrography algorithm using the MTSP approach, was more energy efficient compared to two other tool paths previously mentioned in [33]. Furthermore, in order to correlate precision manufacturing errors with sustainable machining techniques, comparisons were also made between analytical chord error predictions found using four different input process parameters: CAM default, energy efficient tool (EET) path using same CAM default parameters, and an optimized EET using parameters from a specific energy curve.

Section 3 Process

Berthold [45] wrote his thesis about environmental value stream mapping. His focus was a process-oriented approach that enabled small and medium enterprises to have a better overview of the energy and material consumption of their production [45]. This thesis aims for a similar goal which allows large enterprises to obtain a refined understanding of their current supply chain network and its contribution to their value chain. This thesis, however, will only focus on the energy aspect as it is more related to an energy audit process. Yoon et. al. [46] derived power efficiency for milling, micro-milling, drilling, and brushing processes. They determined that power efficiency of a process is dependent on many factors including specific energy consumed; hence, it is important consider the production environment as a whole [46].

Section 4 Assembly line/process chain

Posselt et. al. [47] argued that existing energy value steam analysis methods lack the ability to consider indirect energy demands in a process chain. Indirect energy demands are representations of energy being used for the building services, which are important for the production operation. They aimed to introduce an extended analysis approach that also included indirect demands as well as direct demands [47]. Wang et. al. [48] presented a systematic approach for process planning and scheduling for a milling process. They employed Artificial Neural Networks and several complex algorithms such as the Genetic Algorithm in order to identify optimal solutions. Their intent was to perform a multi-objective optimization to meet the requirements for a sustainable process planning and scheduling [48].

Both studies emphasize that a systematic approach is necessary in order to make optimal decisions that are sustainable. By enabling users of this proposed framework to view energy loss points at a micro-granular scale, such as at the parameter level, it enables users to make precise improvement suggestions while viewing the energy value stream holistically. In the subsequent chapters, the methodologies, results, and discussion for each of the analysis layers above will be presented.

Chapter 3 Methodology
Section 1 Parameter [44]

It is important for a production enterprise to understand the parameter relationship and its effect on energy consumption. One approach to understand this is through process characterization. One can reference the milling energy characterization projects to determine the energy consumption levels while maintaining the same part quality [44, 49]. If the design specifications or processes are to change, one may repeat a similar method in order to obtain such characteristic relationships.

The Energy Model Validation (EMV) Project was a continuation of validating the energy model generated from the constant Material Removal Rate (MRR) experiment conducted by Diaz, et. al. [49]. On top of constant MRR cuts, this project also observed variable MRR cuts to determine the model's validity for cutting parameters that involve a variable nature. MRR follows the formula

$$MRR = d.o.c. * w.o.c. * f \quad (1)$$

where *d.o.c.* is the depth of cut, *w.o.c.* is the width of cut, and f is the feed rate. The experiment was conducted in stages:

1. obtaining a new energy model for the current machine tool, NVD 1500 DCG
2. designing a geometry and programming a tool path that satisfied the variable aspect of the project
3. calculating theoretical energy demand values based on the energy model
4. validating the model accuracy based on six trials of cuts

The experiment was conducted with a 6mm uncoated solid carbide end mill, K600 Series by Kennametal, and with a 1018 AISI Steel work piece. The cutting procedure consisted of continuous x- and y-axis cuts with a slot design. The test piece was designed such that it contains nine features where the MRR was varied at each feature with constant or variable MRR as shown in Figure 10.

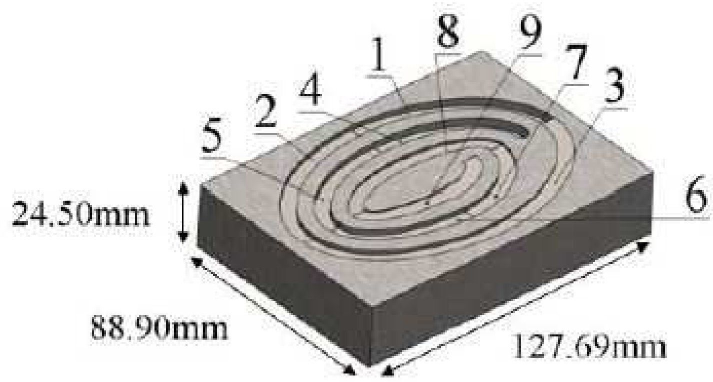

Figure 10: Part design with nine features

The constant and variable MRR entities were varied based on the feature's z-axis geometry, whether the feature was flat or contained a ramp, and were an integral part of the energy prediction and model validation stages.

The first step consisted of deriving the energy model for validation. More specifically, the specific energy model was deduced from the "Specific Energy vs. MRR" curve (see Figure 11) as its best-fit line. The previously obtained plot in [49] was based on the older machine tool, NV 1500 DCG, which had a different spindle speed rating compared to the newer model, NVD 1500 DCG, where the energy model would therefore be different as well. Since each energy model has to be specific to a machine, data was retaken for the newer model, so that a more accurate energy model could be derived.

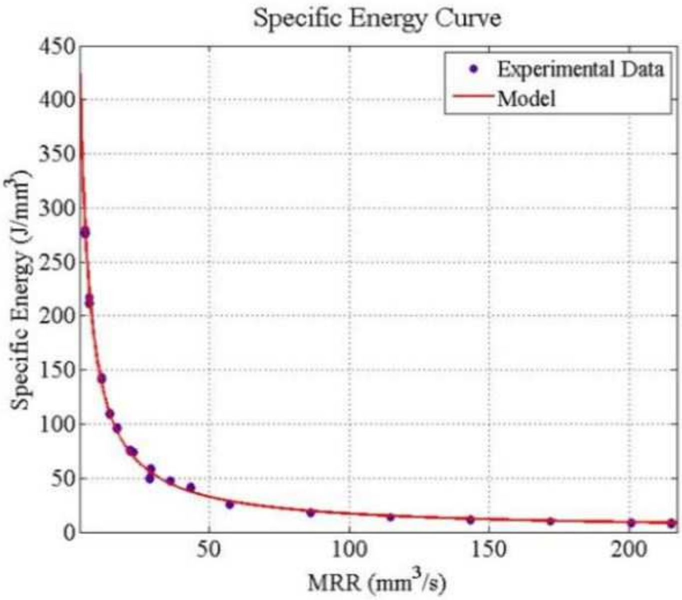

Figure 11: Specific energy curve for 1018 Steel based on constant *MRR* for new machine tool [44]

As one can observe from Figure 2, the curve followed a format shown in Equation (2).

$$E = k * \left(\frac{1}{x}\right) + b \tag{2}$$

where E is the Specific Energy, x is the MRR, and k and b are constants generated from respective "Specific Energy vs. MRR" plots. The specific energy model of the current machine tool was determined to be

$$E = 1556 * \left(\frac{1}{MRR}\right) + 1.475 \tag{3}$$

with an adjusted R-squared value of 0.9698. This equation was later used as part of a series of steps to generate the theoretical energy prediction values per feature. To validate this model, a test part was designed for experimental results of both constant and variable MRRs.

A spiral design was used to incorporate both the constant and variable nature of the experiment. Nine features are used to control various MRR parameters within a single design which included three constant MRR portions. Figure 12(a) illustrates the negative image of the finished part from Figure 9 where Figure 12(b) provides the cross-sectional view of the finished part, both for a closer comparison of the height differences.

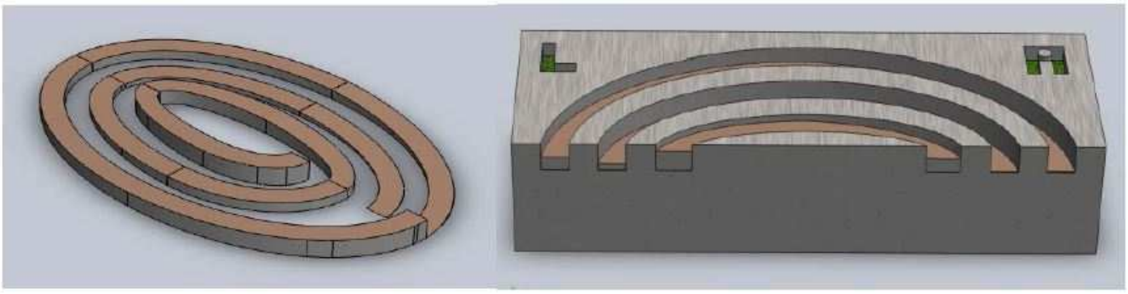

(a) (b)

Figure 12: Spiral design (a) Negative image, (b) Cross-sectional view

The heights were differentiated because ramps along the z-axis were included in six of the features to satisfy variable MRR conditions. In terms of Equation (1), the width of cut and the feed rate were kept constant throughout the cut, while the depth of cut was varied by the addition of the ramp. In terms of the tool path, the end mill plunged into the starting point of feature 1 where the deepest cut is located. Then the tool followed the path set by features 2 and 3 to complete the outer cutting cycle. It slowly exited out of the test piece and re-plunged into the starting point of feature 4, which has the same depth as the starting point of feature 1. The depth was determined by a multiplicative factor, z, that had a span of values from 0 to 1 and the diameter of the cutting tool. Here, $z = 0$ would indicate zero depth or no MRR at the top surface of the stock material, and $z = 1$ would indicate a full diameter worth of depth of cut being performed on the test piece. After all geometries were set with the design, the NC Code was generated and simulated using ESPRIT with assistance from an ESPRIT Applications Engineer, Mr. Julien Durand [50]. After performing a process parameter test, the optimal feed rate and spindle speeds were determined to be 164 mm/min and 3558 rpm, respectively. The process parameter test was based on machine chatter noise through preliminary cuts, aside from the spiral design NC Code. Figures 13(a) and 13(b) show a side view illustration of the end mill slotting up a z-axis ramp and a snapshot of the Advanced Simulation Feature in ESPRIT of the generated tool path, respectively.

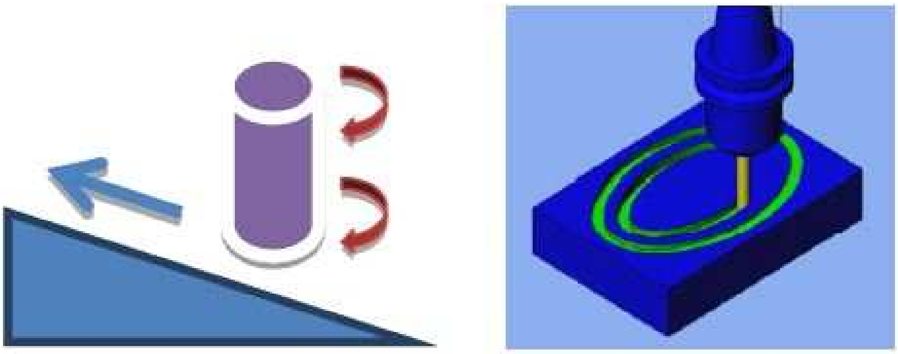

(a) (b)

Figure 13: Simulation illustration (a) Z-axis ramp side view, (b) Advanced Simulation Snapshot

The energy predictions were based on a *MRR* profile and the energy model determined by Equation (3). The MRR profile, plotted as "*MRR* vs. Time," was found for each feature such that the energy predictions could be made based on each feature. Figures 14(a) and 14(b) show the MRR profile for the outer and inner geometry of the spiral design, respectively.

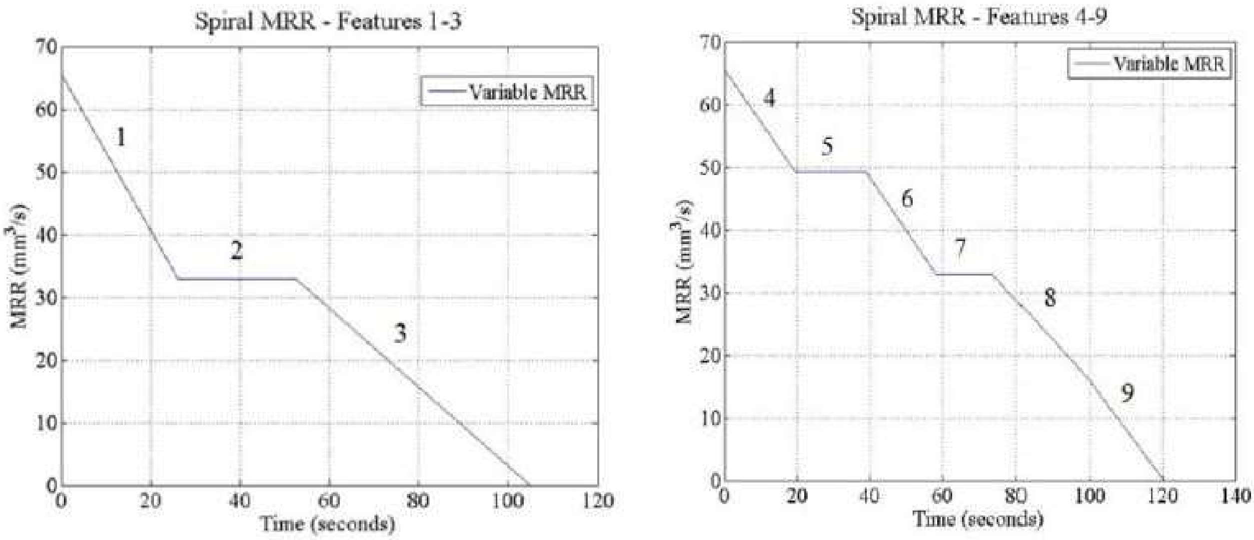

(a) (b)

Figure 14: *MRR* profiles of all nine features (a) Three outer Features, (b) Six inner features [44]

The profiles were found by calculating the MRRs at respective times for the start and end coordinate points, q, of individual features. Equation (1) was modified for finding *MRR* values for each point and the time was calculated based on the quotient of arc length, s, per feature and the feed rate, f.

$$MRR(q) = d.o.c.(q) * w.o.c. * f \quad (4)$$

$$time(q) = \frac{s(q)}{f} \quad (5)$$

These profiles were broken down into desired sample sizes per feature, N, such that a statistical approach could be taken in making energy predictions. The value for N was a user-defined arbitrary value.

Each feature shown in the *MRR* profile was broken into sample sizes, N, where corresponding infinitesimal energy predictions for each feature and entry of the sample size were summed to deduce the final predicted energy value. An illustration of this method is shown in Figure 15 where the sample time, Δt, was calculated by dividing the total time per feature, T, by sample size, N. T was calculated by finding the difference of absolute time value of start and end points from Equation (5). The sample time exists on the same axis as the general time axis because it is a way of breaking the total time per feature, T, into smaller components to take its sum at a later step. For simplicity, the relationship between T and N were considered to be linear for the scope of this thesis.

$$\Delta t = \frac{T}{N} \quad (6)$$

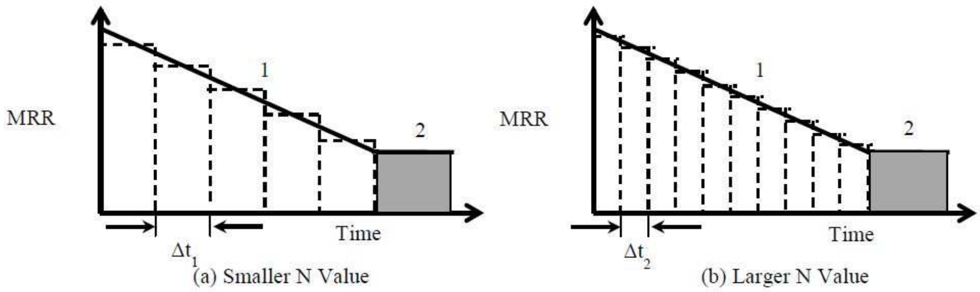

Figure 15: Sample size, *N*, comparison (a) smaller *N* value, (b) larger *N* value [44]

Here, *N*=1000 was used since the predictions converged into a single energy value for *N* values equal to and above 1000. One can deduce that the data sensitivity is dependent on the *N* value from Figure 15, where a smaller *N* value would indicate a larger Δt value. This can potentially result in loss of data sensitivity because infinitesimal data points are found less frequently for a test case with smaller *N* values. Larger *N* values, on the other hand, provide smaller Δt values for more data samples. This was the case for the experiments; thus, a critical *N* value was sought and determined to be 1000 after a few iterations of the modified Matlab energy prediction file. One reason for a fairly high *N* value of 1000 may have been attributed to variability in the data. Then, a time row vector, Δt_{row}, was created with start and end times of zero and total time per feature, *T*, with an increment of Δt shown as Equation (7) in Matlab syntax. The number of indices for the row vector was now equal to the designated sample size, *N*, where a *MRR* value was calculated for each index.

$$\Delta t_{row} = [0{:}\,\Delta t{:}\,T] \qquad (7)$$

$$MRR(\Delta t_{row}) = w.{*}\,\Delta t_{row} + v \qquad (8)$$

An equation that represents each *MRR* profile was derived from the profile plots as either a linear function or a constant. Equation (8) represents the linear function where *w* and *v* are associated constants per feature and $MRR(\Delta t_{row})$ is the *MRR* value as a function of the Δt_{row} indices. Equation (4) is the global feature expression while Equation (8) is the local expression in order to account for the statistical approach of finding infinitesimal points. Referring back to Figure 14, an inclined line and a flat line indicated variable or constant *MRR*s, respectively. The $MRR(\Delta t_{row})$ values were substituted into the modified specific energy model from Equation (3) for multiple indices. The specific energy model became a row vector of $E[MRR(\Delta t_{row})]$ with *N* indices which was an array multiplied (.* = Matlab syntax) with the corresponding $MRR(\Delta t_{row})$ values and the sample time size, Δt, to obtain an average predicted energy row vector, E_{sum}, with *N* indices. E_{sum} indices were then summed in order to obtain the final energy prediction value, E_x, per feature.

$$E_{sum} = E[MRR(\Delta t_{row})].{*}\,MRR(\Delta t_{row}).{*}\,\Delta t \qquad (9)$$

$$E_x = \sum E_{sum} \qquad (10)$$

The steps above are also applicable to constant *MRR* sections but made significantly easier since the *MRR* profile is given as a constant. Equation (11) represents a more summarized form of the steps explained above where the constants *k* = 1556 and *b* = 1.475 are kept from Equation (3) [49].

$$E_x = N * \Delta t \sum_{i=i}^{N}\left(k + b * MRR_{avg,i}\right) \qquad (11)$$

The same formula was used to calculate the energy predictions for all nine features in the design and compared with the actual values obtained from the six trials.

Section 2 Tool path [32]

The collaborative tool path project was conducted such that the newly proposed connectivity algorithm was tested through empirical studies. Energy consumption was measured with Yokogawa power monitoring equipment in order to determine the aggregate energy consumption value for various tool paths as delineated in the subsequent subsections. Please note, this entire section references a previous report written for a graduate level precision engineering course. Please refer to [32] for additional information as some details relevant to the specific purpose of this individual project are neglected for the purposes of this thesis.

Section 2.a. Tool path comparison
Section 2.a.i. Bear design

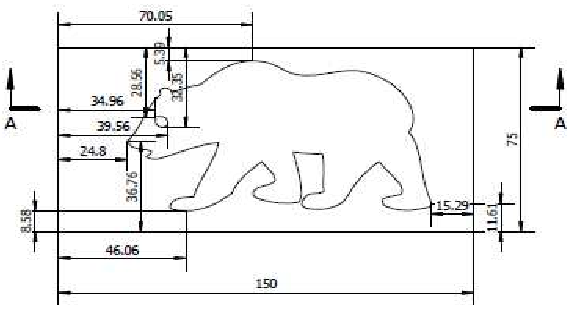

Figure 16: Bear design schematic [51]

Section 2.a.ii. Optimized connectivity algorithm
Section 2.a.ii.A. Vector field generation

The aim was to generate a vector field such that the streamlines within the vector field were coherent. This required the boundary to be aligned through streamline connections that enabled a low curvature. This was challenging since several vector fields limited the cohesiveness of the streamline connections. This was ultimately resolved by relaxing the requirements for the vertex connectivity to allow for a higher tolerance of coherence and curvature.

Section 2.a.ii.B. Streamline generation

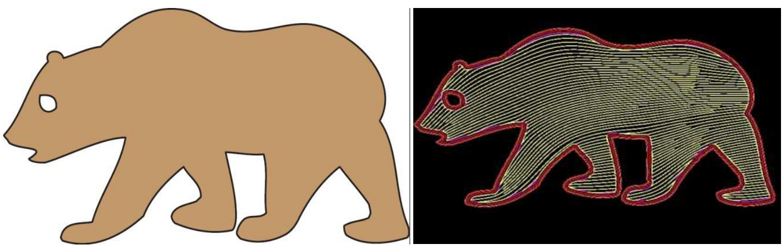

(a) (b)

Figure 17: Bear tool path generation (a) Raw, (b) Streamlined

Once the vector field was generated, the birth points were chosen for new streamlines. As new streamlines were being generated, any points within a fixed distance from the previously generated streamline vertices were chosen as the new birth points for the subsequent streamline. The very first set of birth points were considered to be those near the outer boundary of the vector field. This enabled the algorithm to generate the particular geometry as accurately as possible. A limitation was set in the birth point determination algorithm where the most desirable birth point candidate was determined based on the following criteria in order from most to least importance:

- The birth point candidate to outer boundary distance was shortest
- The birth point candidate to nearby streamline distance is shortest
- The birth point may cause a sharp turn of the tool path if combined with any future birth candidate points

Section 2.a.ii.C. Connectivity data structure

The proposed connectivity algorithm was based on a more traditional optimization problem called the Traveling Salesman Problem (TSP). The intention of this study was to reduce the total tool travel distance by finding the shortest travel displacement possible between the starting and ending coordinates. The TSP was modified to create a Modified TSP (MTSP) version for the particular tool path project. In both the TSP and MTSP, each node was considered to be analogous to the “birth points” or “vertex” of the newly generated streamlines from the previous section. The distance between each vertex was considered to be the cost of travel. Figure 18 portrays the MTSP approach. The streamline generation and the connectivity algorithm were conducted simultaneously in reality since the MTSP used the cost (distance) optimization approach in combination with the three criteria introduced previously for finding an optimal birth point.

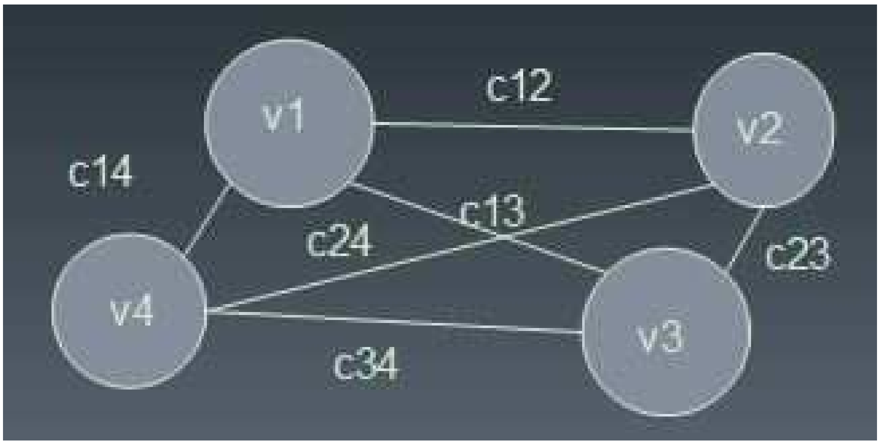

Figure 18: TSP connectivity diagram [50]

Section 2.a.ii.D. Measurement

Other than the newly created tool paths using the EETs created by the proposed MTSP algorithm, tool path CNC codes were generated and submitted to the machineshop for milling and in-process monitoring of energy consumption. These codes were generated using ESPRIT except the EET CNC codes. In the EET cases, the tool path was simulated using a software called NCSim for validation purposes. Air cuts were tested in order to calibrate the Yokogawa power meter's sampling rate in accordance to the experimental design. The aggregate energy consumption values for each tested tool path were derived in order to compare performance.

Section 2.b. Chord error comparison

Chord error, e_r, can be predicted analytically using the following equations based on Figure 7:

$$e_r = R - Rcos\left(\frac{\alpha}{2}\right) = r\left(1 - cos\left(\frac{\alpha}{2}\right)\right) \quad (12)$$

where *R* is the radius, α is an angle. For any angle β, when β is very small,

$$cos\beta \approx 1 - \frac{\beta^2}{2} \quad (13)$$

One can combine Equations (12) and (13) to derive

$$e_r \approx \frac{R*\alpha^2}{8} \quad (14)$$

Therefore, since the error was concerned with the radius and the angle α, it was proved that either a large radius, *R*, or a large angle α would generate a large chord error.

In cases where α is very small it could be approximated such that [33]

$$\alpha \approx \frac{P_i P_{i+1}}{R} = \frac{F_T}{R} \quad (15)$$

$$e_r \geq \frac{{F_T}^2}{8R} \quad (16)$$

where *P* is the vertex coordinates of the chord line from Figure 7 and F_T is the feed rate. If the feed rate were high at a relatively sharp corner (i.e. small radius of curvature) the chord error would be higher. Thus, if the feed rate is held constant when machining a curve with sharp corners it will degrade accuracy. As aforementioned, these values will be predicted for three different input parameters. The feature radius, *R*, can be estimated from the input geometry.

Section 2.b.i. CAM default

The critical variable feed rate, F_T, was the value automatically selected by ESPRIT for the particular tool radius chosen. Other tool paths were chosen to be Figure 9 (a) and (d) (from Chapter 2, Section 2.b.iv.) due to the relatively lower energy consumption value from [33].

Section 2.b.ii. Energy optimized

At the time of project execution, the feed rate, F_T, was chosen for the optimal energy value based on the specific energy curve generated by Diaz et. al. [44]. Since the specific energy curve was plotted based on the *MRR*, it was possible to extract the feed rate from the optimal *MRR* value along the x-axis interpolated with the specific energy y-axis and the *doc* and the *woc* equal to the tool radius of the process.

Section 2.b.iii. Direct

The chord error was predicted for the proposed tool path based on the feed rate found from the aforementioned equations as an analytical prediction. Due to resource limitations with laboratory equipment at the time, the chord error was assumed to be accurate without the use of empirical measurements. For the purposes of this thesis work, since it was assumed in the introduction that all products are made to a certain level of integrity, it will be neglected as a potential source of major error. The error itself, however, will be mentioned in Chapter 5, Discussion, in order to address any future avenues of improvement.

Section 3 Process

The process level consists of projects such as the production cell energy assessment, process utility consumption, and machine utilization with the Autodesk Process Analysis 360 software

Section 3.a. Production cell energy consumption (PCEC) [52]

This section underlays the code methodology that filtered the power data for numerous processes through multiple in-line loops in order to create a "produced part" matrix. Each "produced part" matrix represented a single process whereby accurate time data was extracted for each part matrix. The part matrices were consolidated into a cell matrix in order to examine any selected process.

Section 3.a.i. Setup

Using a comma separated value extension (.csv) editor called CSVed, the given power data file was organized for easy import of the time and corresponding power values. Since the MTConnect time standard was used as the company's acquisition method, the same 24-hour scale was considered to sort the time data. These were imported into Matlab where each time entry was converted in terms of seconds with a maximum value of 86400.000 seconds for the 24^{th} hour. Furthermore, an overall matrix was constructed with two columns consisting of each time entry and its associated power values for filtering purposes.

Section 3.a.ii. Power filter

In order to filter the power values, minimum and maximum power threshold values were found using blocks of actual data sets. A stable state (*SS*) power value of the machine was found first in order to differentiate process and standby times using general index counters and virtual *SS* meta-counters to indicate the specific indices that correlated to the beginning and end of a process. Table 1 shows an example of raw power, counter, and meta-counter matrices using proxy data for one process.

Power Proxy Data [W]	Counter	Meta-Counter (virtual)
3	1	1
4		
5		
6		
7		
7		
3	7	2

Table 1: Example counter matrix construction using proxy data

Considering 3W as the *SS* value, Counter gives the index value of 7 for the second 3W but the Meta-Counter indicates the second 3W as index 2. The power values were rounded to the nearest integer in order to simplify the computation. Although it may seem as though this will potentially trim useful data, 3W was considered *SS* only if it was consistent for a few data points. Hence, the rounding should only cause minimal errors. Working from the higher to lower level, the filtration procedure was now narrowed to individual processes. Using the power values in between the first and second *SS* values, a “virtual part” matrix was created for a single process. In cases where the data acquisition was stopped before completion of the part fabrication, the matrix was considered invalid and nullified due to insufficient data. An exception to this rule was a temporary break within the job with clear indication of a resumed job; in other words, although the acquired time is not continuous, the power data seemed consistent with other tested part processes. This exception will be explained later as part of the final filtration loop.

Given that any single process must contain a peak power output above the *SS* value, the “virtual part” matrix underwent another loop filter that checked for peak power values. As aforementioned, a failsafe code was also implemented to compensate for data flaws. In Table 2, one can see an extended version of Table 1 where the second 3W resides a few data points before a continuous set of 3W values.

Power Proxy Data [W]	Counter	Meta-Counter (virtual)
3	1	1
4		
5		
6		
7		
7		
3	7	2
4		
4		
4		
5		
3	12	3
3	13	4
3	14	5
3	15	6

Table 2: Extension of Table 1 with continuous *SS* values

Until this point, the “virtual part” matrix was only based on single *SS* values that may represent the beginning and end of a process that has peak power outputs. Unfortunately, because of inconsistencies and uncertainties that exist in machine tools, it is possible to have multiple data spikes or dips that may lead to loss of accuracy in the data analysis. In order to minimize this, it was important to verify if this matrix was a “potential part” via a continuous *SS* values test on top of a single ending *SS* value test.

Another source of error was detected to be data that represented incomplete processes. Even with the above filtration steps, certain data sets may still be considered as a “potential part” as long as they pass the above rules even if the total cycle time was significantly less than the factory’s intended 20 seconds. These were named as “ghost parts” as they were “potential parts” which seemed like a real part, but was an incomplete part. Lastly, as introduced earlier, since a specific process may have had a job break where the time is split, but with consistent power trends, a power trend test was performed on these “ghost parts”. All “virtual parts” that passed the above filters were considered “produced parts” and restructured in a cell matrix. These were used to obtain more accurate process time data based on the beginning and ending *SS* values.

Section 3.a.iii. Process time extraction

Time extraction was performed for three categories of single process power data:

- Continuous
- Date change
- Temporary stop/resumption

The first bullet is the most intuitive data set where a single process was performed under normal conditions during its operation. An example of a continuous data would have a process that started at 46000.012 seconds and ended at 46018.560 seconds. The majority of the data were such data sets which involved a simple subtraction to compute the process time. The date change data indicated a process that bridged a date change hour. Given a maximum time of 86400.000 seconds for the 24th hour, a process may have been started at 86397.567 seconds and finished at 00015.123 seconds. A simple subtraction for these types of data would yield a negative time value which is extraneous. For this reason, the calculation was split as an addition of values indicating the daily maximum time minus the process start and the daily minimum (00000.000 seconds) plus the process finish. Similarly, the last category was also found by an addition of before and after the break, but underwent an extra filtration to extract out the break time within the process. The extracted process time and power data were then used to determine the factory's performance relative to their intended total cycle time and the resulting process power output.

Section 3.a.iv. Programming logic

The programming logic is shown as a flow diagram for the previous Section 3.a. subsections:

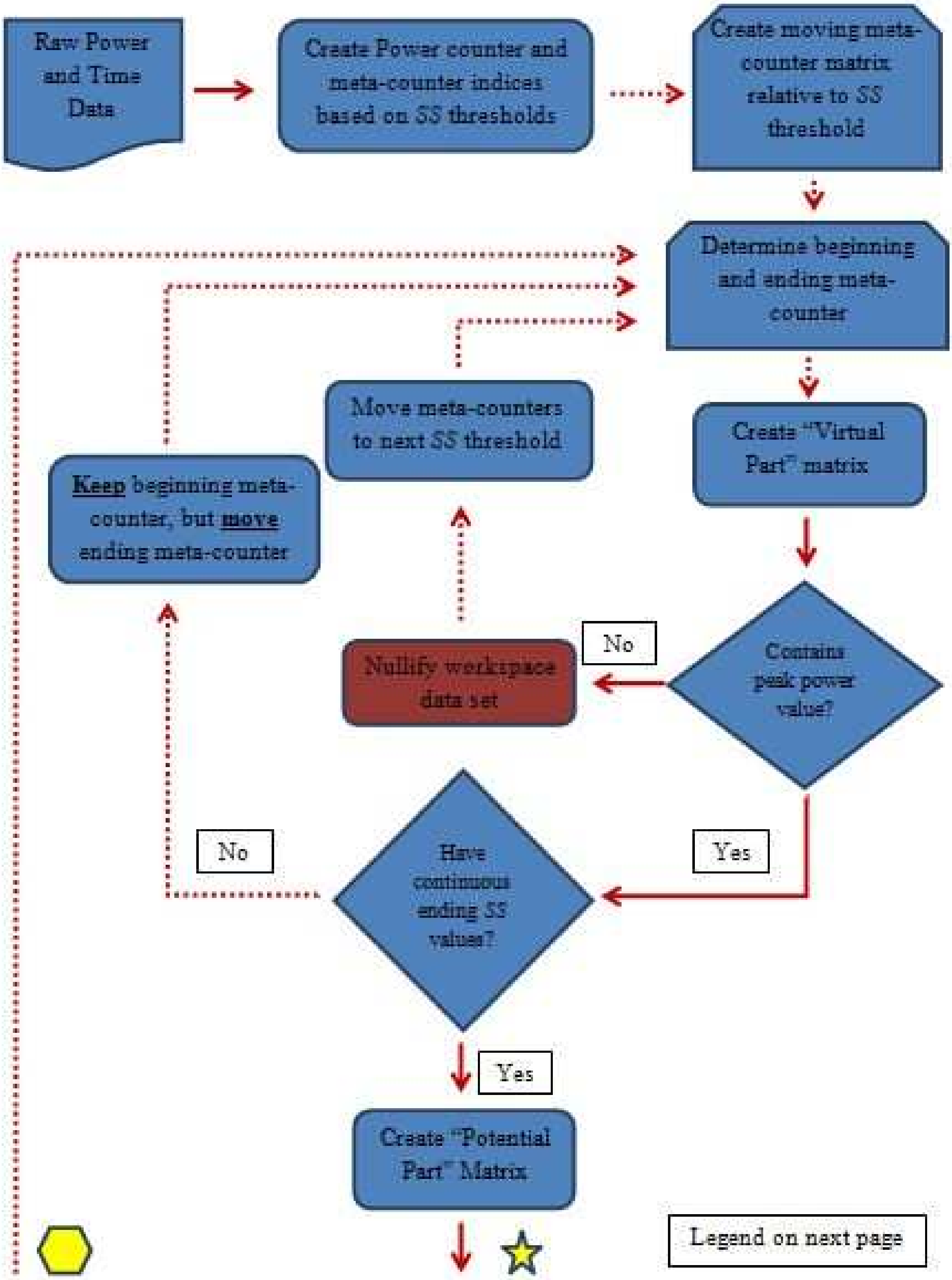

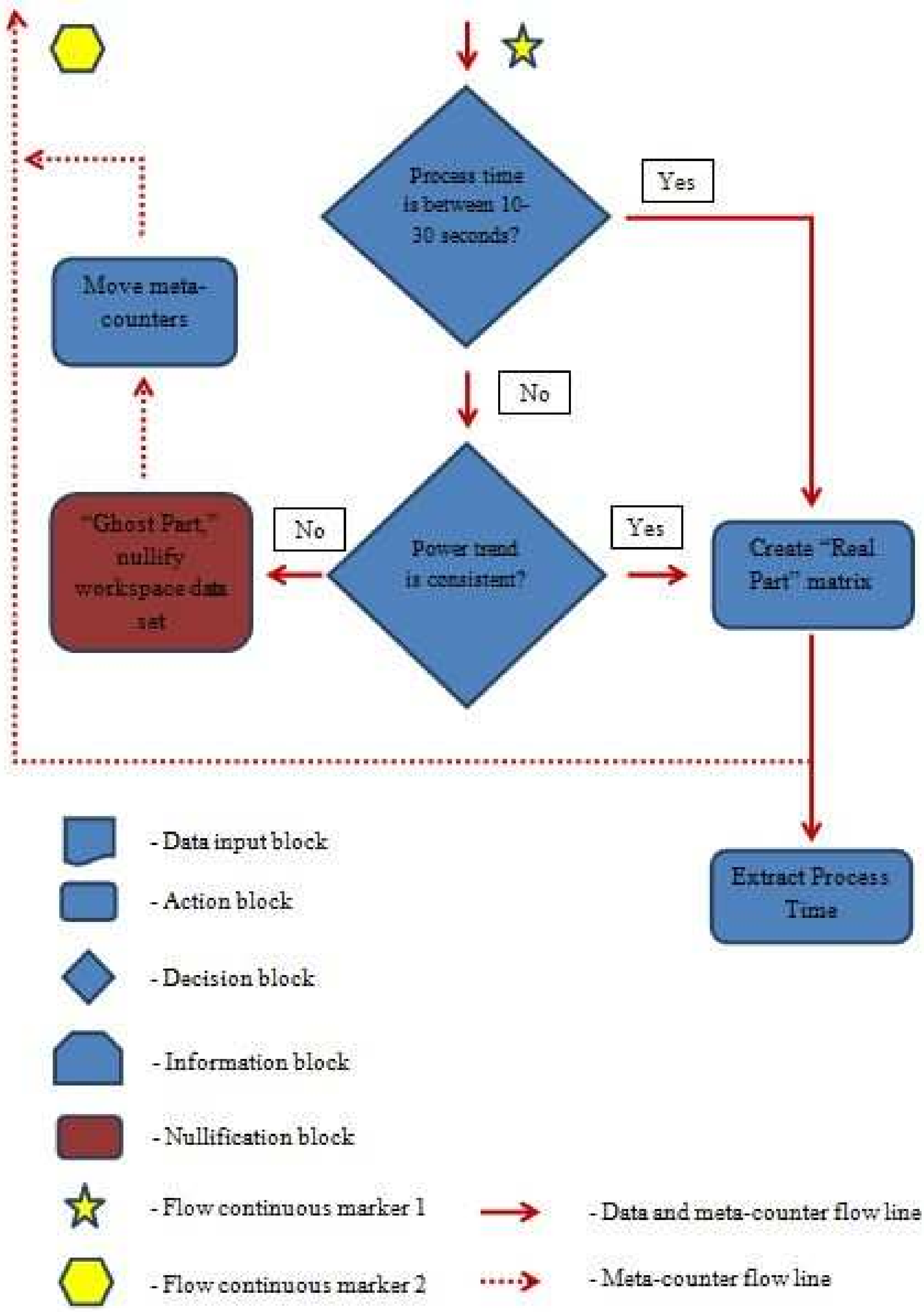

Figure 19: Programming logic for PCEC

Section 3.b. Process I/O stream (PIOS) [53]

This project was a part of an ongoing effort for a software company to identify a process stream for multiple industries. This thesis will focus on the Food Processing Industry due to the data availability and the author's task.

Section 3.b.i. Industry identification

Due to the high dependency on data, it was essential to find an industry that had an abundant amount of data available. Example industries that were initially planned for investigation included automotive, packaging, petroleum, textile, wood, shipbuilding, food processing, and railroad. Out of these industries, the food processing industry was chosen due to the data availability for a variety of products and processes involved.

Section 3.b.ii. Product identification

After an optimal industry was identified, several products were identified based on the fitness to the purpose of the study. The study's objective was to capture an overall trend of the particular industry. Factors such as generic process chains and estimated line energy based on process specifications were considered. Products within a similar sub-category such as orange juice and milk were chosen in order to consider any similarities or differences as well.

Section 3.b.iii. Process chain identification

Please refer to Chapter 3, Section 4.b.

Section 3.b.iv. Process identification

Processes would have been identified with the process chain identification at this stage. In order to understand the process I/O stream, a specific format was established. The material and utility input, value-added output, and waste were identified to the level of data availability. When available, the utility maximum ratings were reported.

Section 3.c. Machine utilization (MU) [22]

The optimal utilization of a machining process can be a key driver of the overall operational efficiency. Operational scheduling depends on reported schedules of each process. Machine utilization can have categories such as process, idle, setup, blocked, and downtime [22]. Machine utilization can be used to save energy by enabling users to improve individual unit cycle times. The Autodesk Process Analysis 360 software was employed for this study. Please note, the project for this particular sub-section is separate from the process I/O stream sub-section.

Section 4 Assembly line/process chain

Section 4.a. Process chain identification (PIOS Plus) [53]

After the desired products were identified for the particular industry, process chains were sought for each of the products. Since the purpose of the study was to identify a generic process chain, more than one process chain was sought for a single product. The more sophisticated process chain was chosen over the others. The process chains for different products were compared in order to derive a generic process chain for the industry, which will be presented in the next chapter.

Section 4.b. Line utilization (LU) [22]

Similar to Chapter 3, Section 3.c. a process analysis was to be performed for each process within a process chain. These would then be displayed as a chain in order to derive the line energy consumption and identify any energy loss points within the process chain. If the energy loss root is obvious at this level of data granularity, then further granularity is unnecessary. However, most energy loss causes tend to be less obvious, which is why an energy loss identification method through an energy audit was proposed to investigate facility and supplier production operations using a high granularity of data.

Chapter 4 Results

Please see subsequent, respective chapter and sections for figure descriptions and discussions.

Section 1 Parameter

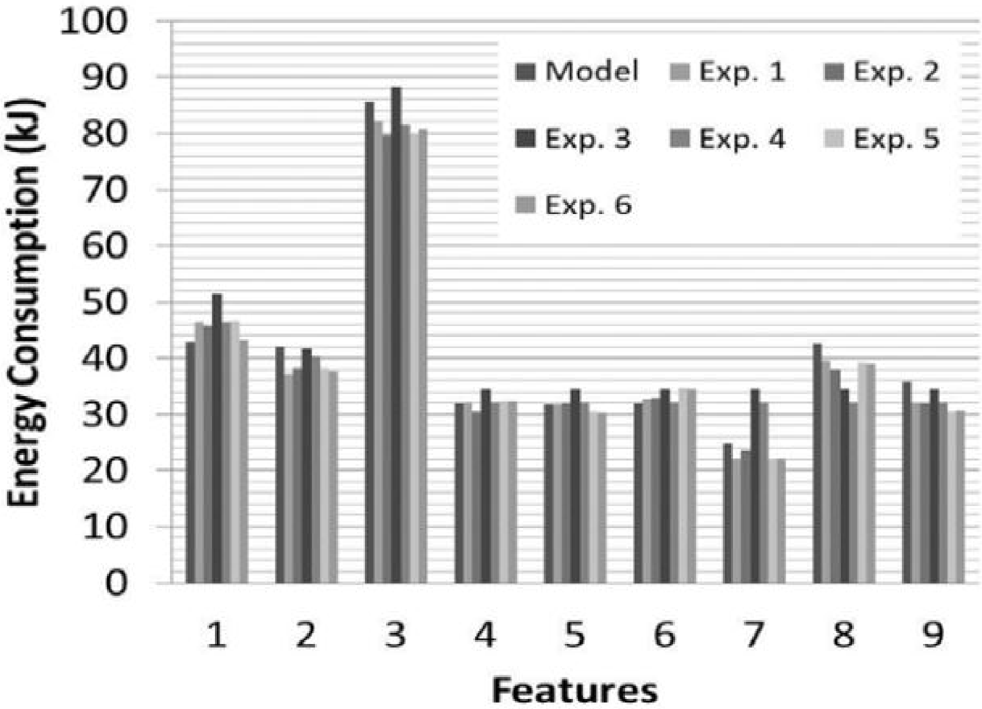

Figure 20: Energy consumption for predicted model and all experiments with 97.4% confidence

Section 2 Tool path

Figure 21: Raw surface finish for all four tool paths

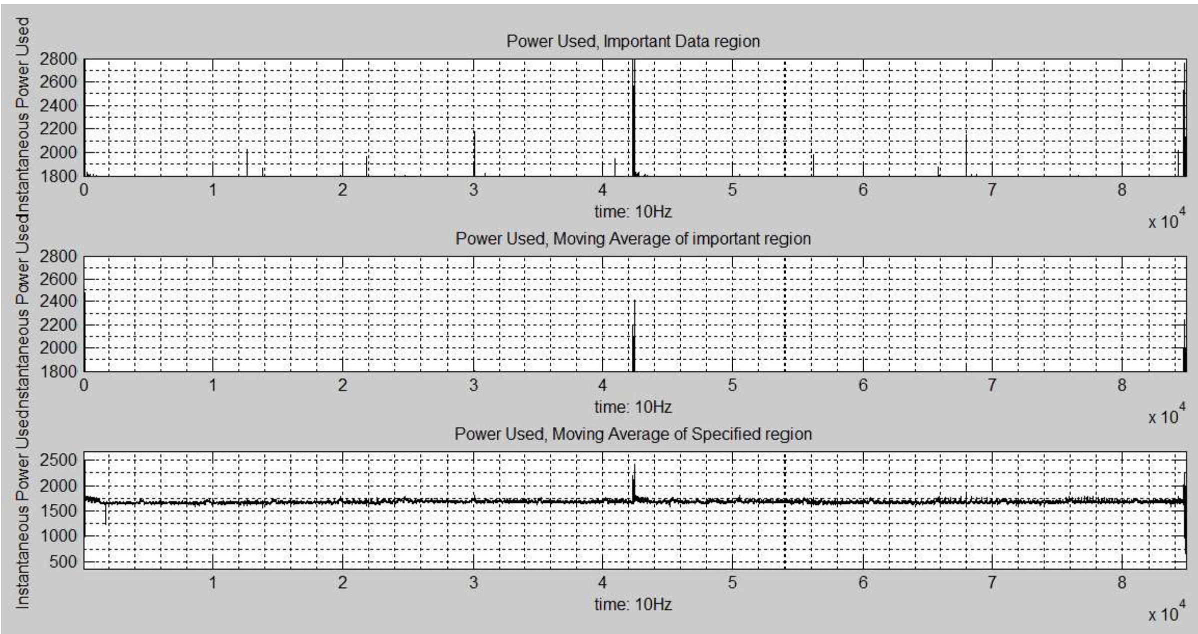

Figure 22: Contour-in data

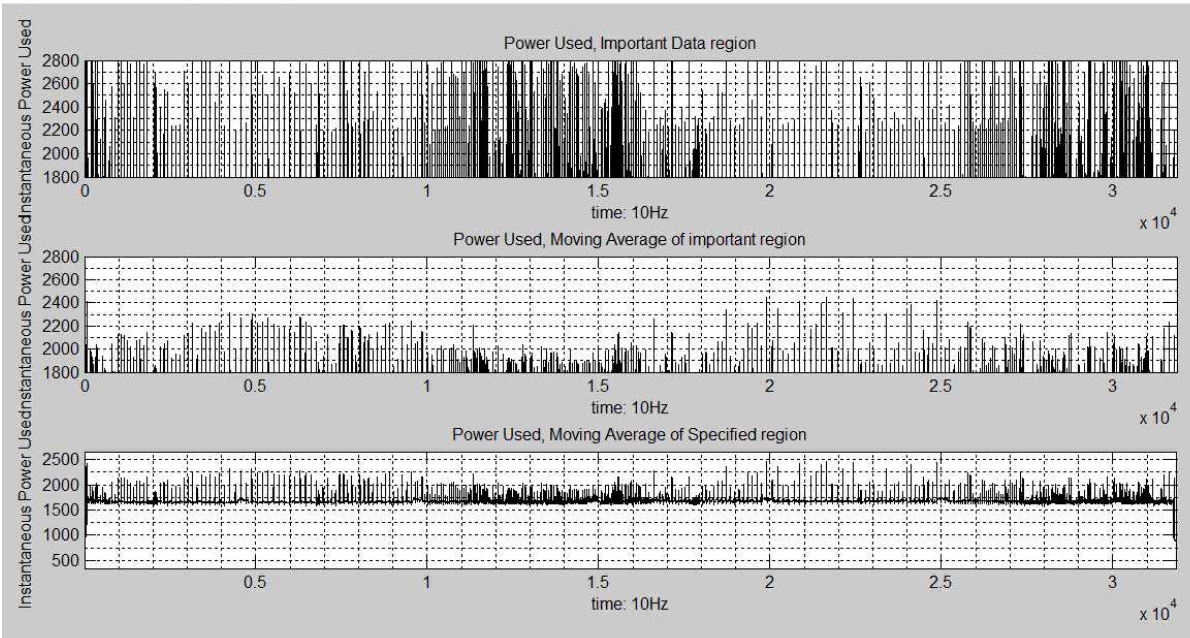

Figure 23: X-direction data

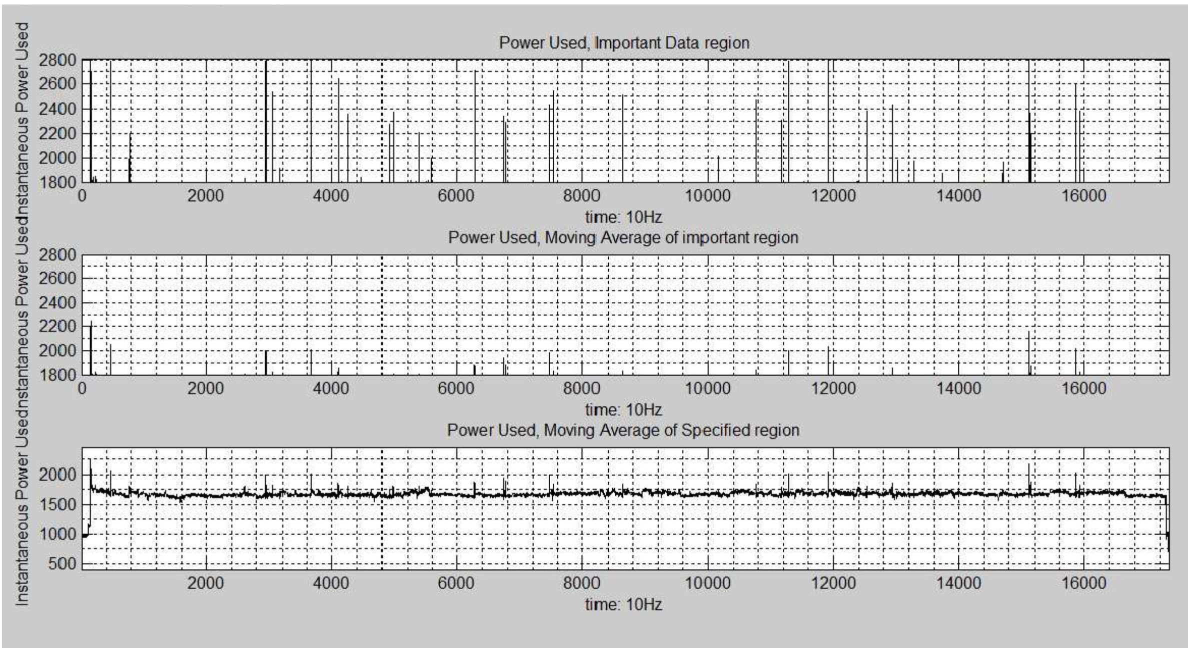

Figure 24: EET data

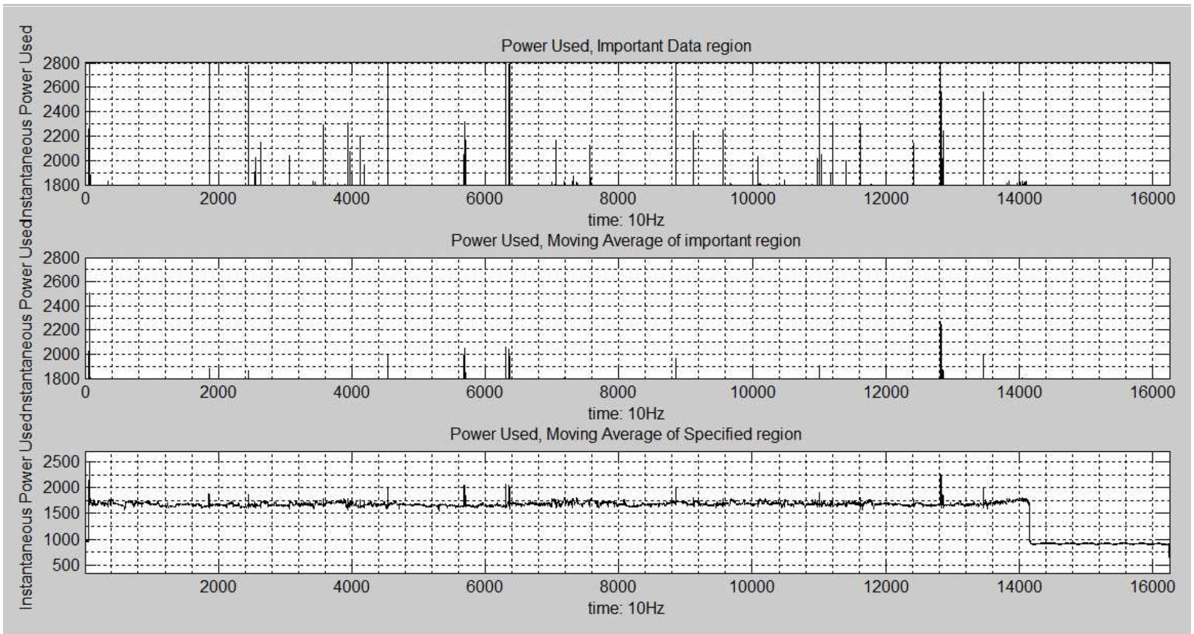

Figure 25: Optimized EET (OEET) data

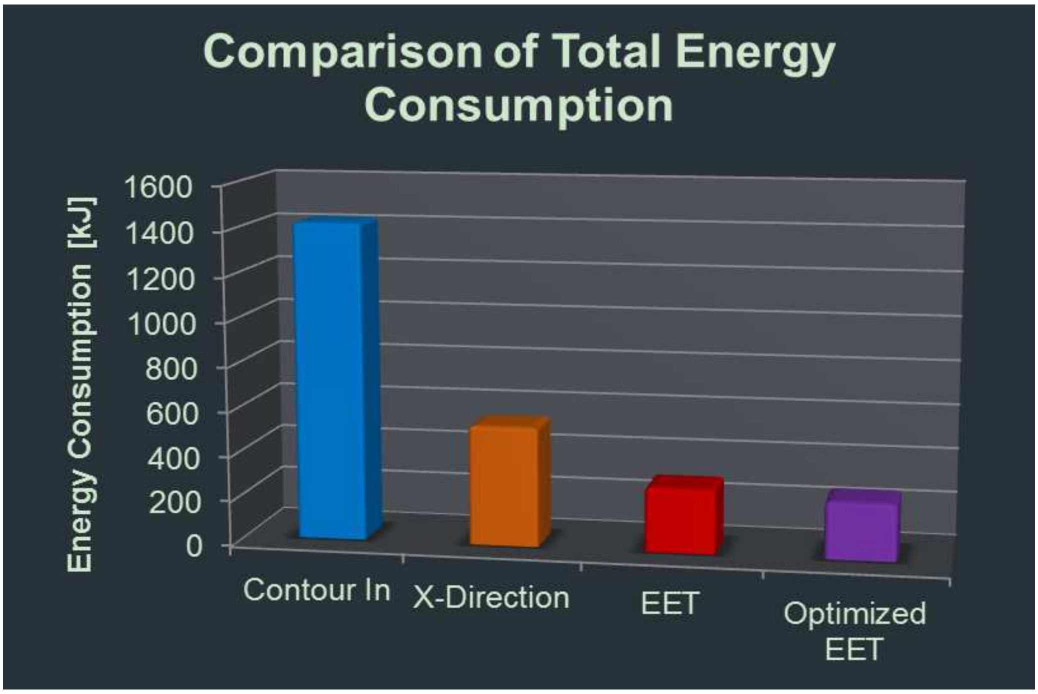

Figure 26: Total energy consumption comparison

	X-Direction	Contour In	Both EET
L [mm]	1.67	0.45	0.57
S [mm]	1.70	0.45	0.57
R [mm]	2.61	1.11	2.45
Θ [rad]	0.65	0.42	0.23
ε_r [mm]	0.134	0.022	0.073

Table 3: Chord error prediction parameters

	Total cycle time, T [mins]
Contour In	112
X-Direction	47
EET	28
Optimized EET	27

Table 4: Total cycle time per tool path

	Energy, E [kJ]
Contour In	1424
X-Direction	537
EET	289
Optimized EET	257

Table 5: Total energy consumed per tool path

	Chord error, ε_r [mm]
Contour In	0.022
X-Direction	0.134
EET	0.073
Optimized EET	0.073

Table 6: Predicted chord error per tool path

	Material Removal Rate, *MRR* [mm^3/min]
Contour In X-Direction	480
EET	1910
Optimized EET	2254

Table 7: *MRR* involved per tool path

Section 3 Process
Section 3.a. Production Cell Energy Consumption (PCEC) [52]

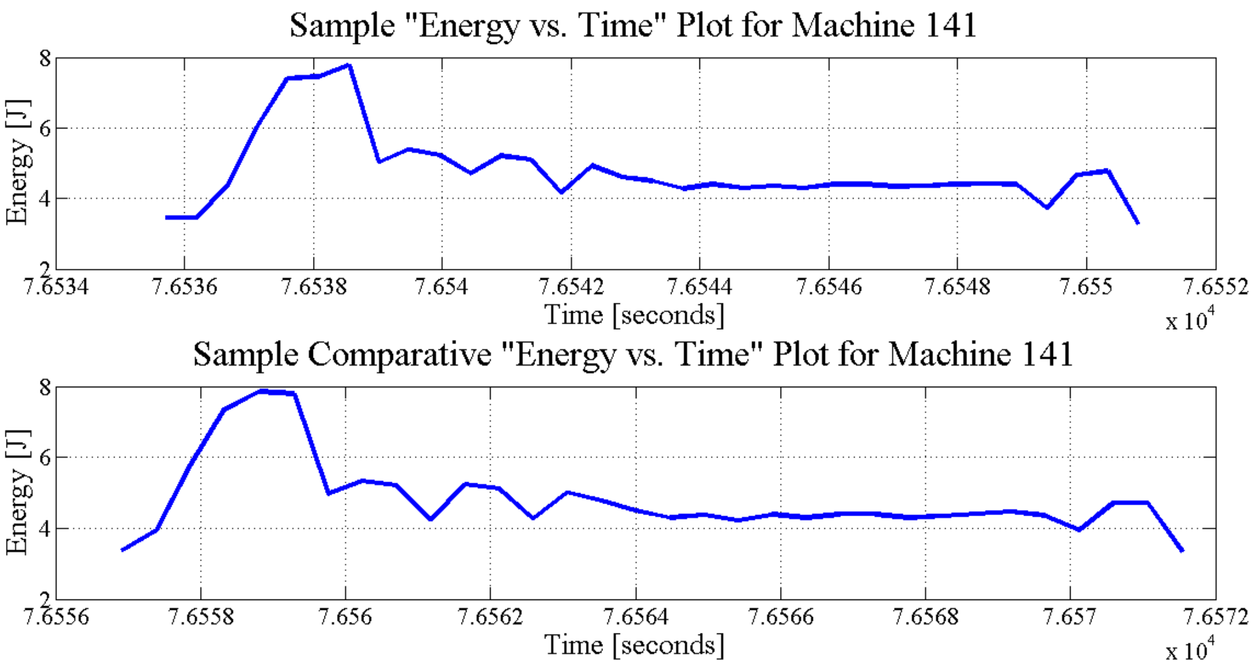

Figure 27: Machine 141 sample energy consumption

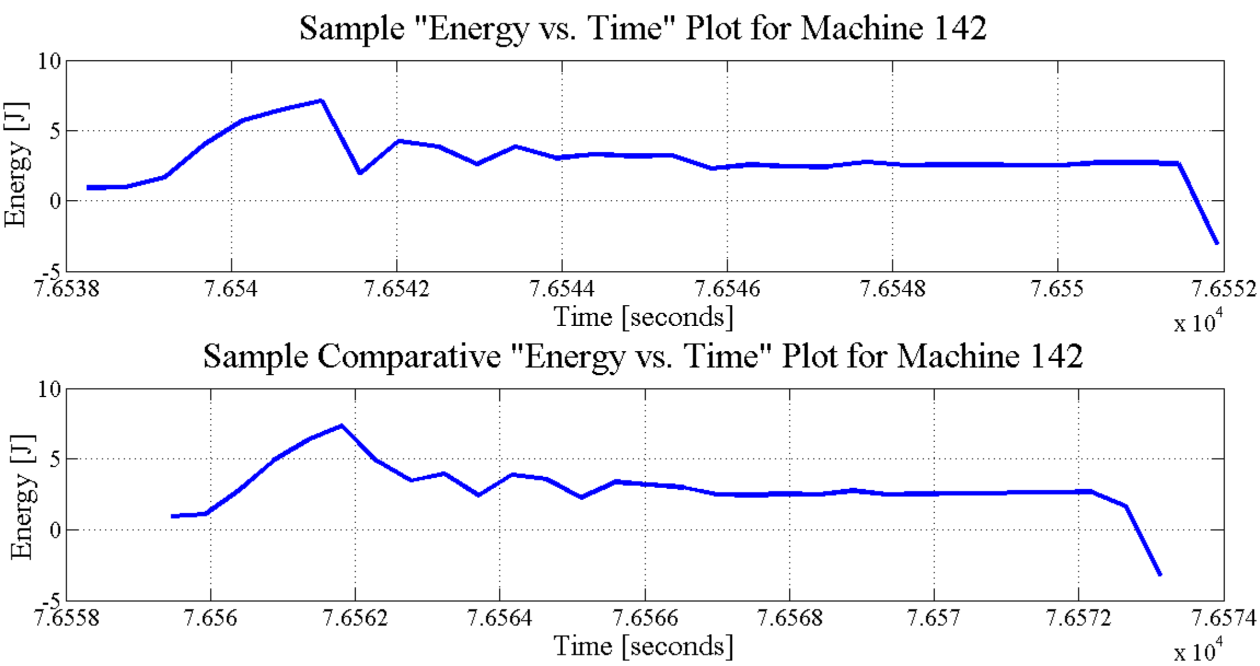

Figure 28: Machine 142 sample energy consumption

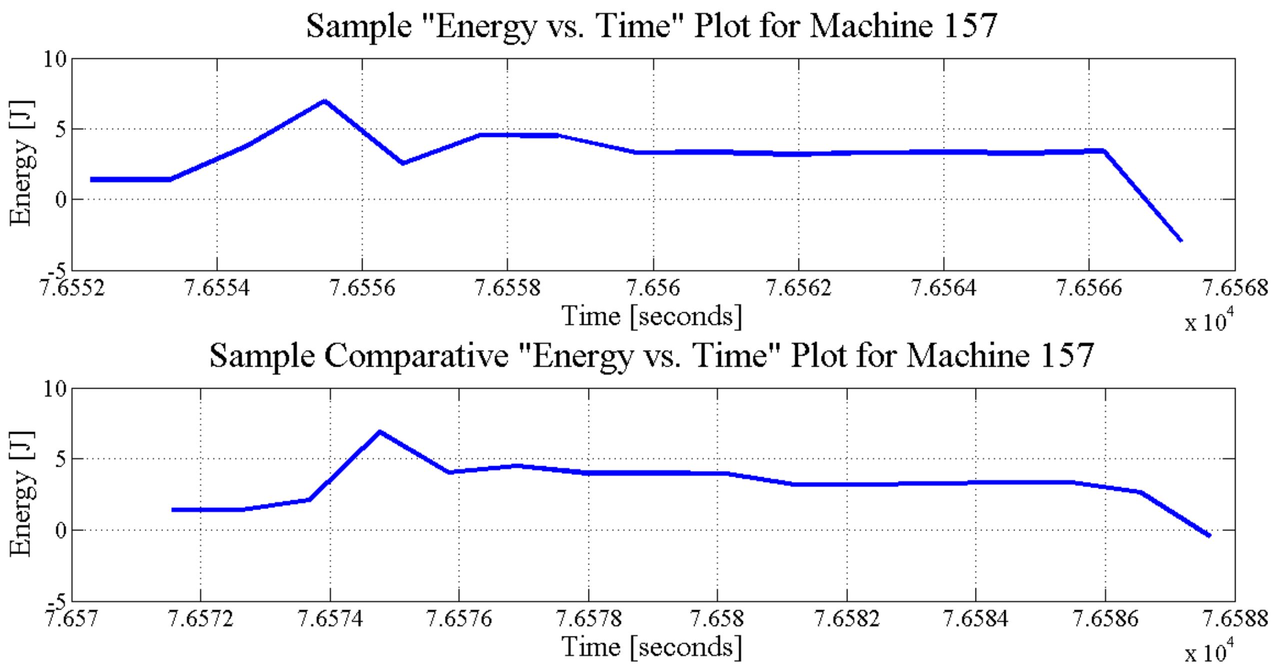

Figure 29: Machine 157 sample energy consumption

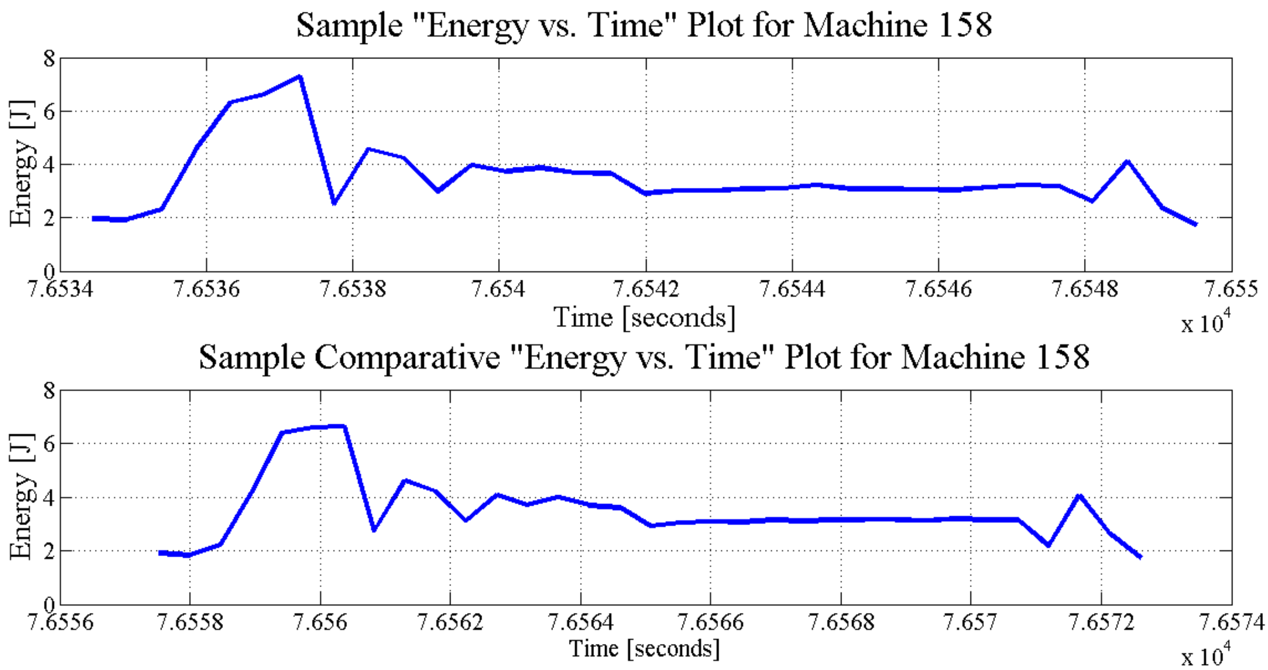

Figure 30: Machine 158 sample energy consumption

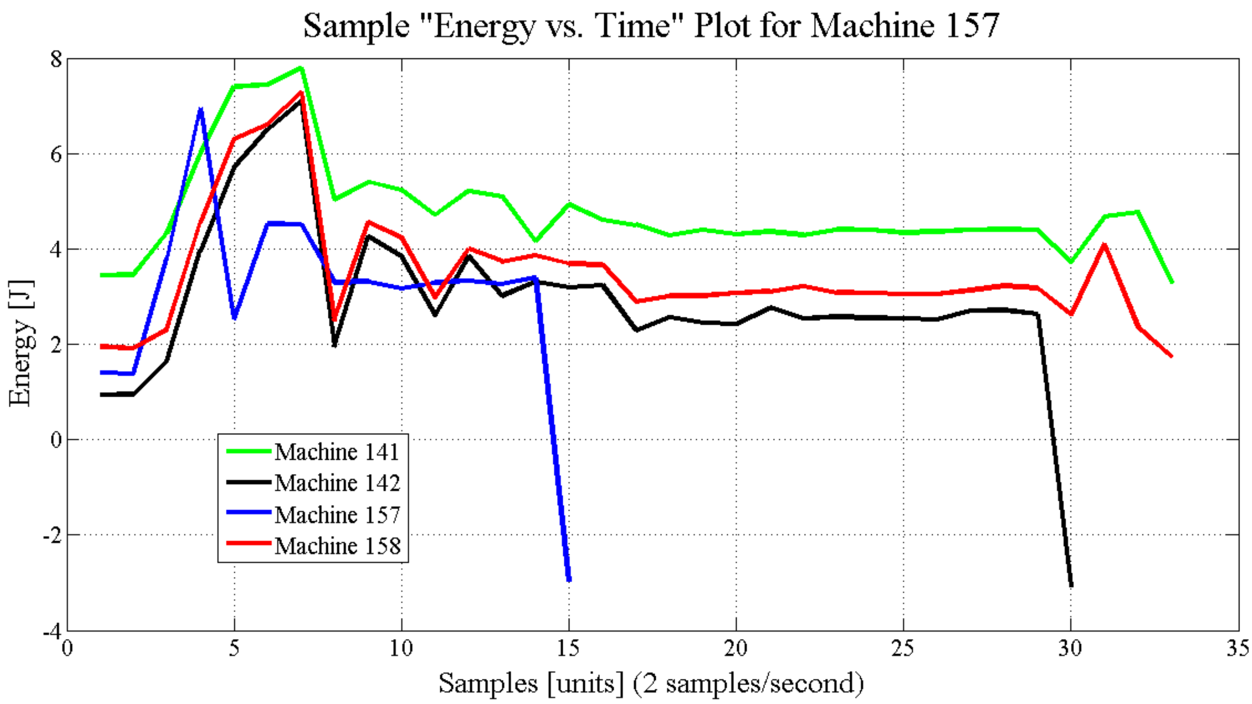

Figure 31: Comparison of all machine using sample data sets

Section 3.b. Process I/O stream (PIOS) [53]

Please refer to Appendix B for more processes

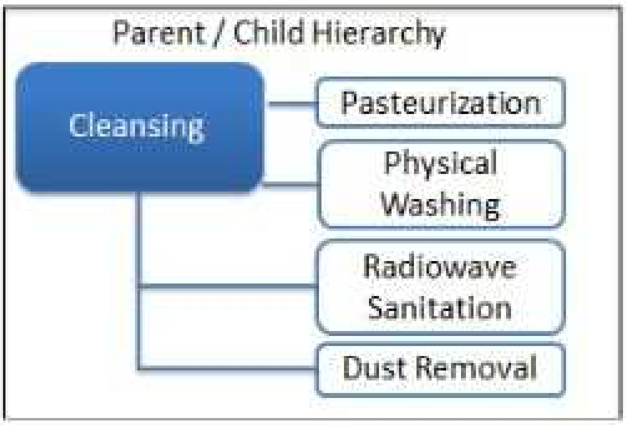

Figure 32: Sample parent/child hierarchy for a cleansing process

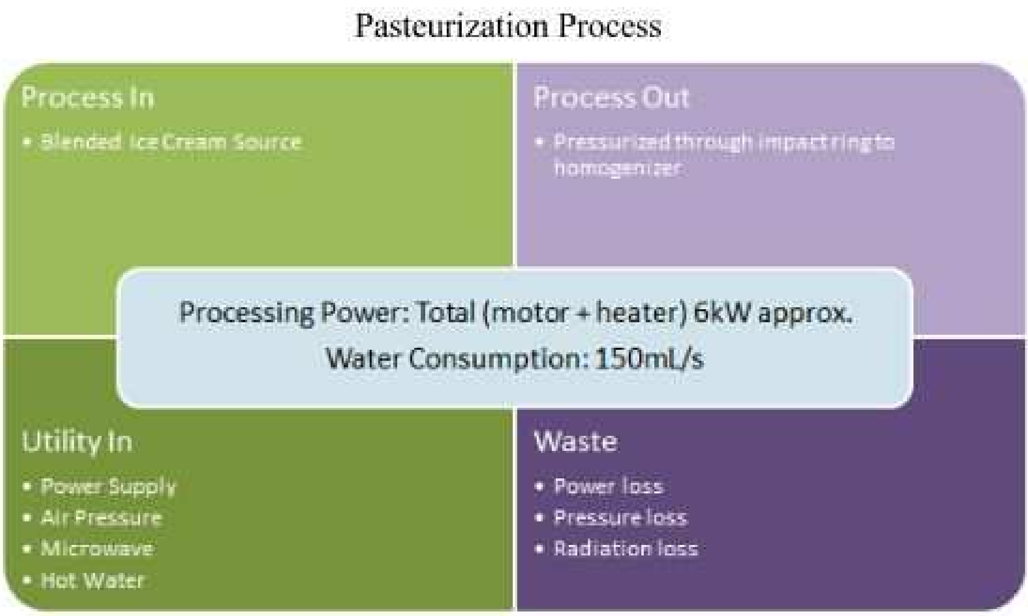

Figure 33: Sample process input/output stream for a pasteurization process

Section 3.c. Machine utilization (hypothetical values) (MU)

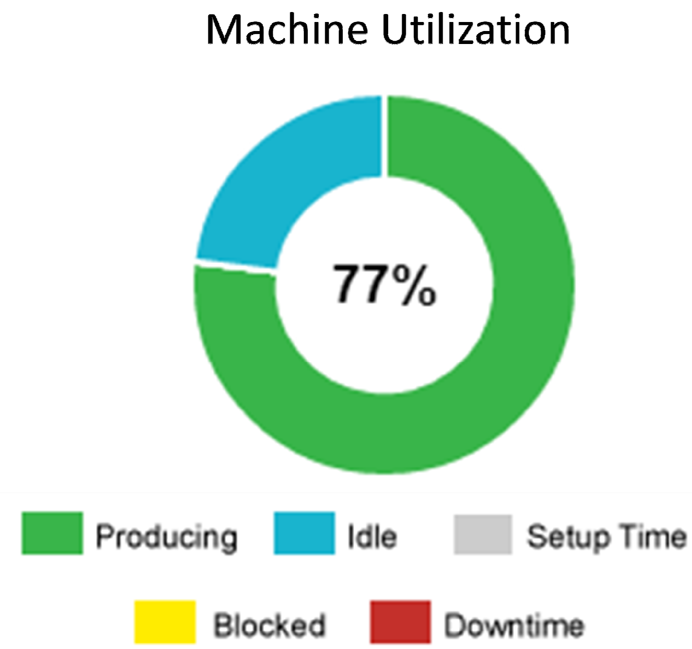

Figure 34: Sample machine utilization visual [22]

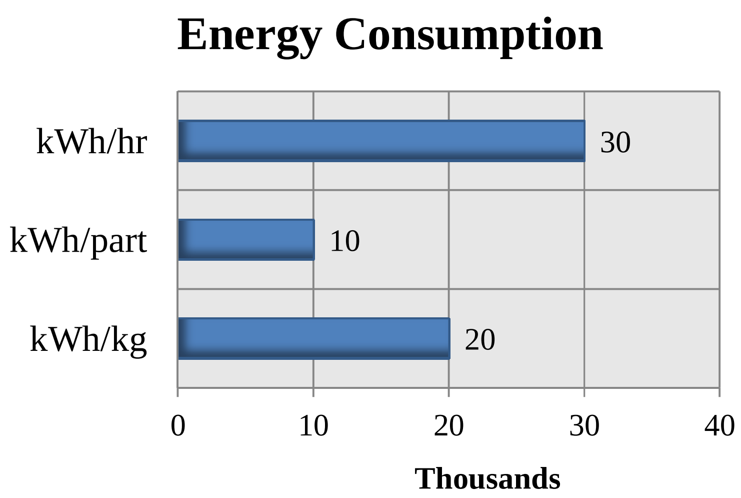

Figure 35: Sample energy consumption diagram with functional units [22]

Section 4 Assembly line/process chain

Please refer to Appendix C for more process chains

Section 4.a. Process chain identification (PIOS Plus) [53]

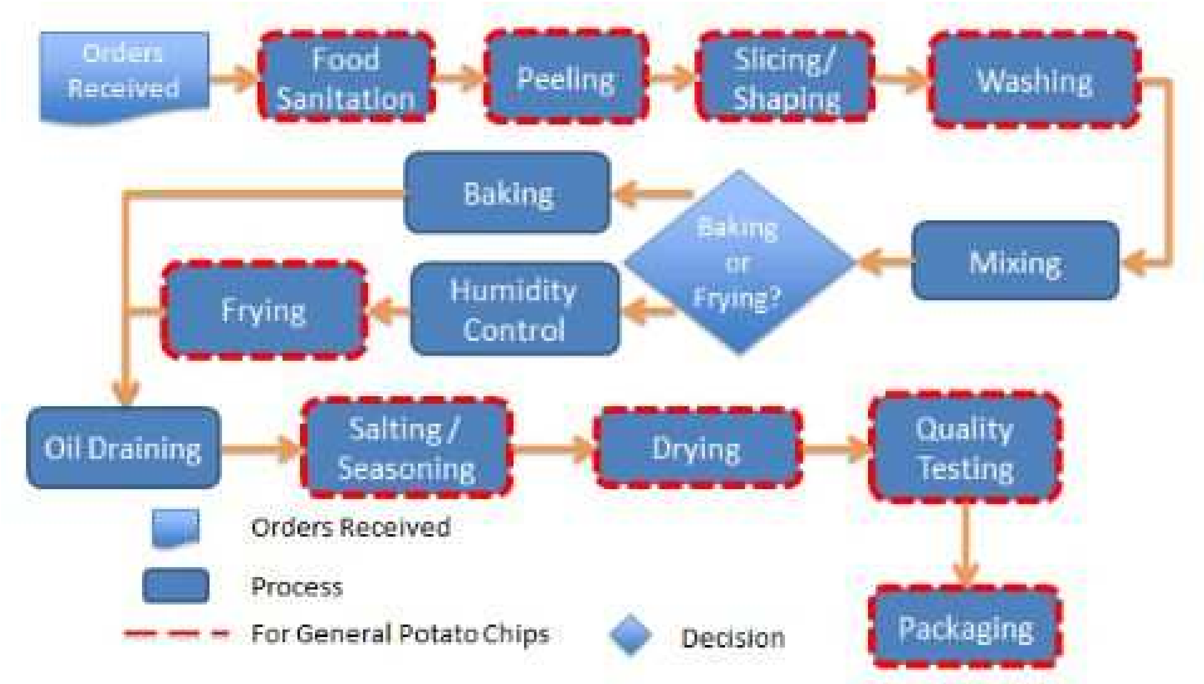

Figure 36: Sample process chain for a potato chip

Section 4.a. Line Utilization (LU) [22]

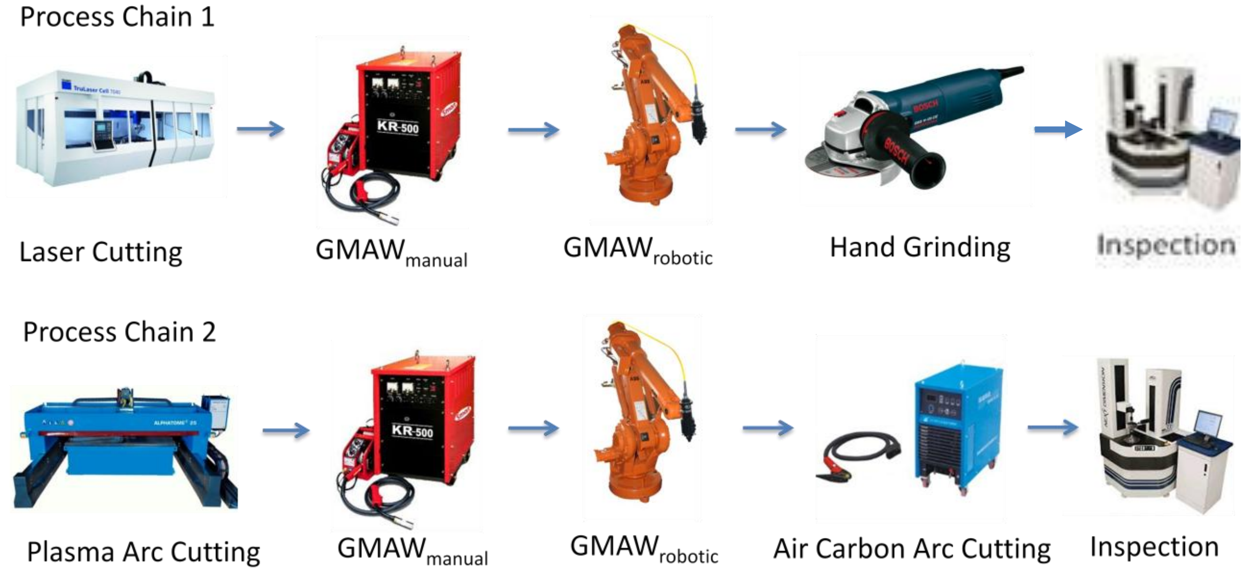

Figure 37: Sample process chain comparison

Process Chain	Energy	Water	Throughput Time	Line Utilization
1	58020 kWh	42 L	28 hrs	75.8 %
2	58003 kWh	40 L	32 hrs	76.8 %

Table 8: Values for sample in Figure 37

Chapter 5 Discussion
Section 1 Parameter [53]

Although the overall accuracy was determined to be very high, some data fluctuation was still observed for the third trial. It can be seen from Figure 20 from Chapter 4, Section 1 that the third trial had outlying values that were much greater or smaller than the values from other trials. This meant that, despite a high accuracy value, the experiment was not quite precise since trial three contained outlying values and led to questionable repeatability of the experiment. However, this was suspected to only be a temporary problem caused by a long machine idle time during the winter recession and a short warm-up cycle of the machine tool following it. Since the coolant was on at full throttle during all experiments, no coolant/lubrication issues were suspected. For this reason, it is recommended that all experiments during the energy data acquisition should be more closely monitored such that machine tools are maintained and warmed-up in a consistent manner to avoid data outliers.

The parameter level data is the most important in attempting to make a larger impact during this proposed energy audit procedure. The continuous monitoring and auditing process is also a vital component to this method when a parameter is changed for any reason. Examples when a parameter maybe changed is during changes of the product, line reconfiguration with existing and/or new process machinery, or changes in operation schedules. For each of these examples, it is highly likely that parameters must be changed in order to meet the demand and requirements of the production system. However, it is important for manufacturers to closely monitor their production facilities and their suppliers in order to stay within compliance and regulatory requirements of their entire enterprise, especially large ones who have a global supply chain base.

In finding an energy characteristic equation for a process, it is recommended to vary the input parameters and configurations as much as possible for a wider coverage of possible manufacturing configuration. For example, one may see that [49] had three variants to find a specific energy based on empirical data. Due to limited experimental time, the particular model was specifically for the application of the 6mm tool as aforementioned in the Methodology section.

The parameter level change is expected to allow a refined, empirical method of suggesting improvements when making energy audits for a facility since it will provide an optimal point using a fitted curve through multiple energy consumption samples for a machine. By building on [49] where they investigated a 2-axis process, this study's focus on a 3-axis process allows potential users to be confident with this method of predicting the energy consumption and making parameter-level changes with a confidence level of 95%. If this level of data granularity is difficult to capture due to the facility or suppliers' circumstances, then it is recommended that the user of this framework examine their system at the next level – Tool path level – to make the greatest impact to their system.

Section 2 Tool path [32]

Overall, the results were as expected where the most time-consuming tool path, Contour-in, showed the highest energy consumption value. The optimized energy-efficient tool path showed the least amount of energy consumption of the four tool paths tested. It is important to note that without the parameter-level data granularity and continuous data monitoring, the next level of data granularity is required to test many variations. This will often take time to measure since each test is a discrete testing procedure specific to the particular tool path with the exact parameters for the exclusive product. In return, this method will cause a slower response time in making changes to the overall energy consumption reduction effort. However, when necessary, this method is recommended and preferred over a more macro-granular auditing level such as the process and process chain level.

One may reasonably guess that, based on past literature, tool paths with less cycle time will consume less energy. However, this statement can only be safely concluded if the parameters are fixed. Based on this methodology, a production enterprise with a machining process can use this approach to generate an energy-optimized tool path in order to manufacture their product sustainably with consideration of precision, mechanistic factors such as chord error. One can easily observe from Figure X that even though the optimized EET achieved less energy consumption values, the non-EET tool paths seemed to have the better surface finish, at least at the macro-level that can be seen by the naked eye (without a microscope). However, even at this level, which is assumed to be relatively granular for the purposes of this thesis, many errors were observed and inferred.

Some possible sources of errors were:

- measurement tool errors such as Abbé error when the work piece was set on the machining table
- Yokogawa power meter errors such as thermal errors due to human proximity and data sensitivity associated with calibration and sampling rate
- machine tool vibration both external and self-excitation causing variation in the energy consumption due to imprecise tool path movement
- algorithmic errors from the streamline generation referenced from UBC and the MTSP approach

Other limitations include the lack of resources to measure chord error, imprecision in placing the work piece onto the table, and that the streamline vector field generation algorithm was proprietary information of the UBC research group. Therefore, alternate streamline generation algorithms were not considered in its generation and only the MTSP method could have been modified, when necessary.

Section 3 Process
Section 3.a. Production cell energy consumption (PCEC) [52]

All machines, overall, performed in-line with the factory's intended total cycle time of 20 seconds. The author's main task in this project was to use energy data in order to describe the process. One way of doing this was by proving that the actual cycle time was within the desired cycle time of 20 seconds. As mentioned above, the processing time was approximately 15 seconds for all machines. If their setup times were intended to be 5 seconds, then this would indicate that they were able to meet their exact production goal with an average peak processing power of 8W per process for each machine. Associated processing energy values, which are proportional to power values for individual machines due to similar trends, can be calculated through integration of power over time for individual processes. Further points of improvement, however, can also be seen. Since the Machine 157 curve was much shorter than the other curves based on Figure 5, it can be concluded that it had a smaller sampling rate. The factory strived for an acquisition sampling rate of 2 samples/second as seen in Machines 141, 142, and 158, but 157 was recorded with a sampling rate of 1 sample/second. This may indicate procedural flaws in data acquisition, which affects the energy performance evaluation.

Furthermore, Machines 142 and 157 had negative power values which were considered to be extraneous; hence, the closest positive value was taken to be the end of the process. Although it is possible to have negative power values based on the acquisition setup, given that the machine and acquisition device setup was the same for all processes, it was also considered as extraneous data caused by procedural and/or possible mechanical flaws inherent within the process. A particular production error could not be identified clearly. One possible error was the power meter itself, but it was assumed that measurement conditions were under normal conditions.

Machines 141 and 158, on the contrary, did not have any negative values, but did show data dips near the end of the process. Machine 158, in particular, also showed power spikes. These dips and spikes could simply indicate machine performance inconsistencies, but may also be an indication that the particular machines are in need of maintenance. Since the dips and spikes consistently existed within the data files for respective machines, it is possible that this could be a service maintenance problem rather than an inherent tolerance of the machine, invalidating the above argument of possible mechanical flaws. If the maintenance cause is deemed true, it may pose avenues of improvement in regards to the factory's maintenance schedule of the machines. With more stabilized data, free of spontaneous power dips and spikes, a more accurate analysis can be made in regards to processing power. However, one can see that the peak power output is near the beginning of every machine. This is one way to confirm that the process and power trends are in-parallel with each other since the initial tool-work piece engagement tends to require the highest amount of processing power for a machine tool. For this reason, the dips and spikes problem may be considered as a minor issue in the bigger picture.

Although not directly relevant to the power vs. time study, it is interesting to see that power values can be used to determine whether a part potentially has failed to complete its entire production cycle or if there was a temporary break during the production. It was apparent that most skipped times occurred around the same timeframe of each day for all machines that indicated, for example, possible lunch breaks or shift changes. This information, however, was unavailable from the data source. There are limitations to the accuracy of this hypothesis, however, since it is difficult to accurately assess the work performance of the factory without knowledge such as holidays and break policies. For example, it is common for automated machines to be unattended while in operation; hence, there should not be any temporary stops during the day caused by worker breaks. However, it may be a factory policy that a machine should be attended at all times. It could also mean that the data acquisition was not set up for automatic assessment, requiring someone to initiate the acquisition process manually.

Section 3.b. Process I/O stream (PIOS) [53]

After the general processes were created for the specific food types, each process was grouped into common processes as a parent/child hierarchy. Figure 32 from Chapter 4, Section 3.b. shows the representative visual of the final product. The child processes all had information on input and output materials, waste, utilities, and utility levels as aforementioned. These were organized into a four box format with the utility consumption levels in the middle as a separate section as shown in Figure 33 from Chapter 4, Section 3.b. for a pasteurization process.

The utility consumption values were found for each process machinery, when available. However, when found, the values were based on machine specifications or ratings given by the manual. For this level and within the scope of this project, the ratings were considered sufficient as long as another acquisition method was assumed such as the previous Production Cell subsection. This subsection emphasizes, instead, on the data organization and visualization since much of the concept is also achieved in a traditional energy auditing methodology.

Section 3.c. Machine utilization (MU)

This subsection emphasized the use of a commercially available software tool for the prediction of machine utilization as it also relates back to the Production Cell subsection. As aforementioned, a machine may be monitored for energy consumption whereby the data is post-processed into operations categories. The author was involved in the early stages of the collaborative project proposal for a Computer-Aided Design software company for the further development of their process analysis product. The product was developed in order to serve customers with needs to analyze their efficiency with given requirements, predict any changes, and simulate for optimal scheduling of the particular process. Ideally, a target user of the proposed energy auditing framework may attempt full utilization of the process level data granularity by combining aspects of the above three subsections.

Section 4 Process chain
Section 4.a. Process chain identification (PIOS Plus) [53]

The particular task for the process chain was to generate an industry table with processes for various industries as aforementioned in Chapter 3, Section 3.b. and 4.a. The food processing industry investigation consisted of defining some of the process chains involved within a factory level. The process chains typically included all steps from orders received to packaging where orders were prepared for shipment or storage. Moreover, after creating a general process chain for a specific type of food, the utilities used and the consumption levels of these utilities were explored. Data was collected by first researching about process chains of a specific food product such as a basic potato chip and moving a level to generate chip production process chains. After completing a few general food chains, the results started to show an industry trend that represented a similar sequence of processes. An example generic process chain was shown in Figure 36 from Chapter 4, Section 4.a. (re-shown below) for chip production. Specific processes were grouped into common processes and organized into a higher level process chain to represent entire food processing industry trends. Several specific foods were researched including potato chips, ice cream, frozen pizzas, pastry, bread, milk, orange juice, beer, and hard-liquor. These represented foods with various main processes including fried products, frozen products, bread products, and both non-alcoholic and alcoholic beverage products. A literature search was conducted to find information on each of these process chains. Furthermore, after the construction of the respective process chains, each process was investigated for input and output materials, waste, utilities, and the utility consumption levels.

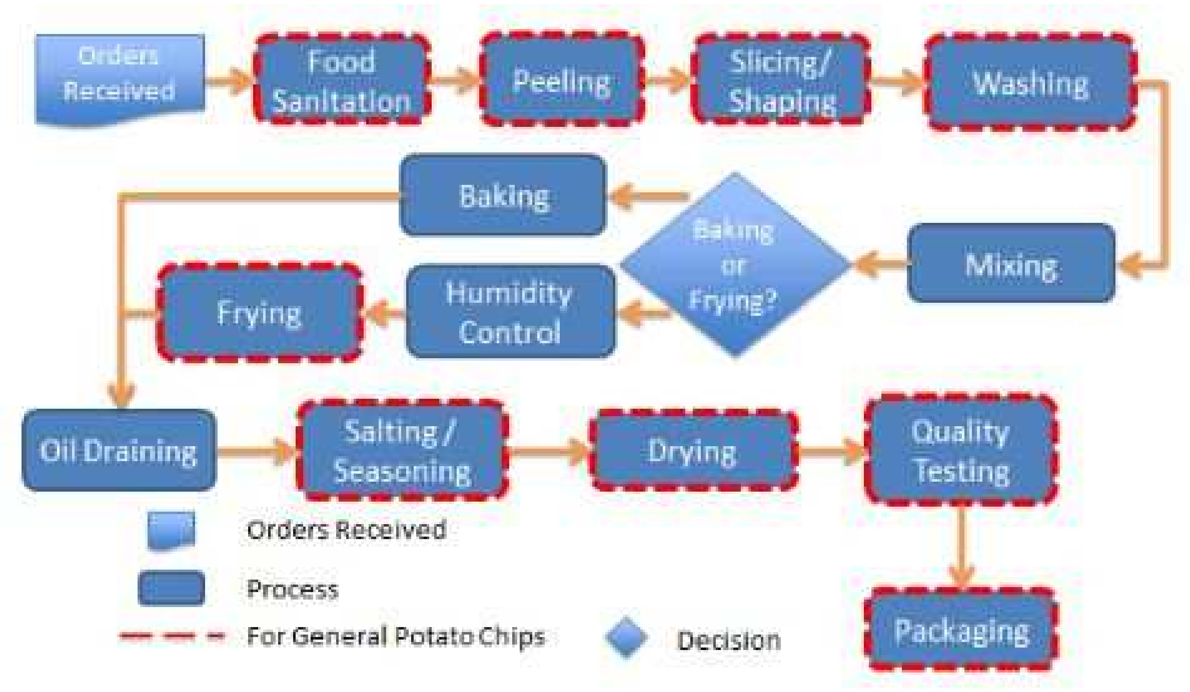

Figure 36: Sample process chain for a potato chip

The process chain was organized such that a manufacturer can select the stages they would like to use, and as long as they follow a similar sequence, they would be able to produce their products. A similar approach can be applied for the purposes of this thesis where the process chains were visualized and organized such that manufacturers can more easily decide to monitor a particular process within the process chain for energy auditing purposes. In fact, boxes surrounded by red dashed lines in Figure 36 are for the most basic form of potato chips. In the potato chip case, some chips are just baked or fried; hence, the decision box. More sophisticated potato chip production is possible with an addition or substitution of other processes into Figure 36. For example, further investigation for chips showed that chips with different cultural background such as those with Asian flavors have extra steps due to different raw materials such as shrimp chips. However, a factory visit to Calbee America for inquiries on their shrimp chips gave a notion that the general underlying processes shown in Figure 36 were still very similar and valid, albeit different raw materials and seasoning choices [54]. For this reason, it was deemed that extra investigation on chips production other than potato-based chips was unnecessary.

Although the general process chain contained other processes that were not always used by individual manufacturers for the potato chip example, other specific food process chains seemed to have similar processes across common food manufacturers. For this reason, the general process chain was equivalent to the specific food process chains themselves for other investigated food types. In fact, the ice cream process chain did not have a generalized version due to the similar processes that exist between frozen dessert products including sherbets and sorbets.

Section 4.b. Line utilization (LU)

Similar to Chapter 5, Section 3.c., each of the process breakdowns were presented as a process chain in order to simulate the total line utilization and energy consumption based on each of the operations categories. This subsection serves as way to visualize a process chain energy consumption based on the categories for users to gain transparency over their facility's energy usage. Much of the process and process chain level data granularity is similar to currently existing energy auditing methodologies. The value added of these sections is in the predictive and visual aspect provided by the aforementioned results and software.

Chapter 6 Conclusion
Section 1 Summary of work

As new regulations and compliance measures encourage production enterprises to manufacture products in more environmentally-benign methods, it is important for these enterprises to monitor and understand their supply chain more transparently. Moreover, in cases where they recognize a problem, it is of utmost importance for them to execute mitigation strategies as early as possible to avoid missing opportunities. Increased transparency of energy losses at facilities and suppliers could be a key factor for enterprises to suggest effective energy consumption improvements that can create a large positive impact to the entire system. This thesis was a consolidation of multiple projects that the author has been associated with, with regards to reduction of energy consumption at manufacturing enterprises. The thesis proposes a guideline that production enterprises can utilize in order to improve upon their traditional energy auditing methods using data with higher granularity and that is more real-time. Data become more granular as acquisition and post-process levels increase in specificity of a facility; i.e., from process chain to process parameter level. The real-time component implies to a frequent iteration and that change enablers are given opportunities to initiate improvement with a faster response time after a continuous energy audit instead of depending on data and reports made by discrete energy audits applicable to the point in time of the report regeneration. The thesis (guideline) was broken down into four levels: parameter, tool path, process, and process chain. Each level contained energy consumption projects, which have been adapted for the guideline's purposes.

Section 2 Guideline levels

The parameter and tool path levels have impacts on the process plan change aspects. Although these levels require more data to be collected and presented in order to suggest a refined improvement plan during the audit, it is considered to have a more precise and large impact to the entire enterprise in lessening the systematic energy consumption.

The parameter level energy consumption was considered to have the highest data granularity; hence, having the most potential for providing the largest impact. Machining processes are executed based on set parameters by the operators, which are commands sent from the line managers or process planners as referenced in Figure 6 from Chapter 1, Section 3.a. Although each processes and machining configuration has a hard, mechanical top-and-bottom limit, tremendous effort and resources are needed to find the optimal set of parameters that can satisfy the product specifications as well as environmental regulations and compliance simultaneously. The parameter level referenced an energy model validation project for a 3-axis machining process. The project itself was based on previous work by [49] for a 2-axis machining process. The result was an energy characterization curve, which was tested with a 3-axis machining process in order to determine the model and generation methodology's validity. For the particular model and its generation methodology, a 95% confidence level was achieved.

The tool path level is less ideal for the purposes of further breaking down the energy consumption and loss points, but it was considered as the next macro-granular level of data possible. In a collaborative project for finding an energy-efficient tool path for a 2.5-axis machining process, multiple tool paths were tested for its energy consumption value. The standard notion of manufacturers is to assume that energy consumption is higher for tool paths that contain more passes since the overall cycle time is increased. This makes the machine vulnerable to higher energy consumption due to the elongated processing time where processing and embodied energy can both affect the energy performance of a process. A new tool path generation algorithm was proposed during this project as part of an example solution to making energy consumption improvements for production enterprises, especially with milling processes. The MTSP algorithm utilized an optimization approach to connect broken down streamlines within a specified geometry. A bear cutout was used as a test case in order to capture data for four tool path types where two were pre-determined tool paths from previous literature, and the other two were: (1) commonly used parameters considered energy-efficient and (2) optimized parameters based on an energy characterization plot, which is generated ideally from the parameter level. The results showed that the OEET was, in fact, the most energy efficient, but the surface integrity was sub-par. There was a secondary component to this particular project in relation to precision engineering with chord error during a milling process. However, it was apparent from the naked eye that the OEET merely provided less energy consumption and sub-par surface integrity. Nonetheless, the level of data granularity provided through acquisition and post-processing at the tool path level will allow change enablers to make a fair impact while the continuous monitoring also enables frequent changes and testing in order to determine the most optimal tool path for a specified product design.

The process and process chain levels were considered to have more impact to the operations scheduling change aspects. These levels required less data, but the act of making energy streams more transparent was less impactful. For the purpose of this thesis's value addition, these levels were presented in order to suggest data post-processing, visualization, and organization methodologies.

The process level was based on three different projects: production cell, process input/output stream, and machine utilization. Production cell output a Matlab script in order to separate the energy consumption per operational category such as setup time, processing time, etc. of a machine(s) within a production cell. Please refer to Appendix A for an example script. The process input/output stream was part of a collaborative industrial project in order to investigate example energy requirements for machinery in multiple industries. The author's project realm included the food processing industry. Multiple products and its manufacturing processes were investigated in order to determine the energy rating based on the machinery specifications. This project was presented in the thesis for the purposes of visualization and organization. The machine utilization project was also a part of a collaborative industrial project. The author participated in the initial proposal stage where they used process analysis software to analyze the process's utilization and categorize that under a specific operational breakdown such as the production cell project. The output of this project was a method to visualize the machine utilization and potentially estimate the energy consumption per operational category for the purposes of predicting the process's energy consumption. The post-processing aspect was emphasized during the production cell project through the Matlab script.

The process chain level consisted of higher levels of the process level projects. This was the level with least data granularity. This level was the least ideal during the thesis's proposition for an improved energy auditing method to increase transparency. Since it is very similar to the existing energy auditing level of data granularity, the author's value addition was placed on the data visualization and organization method. The process chain versions of the aforementioned process I/O stream and machine utilization were found.

Each level contained an inherent argument for real-time data being acquired (monitored) frequently in order to make multiple iterations in a short amount of time. It is critical to have real-time data for a quicker response time by the change enablers in order to make the most impact per change without the delay from an energy audit report.

Section 3 Future work

Although each level of data was a composition of the prior level of data, the error for each level was assumed to be discrete. In reality, each level of analysis would contain an inherent uncertainty or error associated with its data set and a propagation to the error of the entire experiment or a higher level system. For this reason, it is important to incorporate a level-to-level uncertainty analysis and error propagation methodology such as those in [55] in order to determine the overall uncertainty for the systematic energy audit results in the future. Moreover, a facility-level analysis addition would also add precision to the audit and analysis since indirect items were excluded from the audit; i.e., heating, ventilation, air conditioning, and building certifications such as LEED. This would enable auditors and change enablers of the enterprise to suggest improvements more accurately since these are data that are only associated indirectly to the previous levels of data sets. Although levels of higher data granularity such as parameter and tool path levels are less applicable, it would be interesting to observe any implications or effects caused by the data quality of energy ratings given by the manufacturers of different components. Some audits may include and depend on energy ratings that are given by the component manufacturers of process machinery. However, it is important to note the possible errors associated with the given energy ratings in the specifications.

Finally, this audit can provide a comprehensive framework for production enterprises if it incorporates all TBL factors: economic, environmental, and social. Due the limited availability of data and undefined nature of some social factor data sets, the energy audit approach was taken first. For this reason, further expansion of the framework into other factors is highly desirable. With the consideration of all TBL factors, it also opens possibilities to research for a TBL-based benchmarking methodology while enabling companies to find losses within their value chain and make corrections/improvements where necessary in order to maintain a green-competitiveness edge.

Bibliography

[1] LMAS Overview Slides. University of California, Berkeley. Laboratory for Manufacturing and Sustainability. September 16, 2014.

[2] “Integrated Bottom Line”. The Dictionary of Sustainable Management. Presidio Graduate School and TriplePundit. 2014. Obtained on December 15, 2014. Obtained from < http://www.sustainabilitydictionary.com/integrated-reporting/>.

[3] Lewis, J. “Looking Backward: A Historical Perspective on Environmental Regulations”. United States Environmental Protection Agency. March 1988. Obtained on December 15, 2014. Obtained from < http://www2.epa.gov/aboutepa/looking-backward-historical-perspective-environmental-regulations>.

[4] “Summary of the Clean Water Act”. United States Environmental Protection Agency. November 12, 2014. Obtained on December 15, 2014. Obtained from < http://www2.epa.gov/laws-regulations/summary-clean-water-act>.

[5] “Summary of the Clean Air Act”. United States Environmental Protection Agency. November 12, 2014. Obtained on December 15, 2014. Obtained from < http://www2.epa.gov/laws-regulations/summary-clean-air-act>.

[6] “History of RCRA”. United States Environmental Protection Agency. November 1, 2013. Obtained on December 15, 2014. Obtained from < http://www.epa.gov/osw/laws-regs/rcrahistory.htm>.

[7] Appel, M. “Penalties for excessive energy use”. SouthAfrica.info. June 9, 2008. Obtained on December 15, 2014. Obtained from < http://www.southafrica.info/services/consumer/energy-090608.htm#.VI_j9snxsfC>.

[8] “Kyoto Protocol”. United Nations: Framework Convention on Climate Change. 2014. Obtained on December 15, 2014. Obtained from < http://unfccc.int/kyoto_protocol/items/2830.php>.

[9] “2050 GHG Reduction Goals and a Regional Climate Protection Strategy”. Bay Area Air Quality Management District. December 9, 2014. Obtained on December 15, 2014. Obtained from < http://www.baaqmd.gov/Divisions/Planning-and-Research/Climate-Protection-Program.aspx>.

[10] “Assembly Bill 32 Overview”. California Environmental Protection Agency: Air Resources Board. August 5, 2014. Obtained on December 15, 2014. Obtained from < http://www.arb.ca.gov/cc/ab32/ab32.htm>.

[11] “Future of EU Environmental Policy: Towards the 7th Environmental Action Programme.” European Environmental Bureau. November 2010.

[12] Nyhus, E. “Environmental regulations towards 2020”. Det Norske Veritas, Inc.

[13] “The Life Cycle: From Cradle to Grave”. AkzoNobel Sustainable Development. 2010. Obtained on December 15, 2014. Obtained from < https://www.akzonobel.com/sustainabledevelopment/approach/assessment/lifecycle/>.

[14] “Living Progress: Audit Findings”. Hewlett-Packard (HP). 2014. Obtained on December 15, 2014. Obtained from < http://www8.hp.com/us/en/hp-information/global-citizenship/society/auditresults.html#asia-pacific>.

[15] O’Toole, J.O. “Apple supplier faces scrutiny over labor conditions in China”. CNN Money. September 4, 2014. Obtained on December 15, 2014. Obtained from < http://money.cnn.com/2014/09/04/technology/apple-china/>.

[16] “LEED Overview”. United States Green Building Council. 2014. Obtained on December 15, 2014. Obtained from <http://www.usgbc.org/leed>.

[17] “Volkswagen Chattanooga earns highest LEED certification”. Auto Alliance: Driving Innovation. Obtained on December 15, 2014. Obtained from December 15, 2014. < http://www.autoalliance.org/index.cfm?objectid=6497FBE0-B49E-11E1-875B000C296BA163>.

[18] “ISO 14000 – Environmental management”. International Organization for Standardization. Obtained on December 15, 2014. Obtained from < http://www.iso.org/iso/iso14000>.

[19] “ISO 14001 and ISO 50001”. International Business Machines. Obtained on December 15, 2014. December from < http://www.ibm.com/ibm/environment/iso14001/>.

[20] Kaiser, T. “Apple’s Chinese Suppliers in Trouble for Environmental Pollution.” DailyTech. August 5, 2013. Obtained on December 15, 2014. Obtained from < http://www.dailytech.com/Apples+Chinese+Suppliers+in+Trouble+for+Environmental+Pollution/article33103.htm>.

[21] Hasanbeigi, A. and Lynn, P. “Industrial Energy Audit Guidebook: Guidelines for Conducting an Energy Audit in Industrial Facilities.” Ernest Orlando Lawrence Berkeley National Laboratory. China Energy Group. Energy Analysis Department. Environmental Energy Technologies Division. October 2010.

[22] D’Alessio, A.; Bhinge, R.; Ninomiya, K.; Robinson, S. and Dornfeld, D. “Midterm Presentation: Integrating Sustainability into Process Analysis 360.” University of California, Berkeley. Laboratory for Manufacturing and Sustainability. February 26, 2014.

[23] Phornprapha, M. “Production Management I, Lecture 6, Process planning and Operations Scheduling” RWTH Aachen. Obtained on December 15, 2014. Obtained from < http://www.wzl.rwth-aachen.de/en/080d8d8c949a1ac0c1256f190035d886/pm_i_eng_v6.pdf>.

[24] Beil, D. “Supplier Selection”. Stephen M. Ross School of Business. July 2009.

[25] Akili, E.A. “Green Supplier selection criteria”. University of Wisconsin, Whitewater.

[26] Vance, L.; Heckl, I.; Bertok, B; Cabezas, H. and Friedler, F. “Designing Energy Supply Chains with the P-graph Framework under Cost Contraints and Sustainability Considerations.” Proceedings of the 24^{th} European Symposium on Computer Aided Process Engineering. (2014).

[27] Xie, G. “Modeling decision processes of a green supply chain with regulation on energy saving level”. Computers & Operations Research 54 (2015): 266-273

[28] Waldemarsson, M.; Lidestam, H. and Rudberg, M. “Including energy in supply chain planning at a pulp company”. Applied Energy 112 (2013): 1056-1065.

[29] Kishawy, H.A.; Hosseini, A.; Moetakef-Imani, B. and Astakhov, V.P. “An energy based analysis of broaching operation: Cutting forces and resultant surface integrity”. CIRP Annals – Manufacturing Technology 61 (2012): 107-110.

[30] Yoon, H.-S.; Moon, J.-S.; Pham, M.-Q. and Lee, G.-B. “Control of machining parameters for energy and cost savings in micro-scale drilling of PCBs”. Journal of Cleaner Production 54 (2013): 41-48.

[31] Liu, F; Xie, J. and Liu, S. “A method for predicting the energy consumption of the main driving system of a machine tool in a machining process”. Journal of Cleaner Production (2014) 1-7.

[32] Chen, C.; Hu, Z.; Ninomiya, K.M. and Pande, S.S. “Generation of energy-efficient tool path algorithm: aspects of optimization to precision and sustainable manufacturing”. University of California, Berkeley. ME 220 Report. Fall 2013 Term.

[33] Kong, D. et. al. “Software-based tool path evaluation for environmental sustainability”. Journal of Manufacturing Systems 30.4 (2011): 241-247.

[34] Rangarajan, A. and Dornfeld, D. “Efficient tool paths and part orientation for face milling”. CIRP Annals-Manufacturing Technology 53.1 (2004): 73-76.

[35] Youngwook, P.K. “Milling Tool-Path based on Micrography”. University of California, Berkeley. CS 285 Final Course Project. Fall 2011 Term.

[36] Zhang, J.Y. “The Quick and Simple Algorithm for Circular Interpolation”. Applied Mechanics and Materials 34 (2010): 1549-1553.

[37] “Chord Error”. Artwork Conversion Software, Inc. Obtained on October 24, 2013. Obtained from < http://www.artwork.com/polygon/gerber/chord_error.htm>.

[38] Yeh, S.-S. and Hsu, P.-L. “Adaptive-feedrate interpolation for parametric curves with a confined chord error.” Computer-Aided Design 34.3 (2002): 229-237.

[39] Yong, T. and Narayanaswami, R. “A parametric interpolator with confined chord errors, acceleration and deceleration for NC machining.” Computer-Aided Design 35.13 (2003): 1249-1259.

[40] Koren, Y. and Lin, R.S. “Efficient tool-path planning for machining free-form surfaces”. Transactions of the ASME Journal of Engineering for Industry 118 (1996): 20-28.

[41] Chaves-Jacob, J.; Linares, J.-M. and Sprauel, J.-M. “Improving tool wear and surface covering in polishing via toolpath optimization”. Journal of Materials Processing Technology (2013).

[42] Marinac, D. “Tool Path Strategies For High Speed Machining”. Modern Machine Shop. February 2000. Obtained on October 24, 2013. Obtained from < http://www.mmsonline.com/articles/tool-path-strategies-for-high-speed-machining>.

[43] Choi, S.H. and Cheung, H.H. “A topological hierarchy-based approach to toolpath planning for multi-material layered manufacturing”. Computer-Aided Design 38.2 (2006): 143-156.

[44] Diaz, N.; Ninomiya, K.; Noble, J. and Dornfeld, D. “Environmental impact characterization of milling and implications for potential energy savings in industry”. 5th CIRP Conference on High Performance Cutting (2012).

[45] Berthold, D. “Process orientated approach of a bottom-up modified environmental value stream management tool suitable for small and medium-sized enterprises”. Diploma-Thesis. University of California, Berkeley: LMAS. RWTH Aachen: WZL. March 26, 2013.

[46] Yoon, H.-S.; Lee, J.-Y.; Kim, M.-S.; Kim, E.-S. and Ahn, S.-H. “Empirical study of the power efficiency of various machining processes”. Procedia CIRP 14 (2014): 558-563.

[47] Posselt, G. et. al. “Extending Energy Value Stream Models by the TBS Dimension – Applied on a Multi Product Process Chain in the Railway Industry”. Procedia CIRP 15 (2014): 80-85.

[48] Wang, S.; Lu, X.X.; Li, W. and Li, D. “A systematic approach of process planning and scheduling optimization for sustainable machining”. Journal of Cleaner Production 87 (2015): 914-929.

[49] Diaz, N.; Redelsheimer, E. and Dornfeld, D. “Energy Consumption Characterization and Reduction Strategies for Milling Machine Tool Use“. Proceedings of the 18th CIRP International Conference on Life Cycle Engineering. (2011).

[50] Durand, J. ESPRIT Software Support Email Communication. (2011).

[51] Cong, C.; Hu, Z.; Ninomiya, K.M. and Pande, S.S. “Final Presentation”. University of California, Berkeley. ME 220. Fall 2013 Term.

[52] Ninomiya, K. “Final Report”. University of California, Berkeley. ME 196. Fall 2012 Term.

[53] Ninomiya, K. “Final Report”. University of California, Berkeley. ME 196. Spring 2012 Term.

[54] Calbee America Factory Visit. Fairfield, CA. USA. (2011).

[55] Clemon,L.M. “Analysis of Uncertainty in Estimating the Resource Intensities and Impacts of Solid Freeform Fabrication Processes”. Master’s Thesis. University of California, Berkeley: LMAS. Spring 2013.

Additional Informational Bibliography

[56] Ice Cream Manufacture. Dairy, Science, and Technology Education Series. University of Guelph. Accessed 01 May, 2012. <http://www.foodsci.uoguelph.ca/dairyedu/icmanu.html>.

[57] Lehmann, T.A. and Dubois, D.: Commissary Methods of Processing Pizza Dough. American Institute of Baking: Vol. VIII **12** (December 1986).

[58] McNulty, M. F. "Potato Chip." How Products are Made. Vol 3. (2012). Accessed 02 May, 2012. <http://www.madehow.com/Volume-3/Potato-Chip.html>

[59] Jen, S. "Dust Removing Machine." Weiku, Free Global Marketplace. (2012). Accessed 02 May, 2012. <http://www.weiku.com/products/7224212/dust_removing_machine.html>

[60] Mike, A. "Potato Peeler PP30." Alibaba.com. (2012). Accessed 02 May 2012. <http://www.alibaba.com/product-gs/356096359/potato_peeler_pp30.html>

[61] Zhang, Ivy. "Automatic Multifunctional Potato Slicing Machine." Alibaba.com. (2012). Accessed 02 May, 2012. <http://www.alibaba.com/product-gs/529836596/automatic_multifunctional_potato_slicing_machine.html>

[62] "Fried Food Processing Line Search Results." Global Sources Machinery and Industrial Supplies. (2012). Accessed 02 May, 2012. <http://www.globalsources.com/gsol/I/Fried-food-suppliers/s/2000000003844/3000000198677/29944.htm>

[63] Yao, K. "Potato Chips Frying Machine." Alibaba.com. (2012). Accessed 02 May, 2012. <http://www.alibaba.com/product-gs/449051345/Potatos_chips_Frying_Machine.html>

[64] Gao, S. "Potato Chips Seasoning Machine." Alibaba.com 2012. Accessed 02 May, 2012. <http://www.alibaba.com/product-gs/485047548/2011_potato_chips_seasoning_machine.html>

[65] "Potato Drying Machine." Blaze Machinery. Accessed 02 May, 2012 <http://www.potatochipsmakingmachine.com/potato-drying-machine.html>

[66] Wang. L. "New Mesh Belt Dryer for Drying." Alibaba.com. (2012). Accessed 02 May, 2012. <http://www.alibaba.com/product-gs/498143366/New_mesh_belt_dryer_for_drying.html>

[67] Zheng, S. "Potato Chips Filling Machine." Alibaba.com. (2012). Accessed 02 May, 2012. <http://www.alibaba.com/product-gs/509796695/potato_chips_filling_machine.html>

[68] Cai, Y. "Potato Chips Fastback Conveyor." Alibaba.com. (2012). Accessed 02 May, 2012. <http://www.alibaba.com/product-gs/473915486/Potato_chips_fastback_conveyor.html>

[69] Xing, J. "Baked Potato Machine." Alibaba.com. (2012). Accessed 02 May, 2012. <http://www.alibaba.com/product-gs/470083770/Baked_potato_machine.html>

[70] "Humidified Holding Cabinet." Henny Penny. (2010). Accessed 02 May, 2012. <http://www.hennypenny.com/documents/products/HHC-980%20data%20sheet.7.16.10.pdf>

[71] Naresh, L. and Shailaja, U. (2006). Stabilizer Blends and their importance in Ice Cream Industry – A Review. New Zealand Food Magazine. (2006).

[72] McNulty, M. F. "Ice Cream." How Products are Made. Vol. 3. (2012). Accessed 02 May, 2012. <http://www.madehow.com/Volume-3/Ice-Cream.html>

[73] "Paddle Blender Specifications and Dimensions." Charles Ross and Son Company. Accessed 02 May, 2012. <http://www.mixers.com/Specifications/Paddle.pdf>

[74] Piasek, A.; Kusznierewicz, B.; Grzybowska, I. et. al.: The influence of sterilization with Enbiojet Microwave Flow Pasteurizer on composition and bioactivity of aronia and blue-berried honeysuckle juices. Journal of Food Composition and Analysis 24 (2011). pg. 880-888

[75] Che, K. “Ice Cream Pasteurizer OPA40.” Alibaba.com. (2012). Accessed 02 May, 2012. <http://www.alibaba.com/product-gs/348632363/Ice_Cream_Pasteurizer_OPA40.html>

[76] “High Pressure Homogenizer.” Changzhou Chaoli Homogenizing Pump Factory. (2012). Accessed 02 May, 2012. <http://www.chinahomogenizers.com/1a-pressure-homogenizer.html>

[77] Tan, W. “Blending Machine.” Alibaba.com. (2012). Accessed 02 May, 2012. <http://www.alibaba.com/product-gs/302951089/Blending_Machine.html>

[78] Sun, A. “VITA 20 60 Gelato Ice Cream Freezing Machine.” Alibaba.com. (2012). Accessed 02 May, 2012. < http://www.alibaba.com/product-gs/537461217/VITA_20_60_gelato_ice_cream/showimage.html>

[79] “Ice Cream Filling Equipment.” Stanpacnet.com. Accessed 02 May, 2012. <http://www.stanpacnet.com/resources/flexefill_specmanual.pdf>

[80] “Hardening Cabinets.” Global Refrigeration, Inc. Accessed 02 May, 2012. < http://www.globalref.com/files/72394_hardening%20cabinets.pdf>

[81] Reisinger, B. “The Ridiculously Thorough Guide to Making Your Own Pizza.” Billyreisinger.com. (2012). Accessed 02 May, 2012. <http://billyreisinger.com/pizza.html>

[82] “Pizza Topping Lines Waterfall System.” Comas S.p.A. Accessed 02 May, 2012. <http://www.comas-spa.com/sp/eng/catalogo_prodotto.php?as_content_id_att12=49>

[83] Wu, S. “Electric Pizza Oven Pizza Maker.” Alibaba.com. (2012). Accessed 02 May, 2012. <http://www.alibaba.com/product-gs/230437937/Electric_pizza_oven_pizza_maker_.html>

[84] “Arctic Industries (1061-R) – 6’ Modular Walk-In Freezer.” Foodservicewarehouse.com. (2012). Accessed 02 May, 2012. <http://www.foodservicewarehouse.com/arctic-industries/1061-r/p521395.aspx>

[85] Zhang, W. “Pizza Packing Machine.” Alibaba.com. (2012). Accessed 02 May, 2012. <http://www.alibaba.com/product-gs/420913240/pizza_packing_machine.html>

[86] “Cake Manufacturing.” Shumaonline.com. Accessed 02 May, 2012. <http://www.shumaonline.com/cakemanufacturing.html>

[87] Jiang, S. “Walnut Cake Molding Machine.” Alibaba.com. (2012). Accessed 02 May, 2012. <http://www.alibaba.com/product-gs/451673295/walnut_cake_molding_machine.html?s=p>

[88] Liu, W. “2012 Hot Selling Cake Baking Deck.” Alibaba.com. (2012). Accessed 02 May, 2012. <http://www.alibaba.com/product-gs/339143413/2012_hot_selling_cake_baking_deck.html?s=p>

[89] Ma, I. “QLH Series Decorating Machine for Production.” Alibaba.com. (2012). Accessed 02 May, 2012. <http://www.alibaba.com/product-gs/538225369/QLH_series_decorating_machine_for_production.html>

[90] Ni, A. “DSH 250S Horizontal Cake Packing Machine.” Alibaba.com. (2012). Accessed 02 May, 2012. <http://www.alibaba.com/product-gs/523056195/DSH_250S_Horizontal_Cake_Packing_Machine.html?s=p>

[91] McNulty, M.F. “Bread.” How Products are Made. Vol. 2. (2012). Accessed 02 May, 2012. <http://www.madehow.com/Volume-2/Bread.html>
[92] Yan, J. “Dough Kneading Machine.” Alibaba.com. (2012). Accessed 02 May, 2012. <http://www.alibaba.com/product-gs/315694357/dough_kneading_machine.html>
[93] Li, N. “New Style Fermentation Room Bread Leaven.” Alibaba.com. (2012). Accessed 02 May, 2012. <http://www.alibaba.com/product-gs/535976090/New_style_fermentation_room_bread_leaven.html?s=p>
[94] Shi, A. “GR Bread Machine Dough Divider.” Alibaba.com. (2012). Accessed 02 May, 2012. <http://www.alibaba.com/product-gs/526436522/GR_bread_machine_dough_divider.html?s=p>
[95] Gu, L. “Bread Shaping Machine (CE ISO9001 Manufacturer).” Alibaba.com. (2012). Accessed 02 May, 2012. <http://www.alibaba.com/product-gs/482581634/bread_shaping_machine_CE_ISO9001_manufacturer_.html>
[96] Li, V. “Proofer (BKF-632S).” Alibaba.com. (2012). Accessed 02 May, 2012. <http://www.alibaba.com/product-gs/332315492/proofe_rBKF_632S_.html>
[97] Jia, C. “Bread Slicing Machine.” Alibaba.com. (2012). Accessed 02 May, 2012. <http://www.alibaba.com/product-gs/371743808/bread_slicing_machine.html>
[98] Wang, R. “Automatic Bread Packing Machine.” Alibaba.com. (2012). Accessed 02 May, 2012. <http://www.alibaba.com/product-gs/526864463/Automatic_bread_packing_machine.html?s=p>
[99] Cavette, C. “Milk.” How Products are Made. Vol. 4. (2012). Accessed 02 May, 2012. <http://www.madehow.com/Volume-4/Milk.html>
[100] Jinhua, X. “Dairy Milk Separator.” Alibaba.com. (2012). Accessed 02 May, 2012. <http://www.alibaba.com/product-gs/548215278/dairy_milk_separator.html>
[101] Wu, W. “Adjustable Speed Precision Peristaltic Pump OEM13.” Alibaba.com. (2012). Accessed 02 May, 2012. <http://www.alibaba.com/product-gs/422417331/Adjustable_speed_precision_peristaltic_pump_OEM13.html>
[102] Ji, J. “Fully Automatic Milk Pasteurizer.” Alibaba.com. (2012). Accessed 02 May, 2012. <http://www.alibaba.com/product-gs/262751899/fully_automatic_milk_pasteurizer.html>
[103] Philip, S. “Juice Milk High Pressure Homogenizer.” Alibaba.com. (2012). Accessed 02 May, 2012. <http://www.alibaba.com/product-gs/481386058/Juice_Milk_High_Pressure_Homogenizer_Machine.html>
[104] Chu, C. “Juice Milk Tea Hot Bottling Machine.” Alibaba.com. (2012). Accessed 02 May, 2012. <http://www.alibaba.com/product-gs/333674171/Juice_milk_tea_hot_bottling_machine.html?s=p>
[105] Schueller, R. “Orange Juice.” How Products are Made. Vol. 4. (2012). Accessed 02 May, 2012. <http://www.madehow.com/Volume-4/Orange-Juice.html>
[106] Zhang, L. “Apple Cherry Mango Orange Fruit Juice.” Alibaba.com. (2012). Accessed 02 May, 2012. <http://www.alibaba.com/product-gs/550157757/apple_cherry_mango_orange_fruit_juice.html>
[107] Lee, H. “Juice Concentrate Machine Fruit Juice Evaporator.” Alibaba.com. (2012). Accessed 02 May, 2012. <http://www.alibaba.com/product-gs/507008602/juice_concentrate_machine_fruit_juice_evaporator_.html>
[108] Betts, D.E. “Beer.” How Products are Made. Vol. 2. (2012). Accessed 02 May, 2012. <http://www.madehow.com/Volume-2/Beer.html>

[109] Tan, A. “Micro Beer Equipment Red Copper Mash.” Alibaba.com. (2012). Accessed 02 May, 2012. <http://www.alibaba.com/product-gs/472196308/micro_beer_equipment_red_copper_mash.html>

[110] Song, D. “Beer Brewery Equipment.” Alibaba.com. (2012). Accessed 02 May, 2012. <http://www.alibaba.com/product-gs/522809000/Beer_brewery_equipment.html>

[111] Wang, S. “Beer Sterilizing Tunnel Machine.” Alibaba.com. (2012). Accessed 02 May, 2012. <http://www.alibaba.com/product-gs/546687325/beer_sterilizing_tunnel_machine.html>

[112] Gu, A. “Beer Filling Machine.” Alibaba.com. (2012). Accessed 02 May, 2012. <http://www.alibaba.com/product-gs/494450220/Beer_filling_machine.html>

[113] Niu, A. “Barley Cleaner.” Alibaba.com. (2012). Accessed 02 May, 2012. <http://www.alibaba.com/product-gs/498186192/barley_cleaner.html>

[114] Putz, J.M. “How is Whisky Made?.” Whisky-distillaries.info (Oct. 2011). Accessed 02 May, 2012. <http://www.whisky-distilleries.info/Fabrication_EN.shtml>

[115] Song, B. “Malt Flour Rotary Sieve Machine.” Alibaba.com. (2012). Accessed 02 May, 2012. <http://www.alibaba.com/product-gs/460946888/Malt_flour_rotary_sieve_machine.html>

[116] Zhou, J. “SAF18-18-6 Whiskey Filling Machine.” Alibaba.com. (2012). Accessed 02 May, 2012. <http://www.alibaba.com/product-gs/540951292/SAF18_18_6_Whiskey_filling_machine.html>

Appendix Program Codes
Appendix A Energy Model Validation (EMV) Matlab Script

```
%% Material Removal Rate Predictive Tool for Z-Direction

%% Ellipse
a = 54.845; % Major Axis Radius with offset
b = 35.45; % Minor Axis Radius with offset
PeriElli = pi*(3*(a+b)-sqrt(3*a^2+10*a*b+3*b^2)); % Using Ramanujan Prediction Method
ArcPerChange = PeriElli/4; % mm
AvgSlotfz = 164/60; % mm/s
EndMilldiam = 4; % mm with offset
deOfCu1 = 1 * EndMilldiam;
wiOfCu = 6; % mm
MRRFull = deOfCu1 * wiOfCu * AvgSlotfz;
deOfCu2 = 0.5 * EndMilldiam;
MRRHalf = deOfCu2 * wiOfCu * AvgSlotfz;
deOfCu3 = 0 * EndMilldiam;
MRRZero = deOfCu3 * wiOfCu * AvgSlotfz;
TimePerChange1 = (ArcPerChange/AvgSlotfz);
TimePerChange2 = 2 * (ArcPerChange/AvgSlotfz);
timeOuter = [0,TimePerChange1, TimePerChange1 * 2, (TimePerChange1 *
2)+TimePerChange2]
MRRzOuter = [MRRFull,MRRHalf,MRRHalf,MRRZero]
plot(timeOuter,MRRzOuter)
grid on
title('Spiral MRR - Features 1-3')
xlabel('Time (seconds)')
ylabel('MRR (mm^3/s)')
legend('Variable MRR')
%% Spiral

ArcLengthMatrix = [(57.85+48.63)/2,(57.85+48.63)/2,(57.11+48)/2,...
   (46.80+37.44)/2,(39.48+30.58)/2,(39.48+30.58)/2,(38.89+30.09)/2,...
   (28.11+18.90)/2];
TimePerChangeMatrix = ArcLengthMatrix ./ AvgSlotfz;
timeInnerStart = timeOuter(end) + 15.37; % [sec]
A = timeInnerStart + TimePerChangeMatrix(1);
B = A+TimePerChangeMatrix(2);
C = B+TimePerChangeMatrix(3);
D = C+TimePerChangeMatrix(4);
E = D+TimePerChangeMatrix(5);
F = E+TimePerChangeMatrix(6);
G = F+TimePerChangeMatrix(7);
H = G+TimePerChangeMatrix(8);
timeInner = [timeInnerStart,A,B,C,D,F,H]
deOfCu4 = 0.75*EndMilldiam;
```

```
deOfCu5 = 0.25*EndMilldiam;
deOfCu6 = 0.125*EndMilldiam;
MRRThQu = deOfCu4 * wiOfCu * AvgSlotfz;
MRRQu = deOfCu5 * wiOfCu * AvgSlotfz;
MRREi = deOfCu6 * wiOfCu * AvgSlotfz;
MRRzInner = [MRRFull,MRRThQu,MRRThQu,MRRHalf,MRRHalf,MRRQu,MRRZero]
plot(timeInner,MRRzInner)
grid on
title('Spiral MRR - Features 4-9')
xlabel('Time (seconds)')
ylabel('MRR (mm^3/s)')
legend('Variable MRR')
hold off

%% Outer Cut
% 1st Pass
timeOuterSampT1 = timeOuter(2)-timeOuter(1);
N = [1,2,5,8,9,10,20,timeOuterSampT1,50,100,200,500,1000,10000];
deltaT1 = timeOuterSampT1./N;
EC6OuterT1 = zeros(length(N),1);

for k = 1:length(N)
   delT_row = [0:deltaT1(k):timeOuterSampT1]; % sample time in [sec]
   MRROuterT1_Proto = -1.250 .* delT_row + 65.6;
   MRROuterT1 = smooth(MRROuterT1_Proto,'moving');
   SpecEnergy6mmOuterT1 = 1556 .* (1./MRROuterT1') + 1.475;
   EC6OuterT1(k) = sum(SpecEnergy6mmOuterT1 .* (MRROuterT1' .* deltaT1(k)));
end
display(EC6OuterT1)

EC6OuterT1Act1 = 46457;
EC6OuterT1Act2 = 45705;
EC6OuterT1Act3 = 51425;
EC6OuterT1Act4 = 46358;
EC6OuterT1Act5 = 46555;
EC6OuterT1Act6 = 43150;
PercError6mmOT1 = zeros(length(EC6OuterT1),6);
for d = 1:length(EC6OuterT1)
   PercError6mmOT1(d,1) = ((EC6OuterT1Act1 - EC6OuterT1(d))./EC6OuterT1Act1).*100;
end

for s = 1:length(EC6OuterT1)
   PercError6mmOT1(s,2) = ((EC6OuterT1Act2 - EC6OuterT1(s))./EC6OuterT1Act2).*100;
end

for x = 1:length(EC6OuterT1)
```

```
    PercError6mmOT1(x,3) = ((EC6OuterT1Act3 - EC6OuterT1(x))./EC6OuterT1Act3).*100;
end

for y = 1:length(EC6OuterT1)
    PercError6mmOT1(y,4) = ((EC6OuterT1Act4 - EC6OuterT1(y))./EC6OuterT1Act4).*100;
end

for t = 1:length(EC6OuterT1)
    PercError6mmOT1(t,5) = ((EC6OuterT1Act5 - EC6OuterT1(t))./EC6OuterT1Act5).*100;
end

for u = 1:length(EC6OuterT1)
    PercError6mmOT1(u,6) = ((EC6OuterT1Act6 - EC6OuterT1(u))./EC6OuterT1Act6).*100;
end

display(PercError6mmOT1)

%%
% 2nd Pass
timeOuterSampT2 = timeOuter(3)-timeOuter(2);
MRROuterT2 = 32.8;
SpecEnergy6mmOuterT2 = 1556 .* (1./MRROuterT2) + 1.475;
EC6OuterT2 = sum(SpecEnergy6mmOuterT2 .* MRROuterT2 .* timeOuterSampT2);
display(EC6OuterT2)

EC6OuterT2Act1 = 37140;
PercError6mmOT2 = zeros(length(EC6OuterT2),6);
PercError6mmOT2(1,1) = ((EC6OuterT2Act1 - EC6OuterT2)/EC6OuterT2Act1)*100;

EC6OuterT2Act2 = 38210;
PercError6mmOT2(1,2) = ((EC6OuterT2Act2 - EC6OuterT2)/EC6OuterT2Act2)*100;

EC6OuterT2Act3 = 41752;
PercError6mmOT2(1,3) = ((EC6OuterT2Act3 - EC6OuterT2)/EC6OuterT2Act3)*100;

EC6OuterT2Act4 = 40294;
PercError6mmOT2(1,4) = ((EC6OuterT2Act4 - EC6OuterT2)/EC6OuterT2Act4)*100;

EC6OuterT2Act5 = 38296;
PercError6mmOT2(1,5) = ((EC6OuterT2Act5 - EC6OuterT2)/EC6OuterT2Act5)*100;

EC6OuterT2Act6 = 37596;
PercError6mmOT2(1,6) = ((EC6OuterT2Act6 - EC6OuterT2)/EC6OuterT2Act6)*100;

display(PercError6mmOT2)
```

```
 %%
% 3rd Pass
timeOuterSampT3 = timeOuter(4)-timeOuter(3);
N = [1,2,5,8,9,10,20,50,timeOuterSampT3,100,200,500,1000,2000];
deltaT3 = timeOuterSampT3./N;
EC6OuterT3 = zeros(length(N),1);

for k = 1:length(N)
   delT_row = [0:deltaT3(k):timeOuterSampT3]; % sample time in [sec]
   MRROuterT3_Proto = -0.6249 .* delT_row + 65.6;
   MRROuterT3 = smooth(MRROuterT3_Proto,'moving');
   SpecEnergy6mmOuterT3 = 1556 .* (1./MRROuterT3') + 1.475;
   EC6OuterT3(k) = sum(SpecEnergy6mmOuterT3 .* (MRROuterT3' .* deltaT3(k)));
end
display(EC6OuterT3)

EC6OuterT3Act1 = 82181;
EC6OuterT3Act2 = 79630;
EC6OuterT3Act3 = 88217;
EC6OuterT3Act4 = 81646;
EC6OuterT3Act5 = 80064;
EC6OuterT3Act6 = 80685;
PercError6mmOT3 = zeros(length(EC6OuterT3),6);
for d = 1:length(EC6OuterT3)
   PercError6mmOT3(d,1) = ((EC6OuterT3Act1 - EC6OuterT3(d))/EC6OuterT3Act1)*100;
end

for s = 1:length(EC6OuterT3)
   PercError6mmOT3(s,2) = ((EC6OuterT3Act2 - EC6OuterT3(s))./EC6OuterT3Act2).*100;
end

for x = 1:length(EC6OuterT3)
   PercError6mmOT3(x,3) = ((EC6OuterT3Act3 - EC6OuterT3(x))./EC6OuterT3Act3).*100;
end

for y = 1:length(EC6OuterT3)
   PercError6mmOT3(y,4) = ((EC6OuterT3Act4 - EC6OuterT3(y))./EC6OuterT3Act4).*100;
end

for t = 1:length(EC6OuterT3)
   PercError6mmOT3(t,5) = ((EC6OuterT3Act5 - EC6OuterT3(t))./EC6OuterT3Act5).*100;
end

for u = 1:length(EC6OuterT3)
   PercError6mmOT3(u,6) = ((EC6OuterT3Act6 - EC6OuterT3(u))./EC6OuterT3Act6).*100;
end
```

```
display(PercError6mmOT3)

%% Inner Cut
% 1st Pass
timeInnerSampT1 = timeInner(2)-timeInner(1);
N = [1,2,5,8,9,10,timeInnerSampT1,20,50,100,200,500,1000,10000];
deltaT1 = timeInnerSampT1./N;
EC6InnerT1 = zeros(length(N),1);

for k = 1:length(N)
   delT_row = [0:deltaT1(k):timeInnerSampT1]; % sample time in [sec]
   MRRInnerT1_Proto = -0.8420 .* delT_row + 65.6;
   MRRInnerT1 = smooth(MRRInnerT1_Proto,'moving');
   SpecEnergy6mmInnerT1 = 1556 .* (1./MRRInnerT1') + 1.475;
   EC6InnerT1(k) = sum(SpecEnergy6mmInnerT1 .* (MRRInnerT1' .* deltaT1(k)));
end
display(EC6InnerT1)

EC6InnerT1Act1 = 32204;
EC6InnerT1Act2 = 30512;
EC6InnerT1Act3 = 34476;
EC6InnerT1Act4 = 32181;
EC6InnerT1Act5 = 32265;
EC6InnerT1Act6 = 32313;
PercError6mmIT1 = zeros(length(EC6InnerT1),6);
for d = 1:length(EC6InnerT1)
   PercError6mmIT1(d,1) = ((EC6InnerT1Act1 - EC6InnerT1(d))/EC6InnerT1Act1)*100;
end

for s = 1:length(EC6InnerT1)
   PercError6mmIT1(s,2) = ((EC6InnerT1Act2 - EC6InnerT1(s))./EC6InnerT1Act2).*100;
end

for x = 1:length(EC6InnerT1)
   PercError6mmIT1(x,3) = ((EC6InnerT1Act3 - EC6InnerT1(x))./EC6InnerT1Act3).*100;
end

for y = 1:length(EC6InnerT1)
   PercError6mmIT1(y,4) = ((EC6InnerT1Act4 - EC6InnerT1(y))./EC6InnerT1Act4).*100;
end

for t = 1:length(EC6InnerT1)
   PercError6mmIT1(t,5) = ((EC6InnerT1Act5 - EC6InnerT1(t))./EC6InnerT1Act5).*100;
end
```

```
for u = 1:length(EC6InnerT1)
    PercError6mmIT1(u,6) = ((EC6InnerT1Act6 - EC6InnerT1(u))./EC6InnerT1Act6).*100;
end

display(PercError6mmIT1)

%%
% 2nd Pass
timeInnerSampT2 = timeInner(3)-timeInner(2);

MRRInnerT2 = 49.2;
SpecEnergy6mmInnerT2 = 1556 .* (1./MRRInnerT2) + 1.475;
EC6InnerT2 = sum(SpecEnergy6mmInnerT2 .* MRRInnerT2 .* timeInnerSampT2);
display(EC6InnerT2)

EC6InnerT2Act1 = 31824;
PercError6mmIT2 = zeros(length(EC6InnerT2),6);
PercError6mmIT2(1,1) = ((EC6InnerT2Act1 - EC6InnerT2)/EC6InnerT2Act1)*100;

EC6InnerT2Act2 = 31890;
PercError6mmIT2(1,2) = ((EC6InnerT2Act2 - EC6InnerT2)/EC6InnerT2Act2)*100;

EC6InnerT2Act3 = 33803;
PercError6mmIT2(1,3) = ((EC6InnerT2Act3 - EC6InnerT2)/EC6InnerT2Act3)*100;

EC6InnerT2Act4 = 32051;
PercError6mmIT2(1,4) = ((EC6InnerT2Act4 - EC6InnerT2)/EC6InnerT2Act4)*100;

EC6InnerT2Act5 = 30473;
PercError6mmIT2(1,5) = ((EC6InnerT2Act5 - EC6InnerT2)/EC6InnerT2Act5)*100;

EC6InnerT2Act6 = 30233;
PercError6mmIT2(1,6) = ((EC6InnerT2Act6 - EC6InnerT2)/EC6InnerT2Act6)*100;

display(PercError6mmIT2)
%%
% 3rd Pass
timeInnerSampT3 = timeInner(4)-timeInner(3);
N = [1,2,5,8,9,10,timeInnerSampT3,20,50,100,200,500,1000,2000];
deltaT3 = timeInnerSampT3./N;
EC6InnerT3 = zeros(length(N),1);

for k = 1:length(N)
    delT_row = [0:deltaT3(k):timeInnerSampT3]; % sample time in [sec]
    MRRInnerT3_Proto = -0.8529 .* delT_row + 82.43;
    MRRInnerT3 = smooth(MRRInnerT3_Proto,'moving');
```

```
    SpecEnergy6mmInnerT3 = 1556 .* (1./MRRInnerT3') + 1.475;
    EC6InnerT3(k) = sum(SpecEnergy6mmInnerT3 .* (MRRInnerT3' .* deltaT3(k)));
end
display(EC6InnerT3)

EC6InnerT3Act1 = 32790;
EC6InnerT3Act2 = 32959;
EC6InnerT3Act3 = 34627;
EC6InnerT3Act4 = 32756;
EC6InnerT3Act5 = 34598;
EC6InnerT3Act6 = 34512;
PercError6mmIT3 = zeros(length(EC6InnerT3),6);
for d = 1:length(EC6InnerT3)
    PercError6mmIT3(d,1) = ((EC6InnerT3Act1 - EC6InnerT3(d))/EC6InnerT3Act1)*100;
end

for s = 1:length(EC6InnerT3)
    PercError6mmIT3(s,2) = ((EC6InnerT3Act2 - EC6InnerT3(s))./EC6InnerT3Act2).*100;
end

for x = 1:length(EC6InnerT3)
    PercError6mmIT3(x,3) = ((EC6InnerT3Act3 - EC6InnerT3(x))./EC6InnerT3Act3).*100;
end

for y = 1:length(EC6InnerT3)
    PercError6mmIT3(y,4) = ((EC6InnerT3Act4 - EC6InnerT3(y))./EC6InnerT3Act4).*100;
end

for t = 1:length(EC6InnerT3)
    PercError6mmIT3(t,5) = ((EC6InnerT3Act5 - EC6InnerT3(t))./EC6InnerT3Act5).*100;
end

for u = 1:length(EC6InnerT3)
    PercError6mmIT3(u,6) = ((EC6InnerT3Act6 - EC6InnerT3(u))./EC6InnerT3Act6).*100;
end

display(PercError6mmIT3)


%%
% 4th Pass
timeInnerSampT4 = timeInner(5)-timeInner(4);

MRRInnerT4 = 32.8;
SpecEnergy6mmInnerT4 = 1556 .* (1./MRRInnerT4) + 1.475;
EC6InnerT4 = sum(SpecEnergy6mmInnerT4 .* MRRInnerT4 .* timeInnerSampT4);
```

```
display(EC6InnerT4)

EC6InnerT4Act1 = 22117;
PercError6mmIT4 = zeros(length(EC6InnerT4),6);
PercError6mmIT4(1,1) = ((EC6InnerT4Act1 - EC6InnerT4)/EC6InnerT4Act1)*100;

EC6InnerT4Act2 = 23578;
PercError6mmIT4(1,2) = ((EC6InnerT4Act2 - EC6InnerT4)/EC6InnerT4Act2)*100;

EC6InnerT4Act3 = 26480;
PercError6mmIT4(1,3) = ((EC6InnerT4Act3 - EC6InnerT4)/EC6InnerT4Act3)*100;

EC6InnerT4Act4 = 21931;
PercError6mmIT4(1,4) = ((EC6InnerT4Act4 - EC6InnerT4)/EC6InnerT4Act4)*100;

EC6InnerT4Act5 = 22089;
PercError6mmIT4(1,5) = ((EC6InnerT4Act5 - EC6InnerT4)/EC6InnerT4Act5)*100;

EC6InnerT4Act6 = 22117;
PercError6mmIT4(1,6) = ((EC6InnerT4Act6 - EC6InnerT4)/EC6InnerT4Act6)*100;

display(PercError6mmIT4)

%%
% 5th Pass
timeInnerSampT5 = timeInner(6) - timeInner(5);
N = [1,2,5,8,9,10,timeInnerSampT5,20,50,100,200,500,1000];
deltaT5 = timeInnerSampT5./N;
EC6InnerT5 = zeros(length(N),1);

for k = 1:length(N)
   delT_row = [0:deltaT5(k):timeInnerSampT5]; % sample time in [sec]
   MRRInnerT5_Proto = -0.6398 .* delT_row + 79.8874;
   MRRInnerT5 = smooth(MRRInnerT5_Proto,'moving');
   SpecEnergy6mmInnerT5 = 1556 .* (1./MRRInnerT5') + 1.475;
   EC6InnerT5(k) = sum(SpecEnergy6mmInnerT5 .* (MRRInnerT5' .* deltaT5(k)));
end
display(EC6InnerT5)

EC6InnerT5Act1 = 39540;
EC6InnerT5Act2 = 38016;
EC6InnerT5Act3 = 38178;
EC6InnerT5Act4 = 39260;
EC6InnerT5Act5 = 39269;
EC6InnerT5Act6 = 38928;
PercError6mmIT5 = zeros(length(EC6InnerT5),6);
```

```
for d = 1:length(EC6InnerT5)
   PercError6mmIT5(d,1) = ((EC6InnerT5Act1 - EC6InnerT5(d))/EC6InnerT5Act1)*100;
end

for s = 1:length(EC6InnerT5)
   PercError6mmIT5(s,2) = ((EC6InnerT5Act2 - EC6InnerT5(s))./EC6InnerT5Act2).*100;
end

for x = 1:length(EC6InnerT5)
   PercError6mmIT5(x,3) = ((EC6InnerT5Act3 - EC6InnerT5(x))./EC6InnerT5Act3).*100;
end

for y = 1:length(EC6InnerT5)
   PercError6mmIT5(y,4) = ((EC6InnerT5Act4 - EC6InnerT5(y))./EC6InnerT5Act4).*100;
end

for t = 1:length(EC6InnerT5)
   PercError6mmIT5(t,5) = ((EC6InnerT5Act5 - EC6InnerT5(t))./EC6InnerT5Act5).*100;
end

for u = 1:length(EC6InnerT5)
   PercError6mmIT5(u,6) = ((EC6InnerT5Act6 - EC6InnerT5(u))./EC6InnerT5Act6).*100;
end

display(PercError6mmIT5)

%%
% 6th Pass
timeInnerSampT6 = timeInner(7) - timeInner(6);
N = [1,2,5,8,timeInnerSampT6,9,10,20,50,100,200,500,1000];
deltaT6 = timeInnerSampT6./N;
EC6InnerT6 = zeros(length(N),1);

for k = 1:length(N)
   delT_row = [0:deltaT6(k):timeInnerSampT6]; % sample time in [sec]
   MRRInnerT6_Proto = -0.7729 .* delT_row + 93.0949;
   MRRInnerT6 = smooth(MRRInnerT6_Proto,'moving');
   SpecEnergy6mmInnerT6 = 1556 .* (1./MRRInnerT6') + 1.475;
   EC6InnerT6(k) = sum(SpecEnergy6mmInnerT6 .* (MRRInnerT6' .* deltaT6(k)));
end
display(EC6InnerT6)

EC6InnerT6Act1 = 31978;
EC6InnerT6Act2 = 31895;
EC6InnerT6Act3 = 33336;
EC6InnerT6Act4 = 31707;
```

```
EC6InnerT6Act5 = 30445;
EC6InnerT6Act6 = 30646;
PercError6mmIT6 = zeros(length(EC6InnerT6),6);
for d = 1:length(EC6InnerT6)
   PercError6mmIT6(d,1) = ((EC6InnerT6Act1 - EC6InnerT6(d))/EC6InnerT6Act1)*100;
end

for s = 1:length(EC6InnerT6)
   PercError6mmIT6(s,2) = ((EC6InnerT6Act2 - EC6InnerT6(s))./EC6InnerT6Act2).*100;
end

for x = 1:length(EC6InnerT6)
   PercError6mmIT6(x,3) = ((EC6InnerT6Act3 - EC6InnerT6(x))./EC6InnerT6Act3).*100;
end

for y = 1:length(EC6InnerT6)
   PercError6mmIT6(y,4) = ((EC6InnerT6Act4 - EC6InnerT6(y))./EC6InnerT6Act4).*100;
end

for t = 1:length(EC6InnerT6)
   PercError6mmIT6(t,5) = ((EC6InnerT6Act5 - EC6InnerT6(t))./EC6InnerT6Act5).*100;
end

for u = 1:length(EC6InnerT6)
   PercError6mmIT6(u,6) = ((EC6InnerT6Act6 - EC6InnerT6(u))./EC6InnerT6Act6).*100;
end

display(PercError6mmIT6)

%% Energy Consumption Bar Graph
ECOT1 = [EC6OuterT1(end), EC6OuterT1Act1, EC6OuterT1Act2, EC6OuterT1Act3,
EC6OuterT1Act4, EC6OuterT1Act5, EC6OuterT1Act6];
ECOT2 = [EC6OuterT2(end), EC6OuterT2Act1, EC6OuterT2Act2, EC6OuterT2Act3,
EC6OuterT2Act4, EC6OuterT2Act5, EC6OuterT2Act6];
ECOT3 = [EC6OuterT3(end), EC6OuterT3Act1, EC6OuterT3Act2, EC6OuterT3Act3,
EC6OuterT3Act4, EC6OuterT3Act5, EC6OuterT3Act6];
ECIT1 = [EC6InnerT1(end), EC6InnerT1Act1, EC6InnerT1Act2, EC6InnerT1Act3,
EC6InnerT1Act4, EC6InnerT1Act5, EC6InnerT1Act6];
ECIT2 = [EC6InnerT2(end), EC6InnerT2Act1, EC6InnerT2Act2, EC6InnerT1Act3,
EC6InnerT1Act4, EC6InnerT2Act5, EC6InnerT2Act6];
ECIT3 = [EC6InnerT3(end), EC6InnerT3Act1, EC6InnerT3Act2, EC6InnerT1Act3,
EC6InnerT1Act4, EC6InnerT3Act5, EC6InnerT3Act6];
ECIT4 = [EC6InnerT4(end), EC6InnerT4Act1, EC6InnerT4Act2, EC6InnerT1Act3,
EC6InnerT1Act4, EC6InnerT4Act5, EC6InnerT4Act6];
ECIT5 = [EC6InnerT5(end), EC6InnerT5Act1, EC6InnerT5Act2, EC6InnerT1Act3,
EC6InnerT1Act4, EC6InnerT5Act5, EC6InnerT5Act6];
```

```
ECIT6 = [EC6InnerT6(end), EC6InnerT6Act1, EC6InnerT6Act2, EC6InnerT1Act3,
EC6InnerT1Act4, EC6InnerT6Act5, EC6InnerT6Act6];
EnergyConsump = cat(1,ECOT1,ECOT2,ECOT3,ECIT1,ECIT2,ECIT3,ECIT4,ECIT5,...
   ECIT6);
xlswrite('EnergyConsumption_copy.xls',EnergyConsump)

%% Min, Max, and Mean of Aggregate
min((cell2mat({PercError6mmOT1(end,:), PercError6mmOT2,
PercError6mmOT3(end,:),PercError6mmIT1(end,:),PercError6mmIT2,PercError6mmIT3(end,:),
PercError6mmIT4,...
   PercError6mmIT5(end,:),PercError6mmIT6(end,:)})))
max((cell2mat({PercError6mmOT1(end,:), PercError6mmOT2,
PercError6mmOT3(end,:),PercError6mmIT1(end,:),PercError6mmIT2,PercError6mmIT3(end,:),
PercError6mmIT4,...
   PercError6mmIT5(end,:),PercError6mmIT6(end,:)})))
mean((cell2mat({PercError6mmOT1(end,:), PercError6mmOT2,
PercError6mmOT3(end,:),PercError6mmIT1(end,:),PercError6mmIT2,PercError6mmIT3(end,:),
PercError6mmIT4,...
   PercError6mmIT5(end,:),PercError6mmIT6(end,:)})))

%% Min, Max, and Mean Per Feature
minPerFeature = [min(PercError6mmOT1(end,:)), min(PercError6mmOT2(end,:)),
min(PercError6mmOT3(end,:)), min(PercError6mmIT1(end,:)), min(PercError6mmIT2(end,:)),
min(PercError6mmIT3(end,:)),...
   min(PercError6mmIT4(end,:)), min(PercError6mmIT5(end,:)),
min(PercError6mmIT6(end,:))]
maxPerFeature = [max(PercError6mmOT1(end,:)), max(PercError6mmOT2(end,:)),
max(PercError6mmOT3(end,:)), max(PercError6mmIT1(end,:)), max(PercError6mmIT2(end,:)),
max(PercError6mmIT3(end,:)),...
   max(PercError6mmIT4(end,:)), max(PercError6mmIT5(end,:)),
max(PercError6mmIT6(end,:))]
meanPerFeature = [mean(PercError6mmOT1(end,:)), mean(PercError6mmOT2(end,:)),
mean(PercError6mmOT3(end,:)), mean(PercError6mmIT1(end,:)),
mean(PercError6mmIT2(end,:)), mean(PercError6mmIT3(end,:)),...
   mean(PercError6mmIT4(end,:)), mean(PercError6mmIT5(end,:)),
mean(PercError6mmIT6(end,:))]
```

Appendix B Product Cell Energy Consumption (PCEC) Matlab Script

```
% Import Test File
[Power] = csvread('141new.csv', 1, 3, [1,3,1394147,3]);

% Please note, this script block will produce an error since the directory
% information is deleted for privacy protection reasons.

%% Hour Column Import - Raw
% Convert to seconds
[Raw_1] = csvread('141new.csv', 1, 0, [1,0,1394147,0]);
Hours = Raw_1 .* 3600;

%% Minute Column Import - Raw
% Convert to seconds
[Raw_2] = csvread('141new.csv', 1, 1, [1,1,1394147,1]);
Minutes = Raw_2 .* 60;

%% Second Column Import
[Raw_3] = csvread('141new.csv', 1, 2, [1,2,1394147,2]);

%% Sort
SecondsNet = Hours + Minutes + Raw_3;
NetData = horzcat(SecondsNet, Power);

%% Short Testing
%% Test Data Declaration
NetData_Test_1 = NetData(1:60, :);
NetData_Test_2 = NetData(41:100,:);

%% Test_1
keyIndices = find(NetData_Test_1<4);
keyIndNorm = keyIndices - 60;
for s = 1:length(keyIndNorm)
   p = s+1;
   if p <= length(keyIndNorm)
      x = p;
      if (keyIndNorm(x) - keyIndNorm(s) > 2) && ((NetData_Test_1(keyIndNorm(x)+1, 2)) < 4)
         k = s-1;
         y = k;
         display(y)
         display(x)
         display(s)
         expMat1 = NetData_Test_1(keyIndNorm(y):keyIndNorm(x), :)
         xlswrite('141Analysis_Test_3.xls',expMat1,'Sheet1','A1')
      end
   end
```

```
end

%% Test_2
keyIndices = find(NetData_Test_2<4);
keyIndNorm = keyIndices - 60;
for s = 1:length(keyIndNorm)
   p = s+1;
   if p <= length(keyIndNorm)
      x = p;
      if (keyIndNorm(x) - keyIndNorm(s) > 2) && ((NetData_Test_2(keyIndNorm(x)+1, 2)) < 4)
         k = s-1;
         y = k;
         display(y)
         display(x)
         display(s)
         expMat2 = NetData_Test_2(keyIndNorm(y):keyIndNorm(x), :)
         xlswrite('141Analysis_Test_3.xls',expMat2,'Sheet2','A1')
      end
   end
end

%% Concatenation Testing
%% Declaration
NetData_Test = NetData(1:100,:);

%% Test with Concatenation
keyIndices = find(NetData_Test<4);
keyIndNorm = keyIndices - 100;
expMat = {};

for s = 1:length(keyIndNorm)
   p = s+1;
   if p <= length(keyIndNorm)
      x = p;
      if (keyIndNorm(x) - keyIndNorm(s) > 2) && ((NetData_Test(keyIndNorm(x)+1, 2)) < 4)
         k = s-2;
         y = k;
         display(y)
         display(x)
         display(s)
         expMat3 = NetData_Test(keyIndNorm(y):keyIndNorm(x), :)
         expMat = {cell2mat(expMat) expMat3}
       end
   end
end
```

```
%% Plotting/Export if desired
Trend1 = cell2mat(expMat(1));
Trend2 = cell2mat(expMat(2));
subplot(2,1,1); plot(Trend1(:,1),Trend1(:,2))
subplot(2,1,2); plot(Trend2(:,1),Trend2(:,2))
```

Appendix C Process Input/Output Stream (PIOS)

1. Forming/Shaping

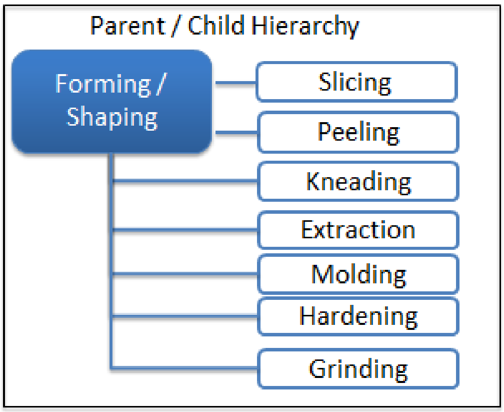

2. Mixing

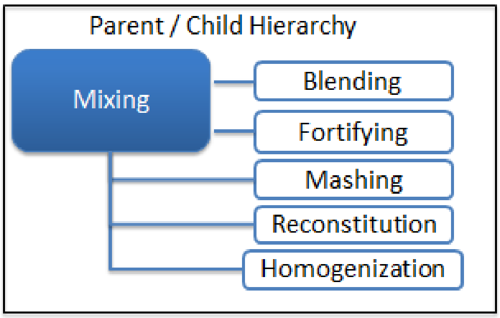

3. Food Addition/Subtraction

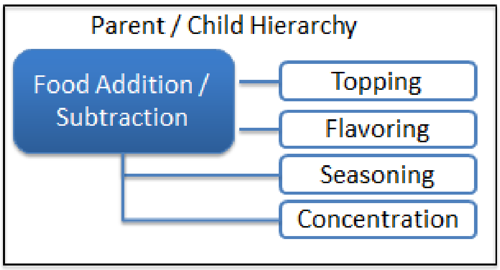

4. Heating / Cooling

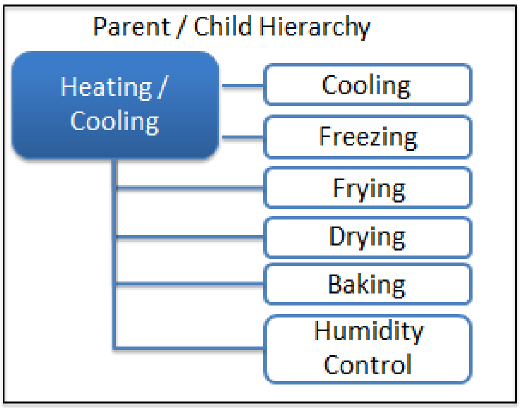

5. Growth

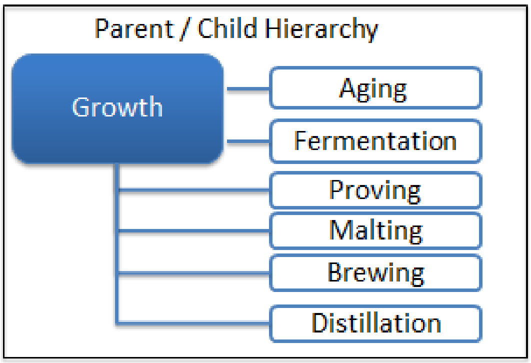

6. Packaging

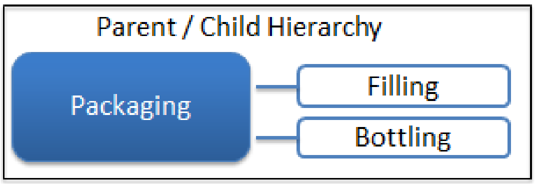

Appendix D Process Chain Stream (PIOS Plus)

1. Ice cream [56], [71]-[80]

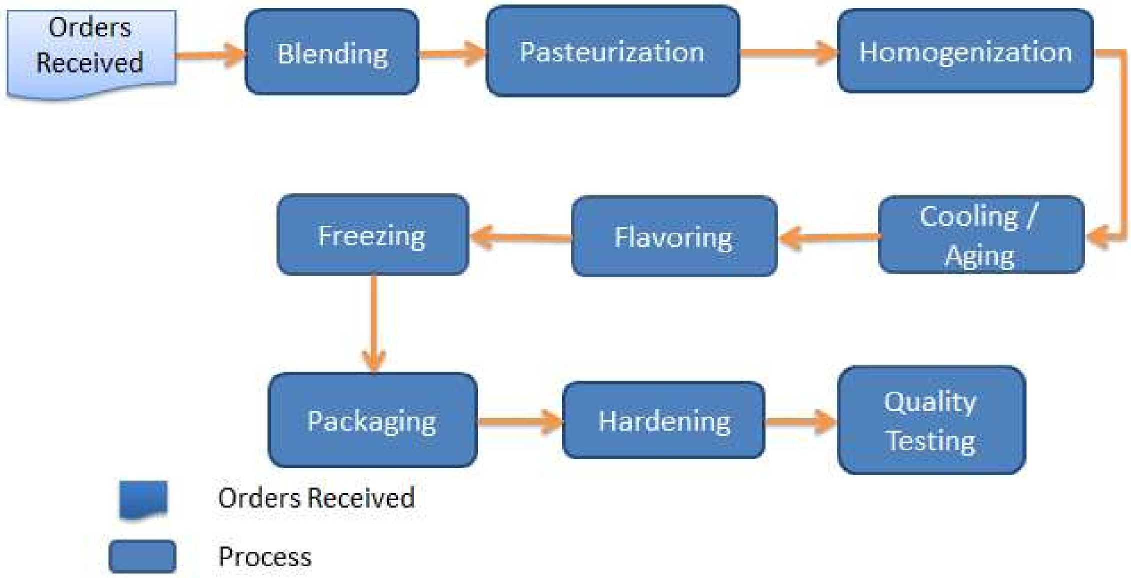

2. Pizza with optional freezing option [57], [81]-[85]

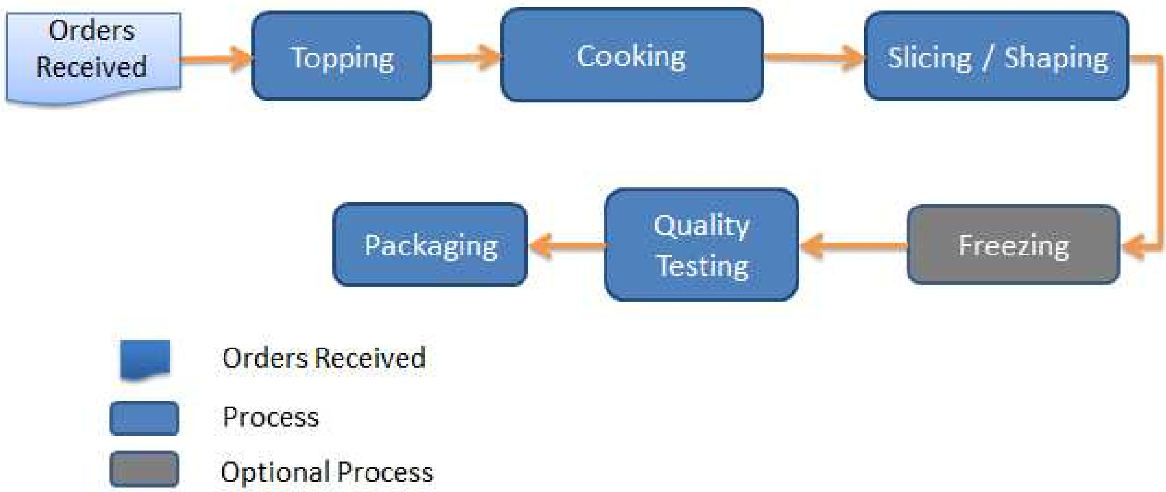

3. Orange juice [59], [77], [102], [104]-[107]

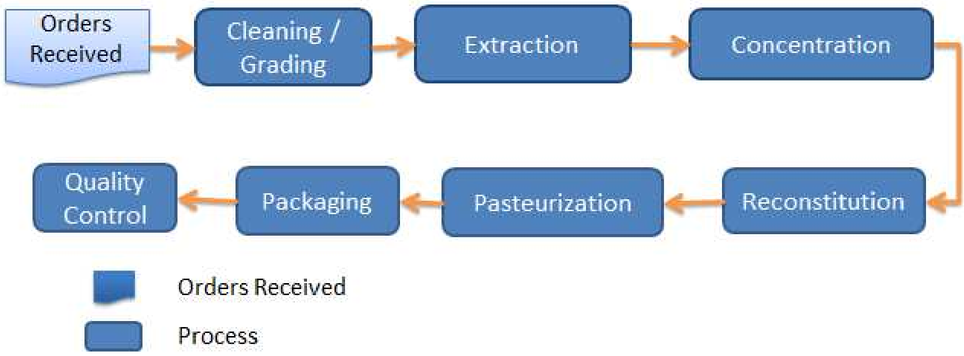

4. Industry trend

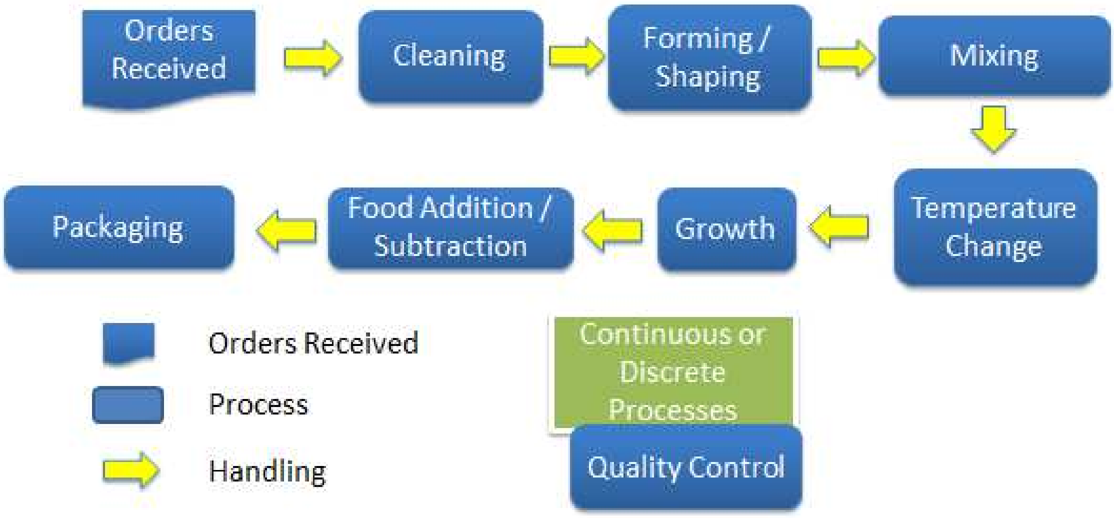

5. Pastry [77], [86]-[90]

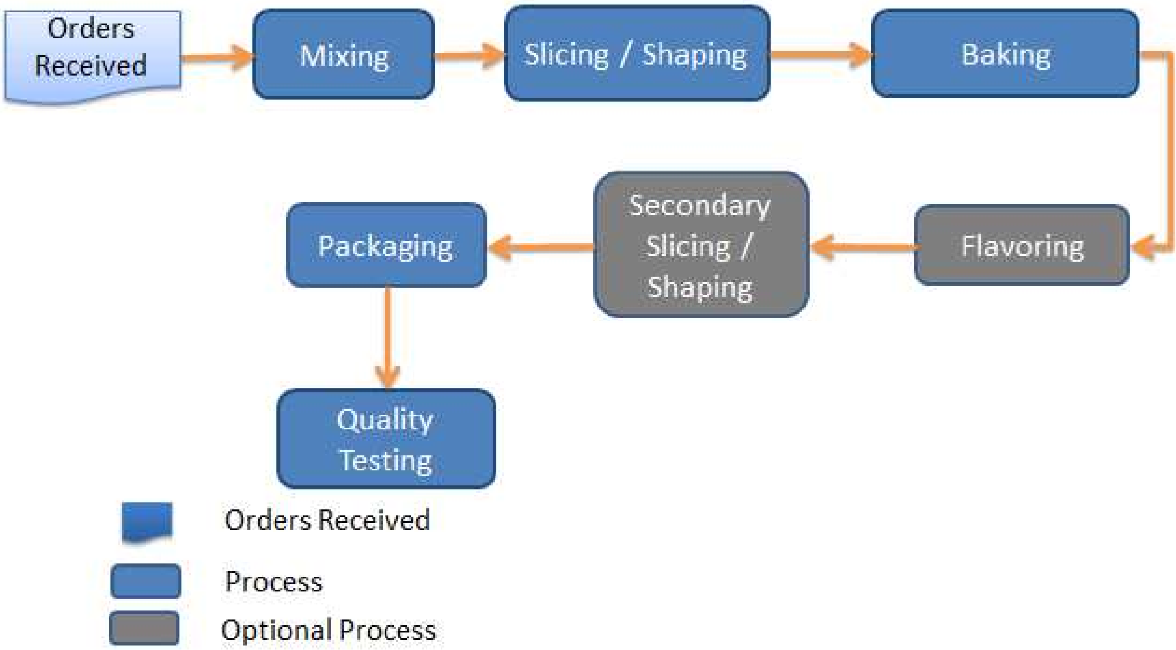

6. Bread [84], [91]-[98]

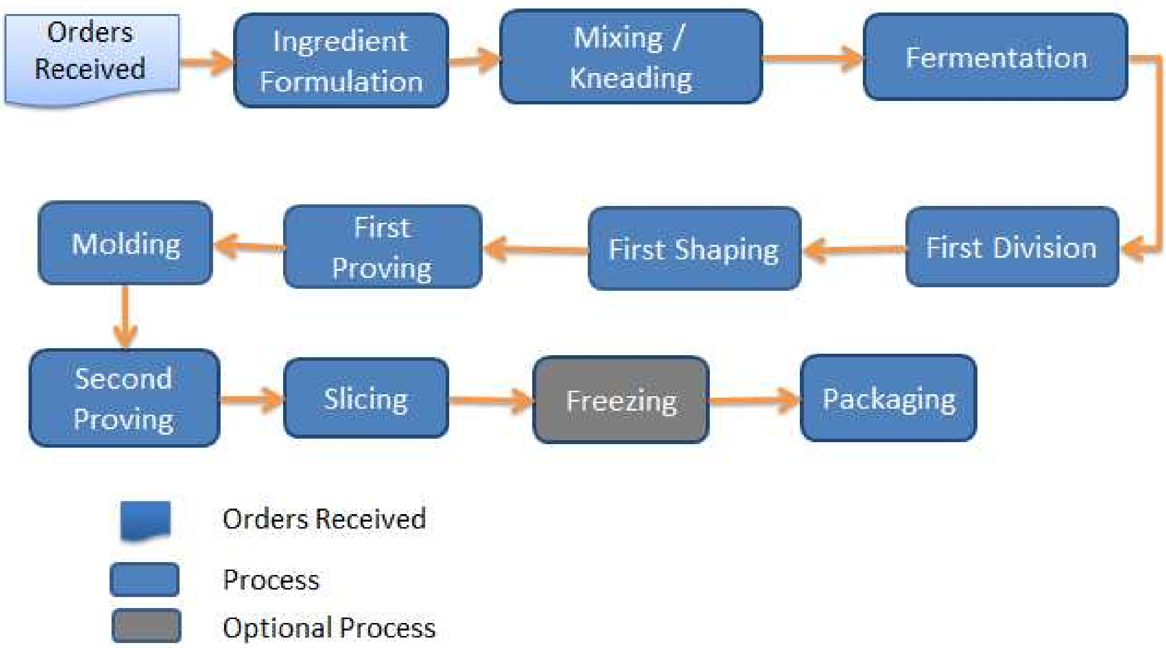

7. <u>Milk</u> [99]-[104]

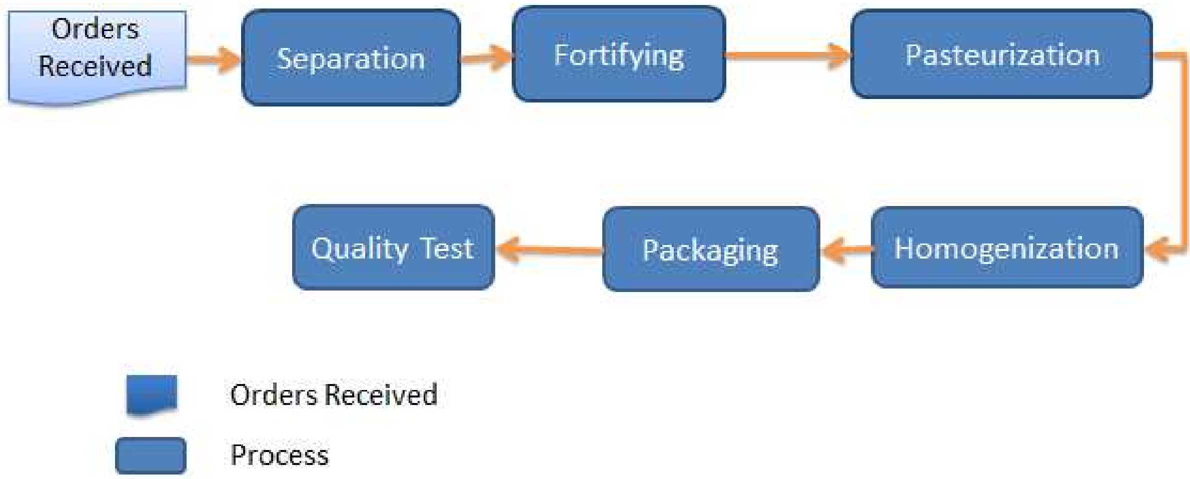

8. <u>Beer</u> [108]-[112]

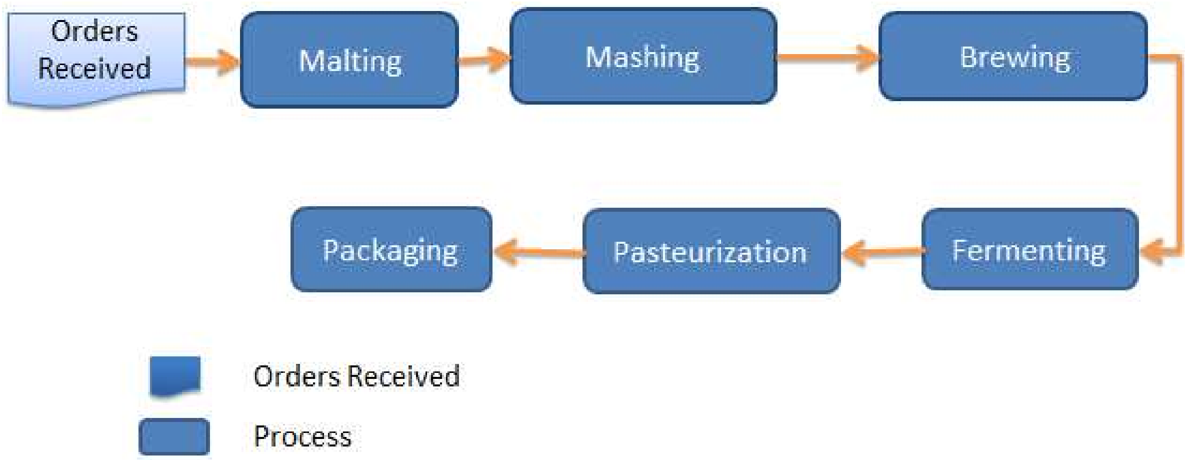

9. <u>Whiskey</u> [113]-[116]